ANALYSIS AND DESIGN OF A SOLAR-POWERED LIQUID-DESICCANT AIR CONDITIONER FOR USE IN HOT AND HUMID CLIMATES

BY

AMMAR CHEBBAH

A DISSERTATION PRESENTED TO THE GRADUATE SCHOOL
OF THE UNIVERSITY OF FLORIDA IN
PARTIAL FULFILLMENT OF THE REQUIREMENTS
FOR THE DEGREE OF DOCTOR OF PHILOSOPHY

UNIVERSITY OF FLORIDA

1987

To my parents
for their love and encouragement

ACKNOWLEDGEMENTS

I wish to express my sincere gratitude to Dr. Erich A. Farber, chairman of the supervisory committee, for his generous support, guidance and advice throughout the preparation of this dissertation.

I am indebted to the supervisory committee members, Dr. H. A. Ingley, Dr. C. K. Hsieh, Dr. R. A. Gater, Dr. U. H. Kurzweg and Dr. R. Pagano, for their suggestions and encouragement and to Dr. R.K. Irey, former faculty member.

I am also indebted to T. E. Barrup, R. W. Dixon, K. E. Davis, John West, C. C. Garretson and Howard Purdy of the Solar Energy and Energy Conversion Lab, for their friendship, advices and help.

I am grateful to Connie Crawford for her consultation and patience in typing this dissertation.

Last, but not least, I would like to especially thank Patricia A. Sickler for her general support and encouragement.

TABLE OF CONTENTS

ACKNOWLEDGEMENTS..iii

LIST OF TABLES..vii

LIST OF FIGURES..viii

KEY TO SYMBOLS..xiv

ABSTRACT..xxi

CHAPTER

I. INTRODUCTION..1

II. PROCESS DESCRIPTION AND RELATED PREVIOUS WORK 8

- 2.1. Solid Desiccant Systems..........................8
- 2.2. Liquid Desiccant Systems........................15
  - 2.2.1. Process Description..........................15
  - 2.2.2. Liquid Desiccant-Moist Air Contactors........23
    - 2.2.2.1. Absorbers................................25
    - 2.2.2.2. Regenerators.............................28

III. THEORETICAL BACKGROUND AND DEVELOPMENT OF A SIMPLIFIED MODEL...............................33

- 3.1. Phase Equilibrium...............................33
- 3.2. Interphase Mass Transfer Coefficients...........35
- 3.3. Heat, Mass and Momentum Transfer Analogies......41
- 3.4. Falling Film Analysis and Non-Entrainment Condition...48
- 3.5. Non-Adiabatic Packed Tower Analysis.............55
  - 3.5.1. Generalysed Differential Analysis............55
  - 3.5.2. Simplified Model for Liquid Desiccant Systems (Nearly Isothermal Processes)..............68

IV. COMPONENT MODELS AND NUMERICAL SOLUTION PROCEDURE....78

4.1. Transfer Coefficients and Friction Losses in Finned Tube Heat Exchangers......78
4.2. Recovery Heat Exchangers....84
4.3. Evaporative Cooler....86
4.4. Liquid Desiccants--Triethylene Glycol....88
4.5. Numerical Solution Procedure....93

V. THEORETICAL ANALYSIS, RESULTS AND DISCUSSION....99

5.1. Absorber Parametric Analysis....100
  5.1.1. Effect of Desiccant Flow Rate and Packing Depth....102
  5.1.2. Effect of Cooling Water Flow Rate and Inlet Temperature....117
  5.1.3. Effect of Solution Inlet Concentration and Temperature....122
5.2. Regenerator Parametric Analysis....127

VI. SYSTEM DESIGN AND OPTIMIZATION....138

6.1. Liquid Desiccant Air-Conditioner Design Procedure....138
6.2. System Optimization....144
6.3. System Performance at Other Than Design Regenerating Temperature....157

VII. EXPERIMENTAL ANALYSIS, RESULTS AND DISCUSSION....159

7.1. Description of The Experimental Apparatus....159
7.2. Experimental Procedure and Data Collection....164
7.3. Discussion and Evaluation of Experimental Results....166
  7.3.1. Effect of Cooling Water Flow Rate....167
  7.3.2. Effect of Regenerator Water Flow Rate....173
  7.3.3. Effect of Regenerator Hot Water Inlet Temperature....178
7.4. Comparison of Experimental and Theoretical Results....182

VIII. CONCLUSIONS AND RECOMMENDATIONS....198

8.1. Conclusions....198
8.2. Recommendations....201

APPENDIX

A. SIMPLIFIED MODEL FOR LIQUID DESICCANT-AIR CONTACTORS.......................................202

B. THERMODYNAMIC PROPERTIES OF TRIETHYLENE GLYCOL.................................209

C. ECONOMIC ANALYSIS....................................213

D. EXPERIMENTAL AND THEORETICAL DATA AND RESULTS......................................220

E. UNCERTAINTY ANALYSIS.................................223

F. COMPUTER PROGRAM DESYST AND SUBROUTINE DESCON.................................228

REFERENCES 238

BIOGRAPHICAL SKETCH 244

LIST OF TABLES

Table

6-1. Characteristics of the Optimized Liquid Desiccant Contactors....155

6-2. Overall Design Characteristics of the Optimized Liquid-Desiccant Air-Conditioning System....156

6-3. System Performance at other than Design Regenerating Temperatures....158

7-1: Dimensions of the Finned Tube Heat Exchangers Used in the Experimental Prototype....162

D-1: Effect of Cooling Water Flow Rate....220

D-2: Effect of Hot Water Flow Rate....221

D-3: Effect of Hot Inlet Water Temperature....222

E-1: Estimated Errors of Different Variables....226

E-2: Uncertainty of Computer Output Variables, Resulting from Error Propagation....227

LIST OF FIGURES

Figure

1-1: Psychrometric Representation of Desiccant Air-Conditioning Concept..............................3

2-1: Solid Desiccant Rotating Bed.........................10

2-2: Absorption Capacity of Selica Gel and Molecular Sieve as Function of Temperature [16]...............12

2-3: Schematic Diagram of Cooled Dunkle Cycle Air-Conditioning System...............................14

2-4: Schematic Diagram of a Basic Liquid Desiccant Air-Conditioning System...............................16

2-5: Niagara "Hygrol" Liquid Desiccant System (Niagara Blower Company) [23]........................18

2-6: Kathabar "Spray Cel" Liquid Desiccant Unit (Midland-Ross Corporation) [24].....................20

2-7: Kathabar "Twin-Cel" Liquid Desiccant Unit (Midland-Ross Corporation) [25].....................21

2-8: Schematic Diagram of Turner's Liquid Desiccant Air Conditioner [38]................................27

2-9: Liquid Desiccant Collector-Regenerator..............30

3-1: Liquid Falling Film in Counterflow with Rising Gas..42

3-2: Entrainment in a Falling Film.......................51

3-3: Non-Adiabatic Packed Tower...........................56

3-4: Heat and Mass Transfer in a Differential Element....60

4-1: Heat Transfer Correlation for Smooth Plate-fin-tube Coils with 4 Rows of Tubes [60]....................80

4-2: Correlation of Friction Data For Smooth Plate-fin-tube Coils [60]...........................82

4-3: Specific Heat of Triethylene Glycol Solutions versus Temperature and Concentration (Dow Chemical Company) [68]..........................90

4-4: Integral Heat of mixing of Triethylene Glycol Solution versus water molar fraction [56]..........90

4-5: Viscosity of Aqueous Triethylene Glycol Solutions (Dow Chemical Company) [68]..........................91

4-6: Total Pressure over Aqueous Triethylene Glycol Solutions versus Temperature (Dow Chemical Company) [68].......................................92

4-7: Flow Diagram of Subroutine DESCON, a Liquid Desiccant Contractor..............................95

4-8: Flow Diagram of the Computer Program DESYST, for the Analysis of a Continuous Liquid Desiccant Air Conditioner...........................97

5-1: Humidity Ratio of Air Leaving the Absorber versus Packing Depth, for Different Desiccant Flow Rates..103

5-2: Humidity Ratio of Air Leaving the Absorber versus Desiccant Flow Rate, for different Packing Depths..104

5-3: Temperature of Air Leaving the Absorber versus Packing Depth, for different Desiccant Flow Rates..106

5-4: Temperature of Air Leaving the Absorber versus Desiccant Flow Rate, for different Packing Depths..107

5-5: Enthalpy of Air Leaving the Absorber versus Packing Depth, for different Desiccant Flow Rates..108

5-6: Enthalpy of Air Leaving the Absorber versus Desiccant Flow Rate, for different Packing Depths..109

5-7: Outlet Temperature of Cooling Water versus Packing Depth, for different Desiccant Flow Rates..111

5-8: Outlet Temperature of Cooling Water versus Desiccant Flow Rate, for different Packing Depths..112

5-9: Concentration by Weight of the Desiccant Solution Leaving the Absorber versus Packing Depth, for different Flow Rates.............................113

5-10: Mass Transfer Driving Potential at top of Absorber versus Coil Depth, for different Desiccant Flow Rates..............................114

5-11: Mass Transfer Driving Potential at the Bottom of the Absorber versus Packing Depth, for different Desiccant Flow Rates................115

5-12: Temperature of Air Leaving the Absorber versus Coil Depth, for different Cooling Water Flow Rates and Inlet Temperatures.......................118

5-13: Humidity Ratio of Air Leaving the Absorber versus Coil Depth, for different Cooling Water Flow Rates and Inlet Temperatures.................119

5-14: Enthalpy of Air Leaving the Absorber versus Coil Depth, for different Cooling Water Flow Rates and Inlet Temperatures.......................120

5-15: Temperature of Air Leaving the Absorber versus Coil Depth, for different Desiccant Solution Inlet Concentrations and Temperatures.............123

5-16: Humidity Ratio of Air Leaving the Absorber versus Coil Depth, for Different Desiccant Solutions Inlet Concentrations and Temperatures...124

5-17: Enthalpy of Air Leaving the Absorber versus Coil Depth, for different Desiccant Solution Inlet Concentrations and Temperatures.............125

5-18: Humidity Ratio of Air Leaving the Absorber versus Desiccant Solution Inlet Concentrations, for different Coil Depths.........................126

5-19: Desiccant Outlet Concentration (by weight) versus Packing Depth, for different Hot Water Inlet Temperatures................................129

5-20: Hot Water Outlet Temperature versus Packing Depth, for different Inlet Water Temperatures.....130

5-21: Desiccant Outlet Concentration (by weight) versus Packing Depth, for different Inlet Water Temperatures................................132

5-22: Hot Water Outlet Temperature versus Packing Depth, for different Inlet Water Temperatures.....133

5-23: Desiccant Outlet Concentration (by weight) versus Process Water Flow Rate, for different Regenerating Temperatures.........................135

5-24: Desiccant Outlet Concentration (by weight) versus Packing Depth, for different Regenerating Temperatures.........................136

6-1: Present Worth, Initial, and Operating Costs versus Absorber Process Water Flow Rate....................148

6-2: Present Worth, Initial, and Operating Costs versus Regenerator Process Water Flow Rate................149

6-3: Present Worth, Initial, and Operating Costs versus Desiccant Flow Rate..................................150

6-4: Present Worth, Initial, and Operating Costs versus Absorber Packing Height..............................151

6-5: Present Worth, Initial, and Operating Costs versus Regenerator Packing Height..........................152

7-1: Schematic Diagram of the Experimental Liquid Desiccant Air Conditioner..........................160

7-2: Overall View of The Experimental Liquid Desiccant Air Conditioner..........................161

7-3: Absorber Outlet Air and Water, Inlet Solution, and Exit of Evaporative Cooler Temperatures versus Cooling Water Flow Rate....................168

7-4: Humidity Ratio of Dried Air Leaving the Absorber versus Cooling Water Flow Rate....................168

7-5: Enthalpy of Air Leaving the Absorber versus Cooling Water Flow Rate............................169

7-6: Generator Outlet Air and Water, and Inlet Solution Temperatures versus Cooling Water Flow Rate........169

7-7: Strong Solution Concentration versus Cooling Water Flow Rate....................................170

7-8: System's coefficient of Performance versus Cooling Water Flow Rate............................170

7-9: Outlet Air and Water, and Inlet Solution Temperatures versus Hot Water Flow Rate............174

7-10: Strong Solution Concentration versus Hot Water Flow Rate..................................174

7-11: Humidity Ratio of Dried Air Leaving the Absorber versus Hot Water Flow Rate...............175

7-12: Outlet Air and Water, Inlet Solution, and Exit of Evaporative Cooler Air Temperatures versus Hot Water Flow Rate..................................175

7-13: Enthalpy of Air Leaving the Absorber versus Hot Water Flow Rate....176

7-14: System's Coefficient of Performance versus Hot Water Flow Rate....176

7-15: Outlet Air and Water, and Inlet Solution Temperatures versus Hot Water Inlet Temperature...179

7-16: Strong Solution Concentration versus Hot Water Inlet Temperature....179

7-17: Humidity Ratio of Air Leaving Absorber versus Hot Water Inlet Temperature....180

7-18: Outlet Air and Water, Inlet Solution, and Exit-of Evaporative Cooler Air Temperatures, versus Hot Water Temperature....180

7-19: Enthalpy of Air Leaving the Absorber versus Hot Water Inlet Temperature....181

7-20: System's Coefficient of Performance versus Hot Water Inlet Temperature....181

7-21: Temperature of Air Leaving the Absorber versus a) Hot Water Inlet Temperature, b) Hot Water Flow Rare, c) Cooling Water Flow Rate....186

7-22: Temperature of Air Leaving the Regenerator versus a) Hot Water Inlet Temperature, b) Hot Water Flow Rate, c) Cooling Water Flow Rate....187

7-23: Cooling Water Outlet Temperature versus a) Hot Water Inlet Temperature, b) Hot Water Flow Rate, c) Cooling Water Flow Rate....188

7-24: Hot Water Outlet Temperature versus a) Hot Water Inlet Temperature, b) Hot Water Flow Rate, c) Cooling Water Flow Rate....189

7-25: Desiccant Solution Temperature Entering the Absorber versus a) Hot Water Inlet Temperature, b) Hot Water Flow Rate, c) Cooling Water Flow Rate....190

7-26: Desiccant Solution Temperature Entering the Regenerator versus a) Hot Water Inlet Temperature, b) Hot Water Flow Rate, c) Cooling water Flow Rate....191

7-27: Humidity Ratio of Air Leaving the Absorber versus a) Hot Water Inlet Temperature, b) Hot Water Flow Rate, c) Cooling Water Flow Rate..192

7-28: Enthalpy of Air Leaving the Absorber versus a) Hot Water Inlet Temperature, b) Hot Water Flow Rate, c) Cooling Water Flow Rate..193

7-29: Strong Solution Concentration versus a) Hot Water Inlet Temperature, b) Hot Water Flow Rate, c) Cooling Water Flow Rate............194

7-30: System's Coefficient of Performance versus a) Hot Water Inlet Temperature, b) Hot Water Flow Rate, c) Cooling Water Flow Rate......195

KEY TO SYMBOLS

a	Surface density, ft^2/ft^3
a	Annuity
A	Area, ft^2
C, Cp	Specific heat, Btu/Lb.°F
$\bar{C}$	Average Specific heat Btu/Lb.°F
C'	Normalized mass concentration, dimensionless
COP	Coefficient of performance, dimensionless
CFM	Volume flow rate, ft^3/min
D	Mass diffusivity, $ft^2/sec.$
D	Diameter, feet
DD	Degree days, °F
D^*	Hydraulic diameter, ft
DFLEOH	Daily full load equivalent operating hours, hours
DP	Pressure drop, psi
E	Surface effectiveness, dimensionless
ER	Recovery heat exchanger effectiveness
f	Friction factor, dimensionless
F	Wetting factor dimensionless
FP	Friction correlating parameter, dimensionless
g	local acceleration due to gravity, ft/sec^2
G	mass of gaz, Lbm

h	Convective heat transfer coefficient, Btu/hr. ft^2. °F
H	Enthalpy, Btu/Lbm
H^*	Enthalphy expression, Btu/Lbm
IC	Inital cost, dollars
J	Colburn J factor, dimensionless
JP	Heat transfer correlating paramenter, dimensionless
k	Thermal conductivity, Btu/hr.ft.°F
k	individual mass transfer coefficient based on mole fractions
K	Overall mass transfer coefficient, ft^2/hr
L	Length, ft.
L	mass of liquid, Lbm
Le	Lewis number, dimensionless
M	Mass, Lbm
MA	Air flow rate, Lbm/hr.ft^2
MD	Desiccant flow rate, Lbm/hr.ft^2
MPW	Process water flow rate, Lbm/hr.ft^2
n	life span of a project, years
N	Molar flux, Moles/ft^2
NR	Number of rows
Nu	Nusselt number, dimensionless
OP	Operating cost, dollars
P	Perimeter, ft
P	Pressure, lbf/ft^2
P'	Partial pressure, lbf/ft^2

Pr	Parandtl number, Dinensionless
PW	Present worth value, dollar
PWF	Present worth factor, dimensionless
Q	Cooling load, Btu/hr
Q	Heating Load, Btu/hr
Q	heat flux, btu/hr. ft^2
Q	Volume flow rate, ft^3/sec
R	Radius, ft
Re	Reynold number, dimensionless
S	Fin spacing, ft
SFLEOH	Seasonal full load equivalent operating hours, hr
Sc	Schmidt number, dimensionless
Sh	Sherwood number, dimenisonless
t	Thickness, ft
T	Temperature, °F
T'	Normalysed temperature, dimensionless
TDB	Dry bulb tempeature, °F
TPW	Process water temperature, °F
TSIN	Inlet solution temperature, °F
TWB	Wet bulb temperature, °F
u	Velocity in the x direction, ft/sec
U	average velocity, ft/sec
v	Velocity in the y direction, ft/sec
V	Volume, ft^3
W	Humidity ratio, lb.H_2O/Lb.da
W	Width, ft

x, y, z	Length, ft
x	mole fraction in liquid phase
x^*	equilibrium mole fraction in liquid phase
Xa	Tube spacing, ft
Xb	Row spacing, ft
X'	mass ratio in liquid phase
y	fin thickness, ft
y	mole fraction in gas phase
y'	Normalized length, dimensionless
y^*	Equilibrium mole fraction in gas phase
Y'	mass ratio in gas phase

Greek Symbols:

α	Thermal conductivity, ft^2/sec
ν	Momentum diffusivity, ft^2/sec
ε	effectiveness, dimensionless
μ	Viscosity, Lbm/ft.sec
δ	Boundary layer thickness, ft
λ	Latent heat, Btu/Lb
λ	Average latent heat, Btu/Lb
ρ	Mass density, Lbm/ft^3
τ	Shear stress, Lbf/ft^2
ΔHm	Mean enthalpy difference, Btu/Lbm.
$\overline{\Delta Hm'}$	Average heat of mixing per unit mass of solvent, Btu/Lbm of water transferred

Subscripts:

a	air
A	Absorber
A,B	Components of a solutions
B_p	Bypass
C	concentration
c	convective
c	cross section
c	cold
Cs	Cooling season
D	Desiccant
DB	Bry bulb
DHW	Domestic hot water
e	equilibrium
E	exhaust
EEC	Exit of evaporative cooler
G	gas
G	Generator
h	Hydraulic
h	Heat transfer
h	Hot
HS	Heating season
H_2O	Water
i	Interface
in	inlet
lm	Logarithmic near

L	Laminar
L	Liquid
m	mass transfer
max	Maximum
o	Outside conditions
p	pipe
pw	Present worth
r	Reference
R	Room conditions
R	Refrigerant
s	supply
S	sensible load
s	solvent
s	saturated
t	tube
T	Total
TEG	Triethylene glycol
v	vapor
w	water
wb	wet bulb
$(\dot{\ })$	per unit time
$(\ ')$	per unit mass or per unit length

Abstract of Dissertation Presented to the Graduate School
of the University of Florida in Partial Fulfillment of the
Requirements for the Degree of Doctor of Philosophy

ANALYSIS AND DESIGN OF A SOLAR-POWERED LIQUID-DESICCANT AIR CONDITIONER FOR USE IN HOT AND HUMID CLIMATES

By

Ammar Chebbah

May 1987

Chairman: Dr. E. A. Farber
Major Department: Mechanical Engineering

An experimental and theoretical investigation of the feasibility of a solar-powered liquid-desiccant air conditioner, for use in hot and humid climates, was carried out at the Mechanical Engineering Department, University of Florida.

The proposed liquid desiccant system used non adiabatic contactors, packed with finned-tube coils, for both moist air dehumidification and liquid-desiccant regeneration.

A theoretical model was developed to analyze the complex phenomena of simultaneous heat and mass transfer in non adiabatic contactors, as well as the continuous interaction between the dehumidification and regeneration processes. This theoretical model was based on the logarithmic mean differences the inlet and outlet thermodynamic properties of the working fluids.

A computer code was written to assist in the analysis of the dehumidification and regeneration processes separately and coupled, for continuous operation. It was used to investigate the interaction between the different controlling parameters (temperatures, humidities, concentrations, flow rates and packing geometry), and to investigate their effects on the overall performance of the desiccant system.

A fully solar-powered liquid-desiccant air-conditioner, with three tons of capacity was designed and optimized including economical criteria. Taking into account the total electrical energy usage and the efficiency of the solar collectors, which was assumed to be 50%, the overall coefficient of performance (COP) of the optimized system was determined to be 0.312. The optimized system operates at a regenerating temperature of 140°F, requiring 640 ft^2 of solar collectors, based on a daily average solar collection of 1000 Btu/ft^2. day.

A prototype unit was built, and experimental results were obtained. These results verified the validity and accuracy of the theoretical model.

CHAPTER I
INTRODUCTION

Although international politics plays a major role in temporarily controlling energy costs, nature controls the available energy forms and quantities. Fossil fuels, on which modern daily life is strongly dependent, are exhaustible. Nuclear energy, a possible alternative, presents major pollution problems that are not yet solved by today's technology. Energy conservation and search for other nonexhaustible sources of energy, such as solar, geothermal and aeolic, are therefore immediate responsibilities for a brighter energy future.

In recent years, considerable time has been devoted to the use of the sun as an alternative source of energy, in particular for air-conditioning applications where the solar radiation and the cooling requirement are in phase. Several solar-assisted cooling systems have since been investigated, namely the Rankine vapor compression cycle, the absorption cycle, and the dehumidification/evaporative cooling cycle using desiccants. Some absorption systems and desiccant systems can operate at temperatures that are obtainable by available flat-plate solar collectors. The later systems have an advantage that the latent load can be controlled without the necessity to cool the moist air below its dew point, and consequently no reheat is needed and cooling requirements at partial loads may be reduced.

Desiccants are liquid or solid substances which have the property of extracting moisture brought into physical contact with them. The moisture transfer is driven by the vapor pressure difference between the water in the surrounding moist air and the water in the adsorbent.

Regardless of the type of the dehumidification agent used, the basic thermodynamic concept of desiccant air-conditioning systems is the same. Figure 1-1 illustrates such a concept on a psychrometric diagram and also shows the conventional air-conditioning cycle with reheat, for comparison. Air at state (A), which is a mixture of fresh outside air and recirculated room air, is dehumidified by contact with the reactivated desiccant. If no heat is added or removed, the dehumidification process will be adiabatic and the latent energy of the adsorbed water heats both desiccant and air. Line AB shows the decrease in moisture content and increase in temperature of air, resulting from the dehumidification process. Note that line AB will approach a constant enthalpy process if both heat of mixing and change in sensible heat of the desiccant are small. The warm and dry air, state (B), is then sensibly cooled to state (C), then evaporatively

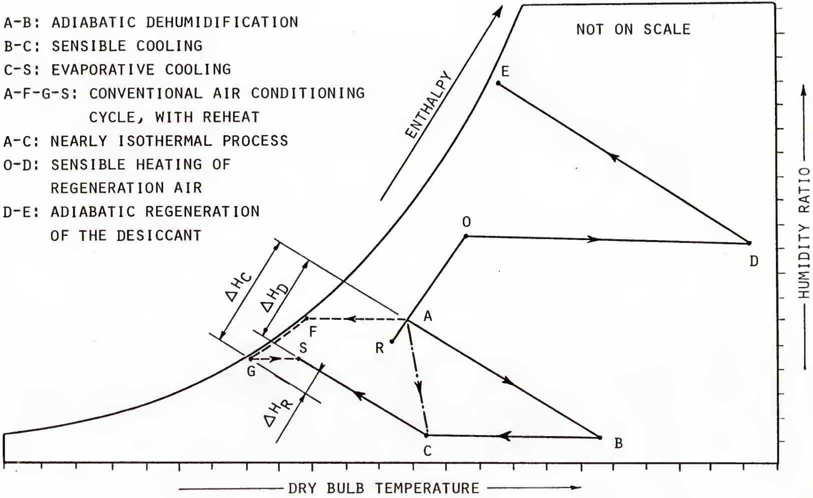
A-B: ADIABATIC DEHUMIDIFICATION
B-C: SENSIBLE COOLING
C-S: EVAPORATIVE COOLING
A-F-G-S: CONVENTIONAL AIR CONDITIONING CYCLE, WITH REHEAT
A-C: NEARLY ISOTHERMAL PROCESS
O-D: SENSIBLE HEATING OF REGENERATION AIR
D-E: ADIABATIC REGENERATION OF THE DESICCANT
NOT ON SCALE
ENTHALPY
E
O
D
A
F
R
S
G
C
B
ΔH_C
ΔH_D
ΔH_R
HUMIDITY RATIO
DRY BULB TEMPERATURE

Figure 1.1: Psychrometric Representation of Desiccant Air-Conditioning Concept.

cooled to the required supply temperature and humidity, state (S). Note that the sensible cooling of the dry air (process B-C) is now achieved at temperatures far above the wet bulb of outside air, and can be accomplished by rejecting heat to available well, lake, or cooling tower water. Meanwhile, the used desiccant, which is saturated with the adsorbed water, is preheated and reactivated by contact with heated outside air, as pictured by path O-D-E.

However, in a conventional air-conditioning system with reheat, as shown by the process A-F-G-S, moist air is cooled to a temperature below its dew point in order to achieve the desired degree of dehumidification, state (G), then heated to the required supply temperature, state (S).

The comparison of the air enthalpy changes, ΔH_D and $\Delta H_C + \Delta H_R$ resulting from the desiccant system and from the conventional cycle with reheat, respectively, demonstrates the advantage of handling the latent load with desiccants, in addition to their suitability to low grade energy sources for additional savings.

It is particularly worth noting that if, in a desiccant system, the dehumidification and sensible cooling of air (paths AB and BC, respectively) are carried out simultaneously, then their combined effects is a nearly isothermal process, which can be represented by path AC on Figure 1-1. Such process requires less concentrated desiccant because of the lower vapor pressure of water in the hydrated desiccant, resulting from the associated lower operating temperatures. Obvious consequences are the lower regenerating temperature requirements and the subsequent higher performance of the solar collectors. Similarly, if the regeneration process is conducted in a nonadiabatic manner, the desiccant solution can be kept hot throughout the operation, thus maintaining higher equilibrium water partial pressures for better mass transfer and hence more efficient reactivation.

As mentioned earlier, desiccants may be solid or liquid. Solid desiccants such as silica gel, activated alumina and hygroscopic salts are also called adsorbents. Although they have the advantage of high adsorption capacity that makes them more attractive for dehumidification purposes, their regeneration temperatures remain high for both efficient and nonexpensive use of solar and low grade geothermal energies. Besides, solid desiccant systems are associated with significant pressure drops taking place in the thick granular beds, and consequently need considerable electric power to circulate both process and regeneration air streams through. A further drawback of solid desiccants is the decline of their adsorption capacity in adiabatic processes, where higher temperatures are attained, and the difficulty to cool the beds during the dehumidification process.

Liquid desiccants on the other hand, also called absorbents, are hygroscopic solutions such as triethylene glycol, lithium chloride and lithium bromide. In spite of their lower desorption capacity as compared to their solid counterparts, they are gaining popularity in dehumidification and/or air-conditioning applications. This renewed interest in liquid desiccant systems stems from the inherent properties they have: a) generally lower regenerating temperatures than solid desiccants, b) lower pressure drop in the air-liquid contactors, c) continuity of the dehumidification-regeneration cycle, d) possibility of heat recovery between the used and regenerated desiccant solution, e) simplicity of controlling the process temperatures through the use of heat exchangers as packing, thus approaching isothermal processes, and f) the air-liquid contactors serve as air washers where bacteria and dust are trapped and then easily filtered out. The above qualities make liquid desiccants a more attractive and promising alternative, suitable for solar and low grade geothermal applications.

Since desiccant regeneration is generally accomplished with outside air, the performance of desiccant air-conditioning systems is then strongly dependent on weather conditions. Whereas a more difficult regeneration is expected in humid areas, still the gains from handling the associated higher latent loads with desiccants are important.

A solar powered liquid desiccant air-conditioning system is considered for use in hot and humid climates.

The proposed desiccant system makes use of the improved mass transfer properties, associated with non-adiabatic dehumidification and regeneration processes, to improve the system performance. The following tasks were performed to design the system and analyze its performance:

- Development of a theoretical model to analyze the complex simultaneous heat and mass transfer phenomena.
- Design of an efficient, yet economically competitive, solar powered liquid desiccant air-conditioner for use in hot and humid climates.
- Construction of prototype to experimentally check the validity and accuracy of the theoretical model.
- Optimization of the proposed liquid desiccant system using the theoretical model and economic criteria.

CHAPTER II
PROCESS DESCRIPTION AND RELATED PREVIOUS WORK

Desiccant dehumidification and/or air conditioning systems have been known for a long time; however, they recently gained special attention as a result of the continuous search for new alternative sources of energy, and for efficient application techniques. Both liquid and solid desiccant systems appear to be promising, yet not fully explored.

2.1. Solid Desiccant Systems

As a result of the high degree of dehumidification achieved by solid desiccants, open cycle solid desiccant air-conditioners have been the subject of intensive research. Different procedures have been used for the dehumidification and regeneration processes; namely single, dual, and multiple desiccant beds for intermittent systems, and rotary wheels for continuous adsorption-desorption operations. Dunkle [1, 2], Dunkle and Maclaine-Cross [3], Johnson [4] and Lunde [5, 6, 7, 8] have used desiccant wheels in conjunction with rotating recovery heat exchangers and evaporative coolers to produce dry and cool air. They used solar heated air for the regeneration of the water saturated desiccant. Several investigators [9-14] worked on theoretical models predicting the heat and mass transfer through desiccant beds; a detailed analysis of a silica-gel rotary bed dehumidifier is presented by Pla-Barby [14].

The mechanism of all solid desiccant dehumidification systems is based on a cyclic adsorption-reactivation process. Rotary beds have been, however, more attractive because of their continuous operation. Figure 2.1 shows a typical rotary bed with a recovery heat wheel. On one side, humid process air at state (1) is brought into contact with a reactivated desiccant structure where water vapor is absorbed. On the other side, the water-saturated desiccant is reactivated by solar heated regeneration air at state (6), where water vapor is desorbed. The rotating wheel motion keeps the absorption-desorption cycle continuous by making freshly reactivated desiccant portions always available for the dehumidification process. An air-to-air rotating heat wheel is incorporated in the system; it recovers heat from the dry process air at state (2), which was heated by the latent heat of dehumidification, and preheats the regeneration air to state (5). The warmand dry air at state (3) can then be sensibly and evaporatively cooled to the required supply conditions.

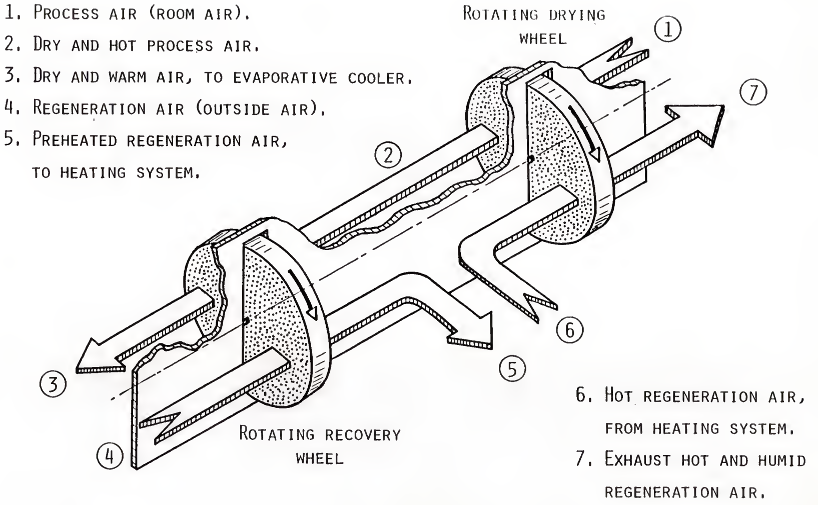
1. PROCESS AIR (ROOM AIR).
2. DRY AND HOT PROCESS AIR.
3. DRY AND WARM AIR, TO EVAPORATIVE COOLER.
4. REGENERATION AIR (OUTSIDE AIR).
5. PREHEATED REGENERATION AIR, TO HEATING SYSTEM.
ROTATING DRYING WHEEL
①
⑦
②
⑥
③
⑤
④
ROTATING RECOVERY WHEEL
6. HOT REGENERATION AIR, FROM HEATING SYSTEM.
7. EXHAUST HOT AND HUMID REGENERATION AIR.

Figure 2-1: Solid Desiccant Rotating Bed.

Several solid desiccants could be used for air dehumidification. Regeneration temperature and adsorption capacity within the working temperature range are important criteria in the selection of a desiccant. For comparison, Figure 2-2 shows the equilibrium absorption characteristics for molecular sieve and silica gel. Molecular-sieve has a better adsorption capacity at high temperatures, making it suitable for adiabatic processes where adsorption energy heats both desiccant and process air. Unfortunately, the regenerating temperature of molecular-sieve is high (300° F); if solar energy is to be used, expensive high performance collectors are necessary.

On the other hand, silica-gel can be reactivated with temperatures around 180° F, obtainable by commercial flat plate collectors. However, the silica-gel adsorption capacity drops rapidly as the bed temperature increases, and it is therefore required to remove the adsorption heat during the dehumidification and thus keep the desiccant at lower temperatures. This cooling of desiccant beds can result in either a dryer dehumidifier outlet condition which in turn increases the cooling capacity, or a lower regenerating temperature which consequently improves the solar collector performance.

Several methods were used to maintain lower solid desiccant temperatures during the dehumidification processes. Lunde [6] proposed the use of a series of desiccant beds with intercooling heat exchangers to cool the air. Robison [15] cooled the process air before it enters the drying wheel, using cooling coils and shallow well water. Barlow and Collier [16] suggested the use of nonhomogeneous or staged beds. By staging the desiccant bed, the range of thermodynamic states where the desiccant must operate is reduced. This permits the use of a more specialized desiccant for each section, thus keeping a high adsorption capacity throughout the bed thickness and the temperature range. Schultz et al. [17] and Jurinak and Beckham [18] used modified Dunkle cycles where the dehumidifier is cooled with evaporatively cooled air as illustrated in Figure 2-3. They claim that the gain in sensible cooling in the associated heat exchangers, combined with the lower dehumidification temperatures, more than offset the deficiency resulting from the higher moisture content in the dehumidifier inlet air stream. At the Illinois Institute of Technology (IIT), a cross cooled dehumidifier was introduced to keep the silica-gel cooler during the dehumidification process. It has since been under intensive theoretical and experimental investigations [19-22]. Cross cooling is achieved with cooling air flowing through rectangular channels, while the process air passes in perpendicular channels, lined with micron-size silica-gel.

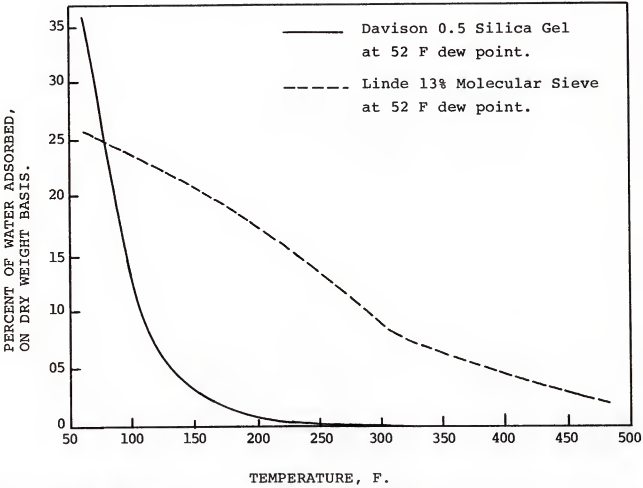

Figure 2-2: Absorption Capacity of Silica Gel and Molecular Sieve as Function of Temperature [16].

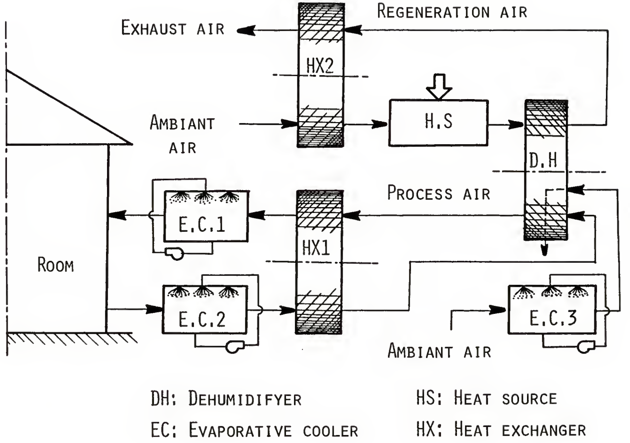

Figure 2-3: Schematic Diagram of Cooled Dunkle Cycle Air-Conditioning System.

2.2. Liquid Desiccant Systems

2.2.1. Process Description

While liquid desiccant systems have the same basic thermodynamic cycle as that of solids, the system design, temperature requirements, equipment and operation, as well as the possibilities of performance improvements, are quite different. A typical liquid desiccant system is shown in Figure 2-4. Its main components are the two liquid-to-air contactors called absorber and regenerator. At the absorber, where the process air to be dehumidified is brought into contact with a concentrated liquid desiccant, moisture is absorbed by the solution of lower water partial pressures. The latent heat resulting from the water vapor absorption as well as the associated heat of mixing are rejected to the cooling water. This permits keeping both the solution and the air stream at lower temperature for a more efficient dehumidification process, due to the consequent lower partial pressure of water in the desiccant solution. The dry and warm air is then sensibly and/or evaporatively cooled to the desired supply temperature and humidity. Meanwhile, the used dilute solution is pumped to the regenerator where either hot air or a heating coil is used. The higher temperature in the regenerator makes water vapor pressure in the desiccant solution higher than

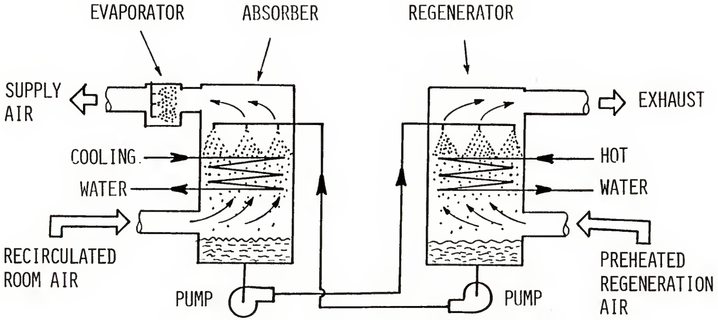

Figure 2-4: Schematic Diagram of a Basic Liquid Desiccant Air-Conditioning System.

that of the air stream, thus forcing water stripping from the desiccant. The resulting hot and humid air is vented outdoors, while the reactivated solution is pumped back to the absorber where it completes the continuous absorption-desorption cycle.

Liquid desiccant cooling-dehumidification systems have been commercially available. They have primarily been used to provide dehumidification, heat recovery and bacteria control. Their operating characteristics make them suitable for a wide range of installations, such as hospitals, laboratories and pharmaceutical and food processing plants, where high quality air is required.

The Niagara "Hygrol" system [23], illustrated by Figure 2-5, uses triethylene glycol as desiccant. In this system, the humidity is controlled by the continuous absorption-desorption cycle, while the sensible cooling is insured by an external source of refrigerated water. The "Hygrol" unit is similar to the basic cycle of Figure 2-4, with the addition of a recovery heat exchanger to respectively preheat and precool the dilute and concentrated solutions before they are sprayed. Mist eliminators, a reflux coil and a fiberglass reclaimer are also introduced to recover the evaporated triethylene glycol otherwise entrained by the air stream.

Two other commercial units are manufactured by Midland-Ross Corporation, the spray and twin cell [24, 25]. Both units use a bacteriostatic solution of lithium

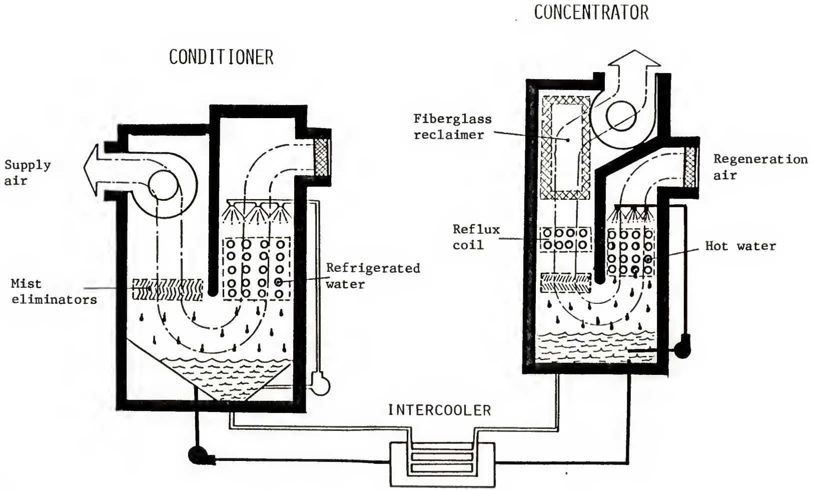

Figure 2-5: Niagara "Hygrol" Liquid Desiccant System (Niagara Blower Company) [23].

chloride and water, called Kathene. The spray cell as pictured in Figure 2-6 is essentially the same as the basic system mentioned earlier. It consists of a conditioner (absorber) and a regenerator, each having its own pumping unit. The air to be conditioned passes over the conditioner coil where it is efficiently contacted by the Kathene solution. The air passes on through an eliminator to the conditioned space, while the solution flows down to the pumping unit. The moisture content of the air stream leaving the conditioner is controlled by the concentration and temperature of the Kathene solution. In the regenerator, dilute solution is reconcentrated by contact with the relatively dry room air exhaust and the hot water coil.

The Kathabar twin-cell unit, however, as shown in Figure 2-7, is an air-to-air enthalpy recovery unit. It consists of two packed columns where the Kathene solution is sprayed and brought into contact with the air streams. The difference in energy content (latent and sensible) between the introduced fresh outside air and the exhausted conditioned air is the key to the twin cell energy recovery process. In summer, the dry and cool exhaust air regenerates and cools the Kathene solution, which in turn dehumidifies and precools the outdoor warm and humid air. In winter, however, the process is reversed; the dry and cold outside air is humidified and preheated during the desiccant regeneration, while the warm and humid exhaust

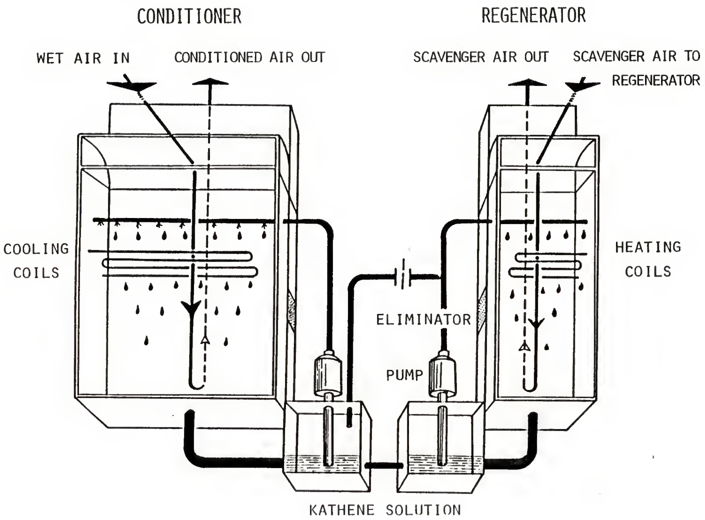

Figure 2-6: Kathabar "Spray Cel" Liquid Desiccant Unit (Midland-Ross Corporation) [24].

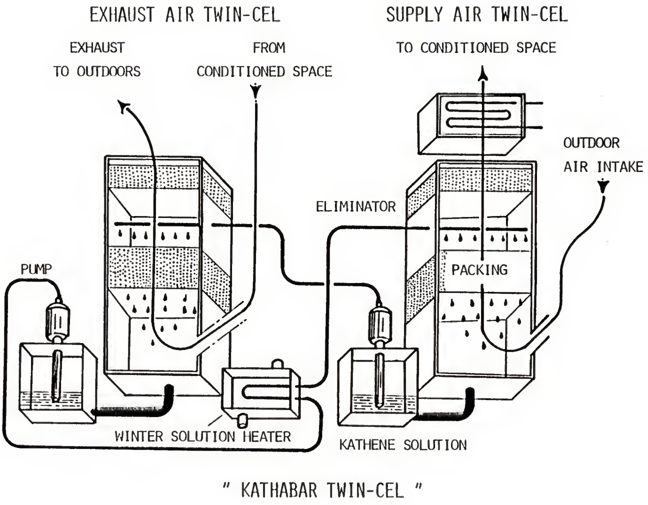

Figure 2-7: Kathabar "Twin-Cel" Liquid Desiccant Unit (Midland-Ross Corporation) [25].

air is both dried and cooled. The continuous circulation of the Kathene solution, between the two cells, insures a continuous moist and heat transfer between the supply and exhaust air streams, and eliminates microbiological and particulate cross contamination between them. Twin cells recover about 65 percent of the energy otherwise lost in the exhaust air; however, final heating or cooling is required to satisfy the desired supply conditions.

Liquid desiccant systems need a source of energy for the regeneration process. That energy serves to heat the regenerating air stream and/or the desiccant solution to force the water stripping. The range of regeneration temperature requirements makes such systems operational with low-grade thermal energy sources such as solar. Lof [26] was the first to suggest a solar powered liquid desiccant air-conditioning system. He tested a four-ton unit operating with triethylene glycol. Regeneration was accomplished with air heated in solar collectors to as low as 140° F (60° C). Lodwig et al. [27] described a solar-assisted liquid desiccant unit using a Niagara "Hygrol" conditioner. Flat-plate collectors provided water at 150° F (65.6° C) for the regeneration of the triethylene glycol solution employed. Robison [28, 29] also designed a solar desiccant air conditioner where energy is stored in the form of concentrated glycol at ambient temperatures. Because of the loss of some triethylene glycol through evaporation, he later redesigned the unit to operate with calcium chloride, and further modified the cycle for heat pump applications. Investigations of liquid desiccant systems have also been reported by Mullick and Gupta [30], Jahannsen [31, 32], Grossman and Shwarts [33], Olsen [34], Kapur [35] and others. Liquid sorbent cooling and dehumidification were found promising for solar applications, especially in humid climates [34, 35].

2.2.2. Liquid Desiccant--Moist Air Contactors

It is obvious that the key components of a liquid desiccant system are the liquid to air contactors. In order to maximize both heat and mass transfer, contactors must provide as large as possible surface area exposure between the solution and the air stream. This can be done by a spray chamber or a packed column for both absorber and regenerator. The packed bed column presents, however, some advantages over the spray chamber. It is more compact, allows a higher residence time, requires less pressure for the liquid distribution, and reduces the mist and droplet entrainment problem. It has, on the other hand, the disadvantage of larger pressure drops through the packing and therefore requires more parasitic power to circulate the air streams. Leboeuf and Lof [36] predicted the feasibility of a lithium chloride open cycle absorption system, where the regeneration is performed in a packed column air-liquid contactor with solar heated air.

Factor and Grossman [37] studied a packed column, in application to dehumidification and regeneration in a liquid desiccant system, utilizing an aqueous solution of lithium bromide. Their computer model, which was closely confirmed by an experimental analysis, concluded that contactor performances were strongly dependent on working temperatures. Cooler absorber and hotter regenerator respectively enhanced the dehumidification and reactivation processes. In the absorber, a solution inlet temperature less than 86° F (30° C) was required to make the drying possible. A regeneration solution temperature above 149° F (65° C) was also mandatory, with satisfactory reactivation accomplished at about 176° F (80° C). Larger desiccant flow rates helped reducing the temperature changes, and therefore maintaining larger desiccant-air water partial pressure differences throughout the contactor for a better mass transfer performance. The main conclusion from Factor and Grossman's work is identical to that deduced earlier for solid desiccants: for an efficient water transfer, the absorber should be kept as cool as possible, while the regenerator should be maintained hot throughout the reactivation process.

2.2.2.1. Absorbers

If no heat is removed or added at the absorber, the process is adiabatic and the latent heat of the absorbed water causes both air and desiccant temperatures to increase. The resulting hot and dry air needs to be sensibly cooled before the evaporative cooling process. It is apparent that a more efficient design would be to simultaneously carry out both dehumidification and sensible cooling, thus maintaining the absorber at the desired lower temperatures. Making use of this concept, Johannsen [32] proposed the isothermal dehumidification process by spraying the strong desiccant solution on the outside surface of a vertically positioned heat exchanger, with cooling water flowing inside the tubes. Such a design permits rejection of the latent heat of the absorbed water vapor, and thus keeps the absorber cool during the dehumidification process. In particular, the desiccant solution is cooler throughout the contactor packing and therefore has lower vapor pressure of water. This results in a larger mass transfer driving potential and lower desiccant concentration requirements. Obvious consequences are lower regenerating temperatures and subsequently better solar collector performances. Keeping the same concept in mind, Peng and Howell [38] employed a falling desiccant film flowing over a bank of water-cooled finned-tube heat exchangers as used in some commercial units. This configuration takes advantage of the heat and mass transfer capability of a thin falling film. Besides, the pressure drop associated with air passing over the falling film is much lower than that through the commonly used packed or bubble-tray columns.

The performance of liquid desiccant systems in general, and of absorbers in particular, is strongly dependent on the available cooling water temperatures. In Johannsen's system, water was cooled in a cooling tower. Robison [28], on the other hand, overcame this problem by using the abundant cool well water from the South Carolina costal area. Turner [39] suggested, however, a solar-powered liquid desiccant conditioner in which the cooling water was internally generated. His system, as illustrated in Figure 2-8 is based on the concept of using a portion of the already processed cool and dry air to evaporatively chill the water for sensible cooling purposes. Briefly, it operates by bringing a mixture of ambient air and recirculated air in contact with a liquid desiccant in a water-cooled absorber. A portion of the dried and cooled air is then diverted through a packed column, called evaporator, where recycled cooling water is evaporatively cooled. The chilled water is then looped through the absorber to cool both the desiccant and the air stream. The used desiccant is regenerated by solar or geothermal heating to about 140° F (60° C), while the remaining

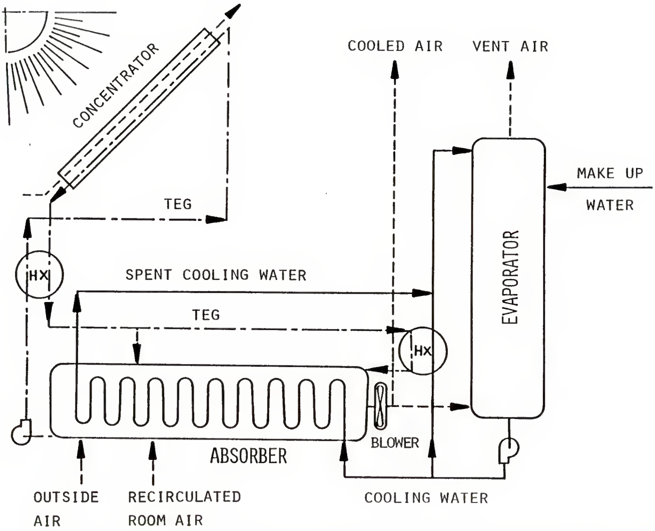

Figure 2-8: Schematic Diagram of Turner's Liquid Desiccant Air Conditioner [38].

processed air is supplied to the conditioned space. It is obvious that the overall thermal performance of this liquid desiccant system, which is self-sufficient cooling-water, is not encouraging, since the unit has to provide cooling for both the chilled water and supply air. Besides, the blower power will be increased because of the larger pressure drop associated with the required larger contact surface in the absorber and the additional evaporator. However, the lower absorber temperature makes the dehumidification process more efficient and makes the system suitable for regions where no cool well-water is economically available.

Peng and Howell [38] slightly modified Turner's system in an attempt to improve its thermal performance. Instead of processed dry and cool air, they utilized exhaust room air to evaporatively cool the water, while all of the processed air is fed to the conditioned space. This modification makes the system thermally more efficient for situations where ventilation is a must and energy can be recovered from the dry and cool exhausted room air, but not for residential application where infiltration is generally sufficient to supply the desired amount of fresh ambient air.

2.2.2.2. Regenerators

Desiccant regeneration is considered as the most important part of a solar powered liquid desiccant system.

It needs to be as efficient as possible to reduce the number of required solar collectors and therefore minimize the total cost. Furthermore, the amount of water desorbed in the regenerator is a direct indication of the moisture that can be stripped out of the air during the dehumidification process. As a result, several theoretical and experimental investigations have been conducted on regenerators only, and different designs have been considered in the search for an efficient and inexpensive regeneration method. Hollands [40] studied the reactivation of lithium chloride brines in a roof-type solar still, in a manner similar to the conventional saline water desalinization with solar energy. He predicted the regeneration performance using the models developed by Dunkle [41] and Lof et al. [42] for solar water distillation.

Kakabaev et al. [43, 44] proposed the use of solar collector-regenerators and investigated the open, as well as the glass covered, collectors with air ventilation as illustrated by Figure 2-9. This regeneration technique consists of a tilted black surface on which the dilute desiccant solution flows down as a falling film in contact with ambient air. The solar radiation is absorbed by the black surface, which in turn heats the thin film and forces the water absorption from the solution to ambient air. The water vapor is then rejected to the environment by wind action, convection and thermosiphon forces, or by forced

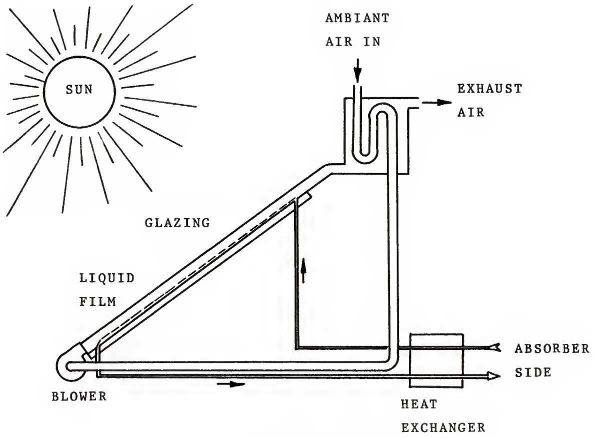

Figure 2-9: Liquid Desiccant Collector-Regenerator.

air circulation. To insure an even liquid film distribution, the inclined surface could be corrugated, v-grooved or textured. Further investigation of such regenerators were conducted by Gandhidasan et al. [45, 46, 47], who studied the regeneration of calcium chloride with laminar forced cocurrent and countercurrent air circulation including buoyancy forces, and by Mullick and Gupta [48], who considered the free convection case for the regeneration of lithium bromide solutions.

Another type of regenerator is the regeneration chamber similar to the absorption column discussed earlier. It can be either a packed bed, with air and/or desiccant preheated before entering the contactor, or a stack of finned tube heat exchanges, with heating water flowing through the tubes.

Peng and Howell [49] compared most of the preceding types of regenerators through detailed computer models. They concluded that although open regenerators are the simplest and least expensive, they present the following drawbacks: a) rain and dust contamination problems, b) their performance is strongly dependent on weather conditions, namely wind speed, temperatures and humidity contents, and c) they are neither efficient nor practical for hot and humid climates. On the other hand, glass-covered collector-regenerators with forced ventilation give a solution to those drawbacks. In addition they improve the performance through the higher mass transfer coefficient resulting from the continuous forced air motion and the lower regenerator heat losses. The finned tube regeneration chamber was, however, found to be the most practical choice because of its good performance even in humid climates, compactness in size, flexibility for multipurpose solar applications, and suitability for other energy sources for back up.

In view of the considerations discussed in this chapter, liquid desiccants appear more attractive than their solid counterparts. However, in order to insure a high system performance, nearly isothermal processes must take place during air dehumidification and desiccant reactivation. For this purpose and because of the advantages mentioned earlier, finned-tube heat exchangers, which provide additional contact surface between the liquid desiccant and air, will be used in this work as packing for both the regenerator and the absorber.

CHAPTER III
THEORETICAL BACKGROUND AND DEVELOPMENT OF A SIMPLIFIED MODEL

3.1. Phase Equilibrium

Every system or state evolves towards equilibrium by transfer of momentum, energy and mass. In particular, if a system consists of coexisting phases, there will be momentum, heat, and mass transfer within and between the phases. The thermodynamic equilibrium is achieved when temperatures, pressures, and component chemical potentials are uniform throughout all the adjacent phases. The degree of freedom, f, of a multiphase system in equilibrium is controlled by the well-known phase rule:

$$f = C - P + 2 \tag{3-1}$$

where P denotes the number of phases, and C is the number of components minus the number of chemical equilibria equations.

For instance, consider the case of a two-phase system consisting of moist air in contact with an aqueous liquid desiccant solution, which is the subject of this work. The amount of air absorbed is very small compared to the amount of water absorbed; and, consequently, air may be considered as insoluble in the adjacent liquid phase. In addition, moisture transfer takes place without chemical reactions; therefore, this system has three degrees of freedom ($f = 3 - 2 + 2 = 3$).

If three intrinsic properties such as temperature, concentration, and total pressure are specified, then all other equilibrium properties are fixed, in particular the solute (water in this case) partial pressure, P_A. If both of the gas components are assumed to obey the perfect gas equation of state, then with the help of Raoult's Law, the equilibrium gas mass ratio, or the humidity ratio for the air-moisture mixture is written as

$$Y' = 0.62198 \frac{P_A}{P_t - P_A} \tag{3-2}$$

where Y' is in pounds moisture per pound dry air, and P_t is the total pressure. This relation will be used throughout this study to compute the interface equilibrium mass ratio from the available water partial pressure and the equilibrium data of aqueous desiccants solutions as a function of temperature and concentration.

3.2. Interphase Mass Transfer Coefficients

The mass transfer of a solute within a fluid is driven by molecular and/or eddy diffusion. The mechanism of molecular diffusion takes place in stagnant fluids or in fluids moving in a laminar flow. It is the result of the random motion of molecules by virtue of their thermal energy. If there are concentration gradients and there are no constraints to the flow of mass, molecules will diffuse from the high concentration zones to the lower ones until a uniform composition is attained throughout the system. The mechanism of eddy diffusion, also called turbulent diffusion, is, however, the result of the mechanical agitation associated with the random motion of eddies in turbulent flows. Although molecular diffusion occurs within its boundaries, each eddy carries with it a large amount of solute. The rapid motion of these eddies makes mass transfer in turbulent flow much greater than that resulting from molecular diffusion.

The process of molecular diffusion is predictable, particularly for gases which can be described in terms of kinetic theory. However, for turbulent flows, it is still impossible to compute mass transfer coefficients because of the nonforeseeable eddies motion, and advantage should be taken of the similarities to certain already solved heat transfer problems.

Even though the use of molecular and eddy diffusions is straight forward in the explanation of mass transfer phenomenon within individual fluids, the problem becomes more complex when mass is transported between adjacent phases at nonequilibrium bulk conditions, gas and liquid for instance. Several theories have been proposed to interpret the behavior of the interphase mass transfer coefficients [50]. The oldest and of most obvious meaning is the two resistance (or two film) theory. In this theory, it is assumed that there is no resistance to the mass transfer at the interface separating the phases. As a consequence, the interface concentrations of both phases correspond to the local equilibrium chemical potential at the local temperature and pressure, and the only diffusional resistances are those residing in the fluids themselves. If the molar fraction differences are considered as the driving force for the mass transfer, then the steady state molar flux may be expressed in terms of the gas and liquid individual mass transfer coefficients k_x and k_y, by

$$\text{Gas} \qquad N_A = k_y (y_A - y_{Ai}) \tag{3-3}$$

$$\text{Liquid} \qquad N_A = -k_x (x_A - x_{Ai}) \tag{3-4}$$

where k_y and k_x are based on mole fractions, y_A and x_A are the bulk mole fractions of solute A in the gas and liquid phase, respectively, and subscript i refers to the interface equilibrium conditions.

Unfortunately, it is practically impossible to measure the interface concentrations; therefore, it is more convenient to determine the overall transfer effect in terms of overall mass transfer coefficients K_y and K_x, and the bulk concentrations. The transfer equations then become

$$N_A = K_y \, (y_A - y_A^*) \tag{3-5}$$

$$N_A = -K_x \, (x_A - x_A^*) \tag{3-6}$$

where y_A^* represents the mole fraction the gas would have if it was in equilibrium with a solution of composition x_A, and conversely x_A^* refers to the mole fraction the solution would have if it was in equilibrium with a gas of concentration y_A.

If the mass transfer rate and the change of liquid concentration are small, as they usually are, the equilibrium distribution $y_A = f(x_A)$ can be assumed linear within a small working concentration range. Hence, the gas and liquid equilibrium compositions can be related by

$$y_A = m\, x_A^* + n \qquad (3\text{-}7a)$$

$$y_{Ai} = m\, x_{Ai} + n \qquad (3\text{-}7b)$$

$$y_A^* = m\, x_A + n \qquad (3\text{-}7c)$$

where m and n are the linearity constants. Note that the slope m is a direct indication of the solubility of the gas in the liquid, and that when $n = 0$, equations (3-7a, b and c) reduce to Henry's Law which is valid only for dilute solutions.

The combination of the flux equations and the equilibrium relations (3-3) through (3-7) permits the deduction of the relationships between the individual and overall mass transfer coefficients:

$$\frac{1}{K_y} = \frac{1}{k_y} + \frac{m}{k_x} \qquad (3\text{-}8)$$

$$\frac{1}{K_x} = \frac{1}{k_x} + \frac{1}{mk_y} \qquad (3\text{-}9)$$

which show that the overall diffusion resistances depend on the solubility of the solute in the liquid. In the case of a highly soluble gas, the slope m is very small, so that the term m/k_x is negligible, and the mass transfer is said to be gas phase controlled. Ultimately, equation (3-8) becomes:

$$\frac{1}{K_y} = \frac{1}{k_y} \qquad (3\text{-}10)$$

which is equivalent to

$$y_A^* = y_{Ai} \qquad (3\text{-}11)$$

Conversely, for insoluble gases, m is very large and the major transfer resistance resides in the liquid phase. Such a system is called liquid phase controlled and Equation (3-9) reduces to

$$\frac{1}{K_x} = \frac{1}{k_x} \qquad (3\text{-}12)$$

which is equivalent to

$$x_A^* = x_{Ai} \qquad (3\text{-}13)$$

Similar individual and overall transfer coefficients may be easily derived if other concentration definitions are used. In air conditioning applications, for example, it is generally more convenient to use the mass ratio (or humidity ratio) rather than the molar fraction y_A. For future reference, relationships between certain mass transfer coefficients need to be determined. In the gas phase, the diffusion of a solute A through a non-diffusing solvent B can be expressed by either of the following versions of equations (3-3) through (3-6), as convenient

$$M_A\ N_A = k_C\ (C_A - C_{Ai}) = K_C\ (C_A - C_{Ai}^*) \qquad (3\text{-}14)$$

$$M_A\ N_A = k_Y'\ (Y_A' - Y_{Ai}') = K_Y'\ (Y_A' - Y_{Ai}'^*) \qquad (3\text{-}15)$$

where k_C and k_Y' are the individual mass transfer coefficients based on the mass concentration C and the mass ratio Y', respectively, K_C and K_Y' are the corresponding overall mass transfer coefficients, and M_A is the molecular mass of solute A. If, in addition, small transfer rates and dilute solutions are assumed, then the different transfer coefficients are simply inter-related by

$$k_Y' = M_B\ k_y = \rho_B\ k_C \qquad (3\text{-}16)$$

$$K_Y' = M_B\ K_y = \rho_B\ K_C \qquad (3\text{-}17)$$

where M_B and ρ_B denote the molecular mass and the mass density of the solvent B, respectively.

Owing to the small range of working concentrations and the high solubility of water vapor into liquid desiccants, overall mass transfer coefficients will be used in this work in conjunction with the gas-phase controlled mass-transfer relationships.

3.3 Heat Mass and Momentum Transfer Analogies

In air conditioning problems, as well as in several other engineering applications, one often has to deal with simultaneous transfer of heat, mass and momentum. It is well known that these transport phenomena are inter-related; therefore, an analysis would help in understanding the complexity of the problem, and in providing necessary relationships and information for design purposes.

Consider the common case as used in liquid desiccant systems, where a liquid and a gas phase are brought into contact in a counterflow configuration, to insure an efficient heat and mass transfer operation. The gas is blown upwards, while the liquid drains down by gravitation in the form of a thin falling film as illustrated by Figure 3-1.

The momentum, heat, and mass transfer are governed by the Navier-Stokes, the energy, and the continuity equations, respectively. The simultaneous solution of such a system of differential equations is complex, and becomes possible only when appropriate simplifying assumptions are made. For present purposes, assume the following:

1. Steady state conditions.
2. Incompressible flow.
3. No chemical reaction.

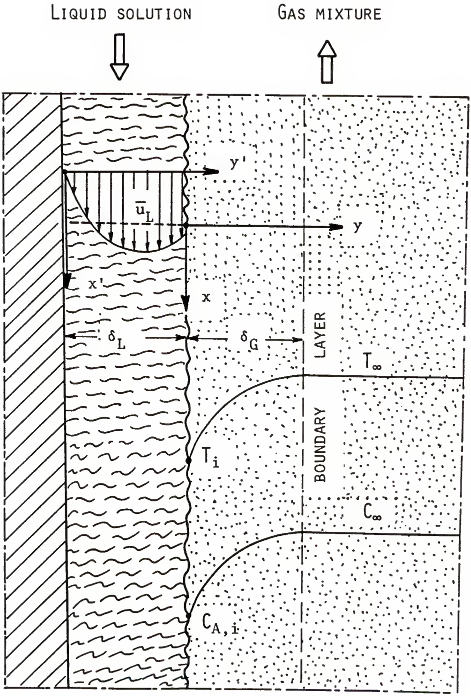

Figure 3-1: Liquid Falling Film in Counterflow with Rising Gas.

4. Constant physical properties.
5. Negligible viscous energy dissipation.
6. Zero pressure gradient.

With these assumptions, the laminar two-dimensional gas boundary layer equations can be deduced:

Momentum:

$$u\frac{\partial u}{\partial x} + v\frac{\partial u}{\partial y} = \nu\frac{\partial^2 u}{\partial y^2} \tag{3-18}$$

Continuity of component A:

$$u\frac{\partial C_A}{\partial x} + v\frac{\partial C_A}{\partial y} = D\frac{\partial^2 C_A}{\partial y^2} \tag{3-19}$$

Energy:

$$u\frac{\partial T}{\partial x} + v\frac{\partial T}{\partial y} = \alpha\frac{\partial^2 T}{\partial y^2} \tag{3-20}$$

Boundary conditions:

at $y = 0$

$$u = 0 \qquad v = v_i \qquad T = T_i \qquad C_A = C_{A,i} \tag{3-21a}$$

at $y = \delta_G$

$$u = u_\infty \qquad v = 0 \qquad T = T_\infty \qquad C_A = C_{A,\infty} \tag{3-21}$$

where C_A is again the mass concentration of solute A, T is temperature, u and v are the velocities in the x and y directions, α, D and ν are the thermal, mass and momentum diffusivities, and the subscripts i and ∞ refer to conditions at the interface and outside the boundary layers, respectively. Notice that the coordinates considered for these equations are the local cartesian coordinates at the gas-liquid interface, and moving at the average bulk velocity of the liquid film.

This system of differential equations shows that there is a certain similarity between the heat, the mass and the momentum transfer. In fact, if the diffusivities α, D and ν are equal and the interface velocity v_i is zero, then the solutions of all three transfer equations aquire identical algebraic forms, and the velocity, concentration and temperature distributions are similar and lead to the same boundary layer thicknesses. The transport phenomena similarities are detailed by Kays and Crawford [51], but for the purpose of this study, only heat and mass transfer analogies are further discussed. The energy and mass balances, performed on the gas-liquid interface (y= 0) can respectively be given by

$$h\ (T_\infty - T_i) = -k\ \left(\frac{\partial T}{\partial y}\right)_{y=0} \tag{3-22}$$

$$k\ (C_{A\infty} - C_{Ai}) = -D\ \left(\frac{\partial C_A}{\partial y}\right)_{y=0} \tag{3-23}$$

where h and k_C are the gas side convective heat and mass transfer coefficients, respectively, and k is the gas thermal conductivity. When the variables are normalized using the following dimensionless temperature, length and concentration:

$$T' = \frac{T - T_i}{T_\infty - T_i} \tag{3-24}$$

$$y' = \frac{y}{L} \tag{3-25}$$

$$C_A' = \frac{C_A - C_{A,i}}{C_{A,\infty} - C_{A,i}} \tag{3-26}$$

where L is an arbitrary reference length. The heat and mass fluxes of Equations (3-22) and (3-23) can then be rearranged to give

$$Nu = \frac{h\ L}{k} = \left(\frac{\partial T'}{\partial y}\right)_{y=0} \tag{3-27}$$

$$Sh = \frac{k_C\ L}{D} = \left(\frac{\partial C_A'}{\partial y}\right)_{y=0} \tag{3-28}$$

where Nu denotes the Nusselt number, a dimensionless heat transfer coefficient, while Sh is the Sherwood number, a dimensionless mass transfer coefficient.

Theoretical and experimental investigations [52] showed that the Nusselt and Sherwood numbers assume the same functional relation and are given by

$$Nu = C_1\ Re^a\ Pr^b \tag{3-29}$$

$$Sh = C_1\ Re^a\ Sc^b \tag{3-30}$$

where Re, Pr, Sc are the Reynold, the Prandtl and the Schmidt numbers, respectively, and are defined by

$$Re = \frac{U\ L}{\nu} \tag{3-31}$$

$$Pr = \frac{\nu}{\alpha} \tag{3-32}$$

$$Sc = \frac{\nu}{D} \tag{3-33}$$

and U is the mean velocity. Several analogies have been proposed. Chilton and Colburn [53] presented one of the most widely accepted similarities, called the J factor analogy, which takes into consideration the Prantl number effects

$$J = J_m = \frac{f}{2} \tag{3-34}$$

where

$$J = \frac{h}{\rho\ Cp\ U}\ Pr^{2/3} \tag{3-34a}$$

$$J_m = \frac{k_c}{U}\ Sc^{2/3} \tag{3-34b}$$

The combination of Equations (3-34) through (3-34b) lead to

$$\frac{h}{\rho\ Cp\ k_C} = \left(\frac{Sc}{Pr}\right)^{2/3} = Le^{2/3} \tag{3-35}$$

where Le is the Lewis number, f denotes the friction factor, ρ is the mass density, and C_p refers to the specific heat. Note that $\rho\ k_C = k_y'$ as defined earlier.

Equation (3-35) is of great importance. If the Lewis number is known, it permits the computation of the mass transfer coefficient from the available heat transfer data. For the transfer of water vapor, the Lewis number was found to be close to one [54]. Notice that under the conditions $Pr = Sc = Le = 1$, the j factor analogy reduces to the well-known Reynolds analogy, which first related the momentum and heat transfer, and was later extended to include the mass transfer

$$\frac{k_C}{U} = \frac{h}{\rho\ Cp\ U} = \frac{f}{2} \tag{3-36}$$

It is also particularly noteworthy that the same analogies, developed for laminar flow, can be recovered for turbulent flow where the better heat and mass transfer characteristics are desired.

3.4. Falling Film Analysis and Non-Entrainment Conditions

Up to this point, only the gas side heat and mass transfer boundary layers are considered; nevertheless, it is important to understand hydrodynamic (momentum) interactions between the gas and liquid phases in the counterflow configuration. The pressure drops, as well as the velocity distributions, are influenced by both fluid flow rates and the geometry of the packing. At a fixed gas velocity, larger liquid rates reduce the free cross section available for the flow of gas, thus resulting in higher gas pressure drops. On the other hand, as the gas rate is increased, the shear action on the falling film increases, causing liquid entrainment that could lead to flooding. In consequence, it is essential to recognize such flooding conditions and to avoid them in the design of a system. Investigations and data on flooding conditions in random packings are reported by Treybal [50], but for the purpose of this work, where finned tube heat exchangers are used for packing, it is more convenient to consider the falling film approach.

Refer again to Figure 3-1. Since the liquid film moves at a low velocity, due only to gravitation, and because the film is thin with a negligible temperature gradient, bouyancy forces can be omitted and the liquid-film flow can be considered as laminar. If, for convenience, a new system of coordinates (x', y',z') is attached to the still wall, then the Navier-Stokes equations, describing the laminar flow in the liquid film with gravity as a body force, can be reduced to

$$\nu \frac{\partial^2 u}{\partial y'^2} + g = 0 \qquad (3\text{-}37)$$

with the boundary conditions

$$u = 0 \text{ at } y' = 0 \text{ (No slip condition)}$$

$$\frac{\partial u}{\partial y'} = -\frac{\tau}{\rho\ \nu} \text{ at } y' = \delta_L \text{ (Interfacial shear stress for Newtonian fluids)} \qquad (3\text{-}38)$$

The solution of Equation (3-37), satisfying the specified boundary conditions, gives the velocity distribution as

$$u = \frac{g}{\nu}\left(\delta_L\ y' - \frac{y'^2}{2}\right) - \frac{\tau y'}{\nu\rho} \qquad (3\text{-}39)$$

which, by integration over the film thickness, makes it possible to find the average velocity

$$\bar{U}_L = \frac{g}{3\nu}\ \delta_L^2 - \frac{\tau\ \delta_L}{2\ \nu\ \rho} \qquad (3\text{-}40)$$

and the volumetric flow rate per unit width

$$Q'_L = \frac{g}{3\nu}\ \delta_L^{\ 3} - \frac{\tau\ \delta_L^{\ 2}}{2\ \nu\ \rho} \qquad (3\text{-}41)$$

This relation can be solved to give the film thickness δ_L if the flow rate Q_L' and the shear stress τ are specified. In addition, it confirms that if τ is negative, which corresponds to a cocurrent flow, Q_L' is always positive, meaning that no flooding occurs. Furthermore, it shows that in a counter-flow configuration, flooding ($Q_L' \leq 0$) will take place if the shear stress

$$\tau \geq 2/3 \ \rho \ g \ \delta_L \qquad (3\text{-}42)$$

It is well known that the shear stress increases with larger gas velocities. At the same time, entrainment of the falling liquid by the ascendant gas increases, causing thicker liquid film, which in turn restricts the gas flow. Figures 3-2a,b and c show this phenomenon for three different gas flow rates and their corresponding, assumed laminar, velocity profiles. Notice that Figure 3-2a represents the case where no entrainment is taking place, while Figure 3-2b illustrates the beginning of entrainment, and finally Figure 3-2c pictures the start of flooding ($U_L = Q_L = 0$) and is an unstable limit condition.

It is unfortunate that Equation (3-42) can not be used explicitly because of mutual dependence between τ and δ_L. Besides, flooding is only a theoretical hydrodynamic limit and an efficient system should not operate under conditions close to it. In practical situations, however, economical considerations are generally needed to optimize the

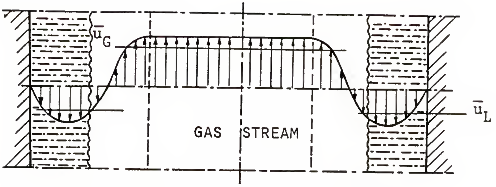

a. Low air velocity, no liquid entrainment.

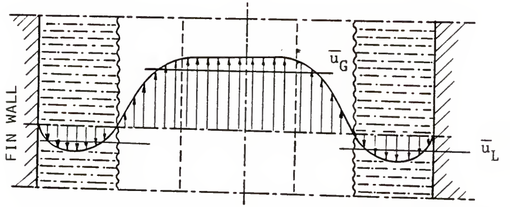

b. Medium air velocity, start of liquid entrainment.

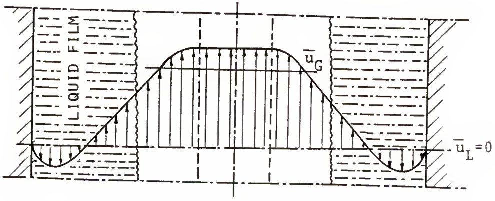

c. High air velocity, flooding conditions.

Figure 3-2: Entrainement in a Falling Film.

performance of any process. In this particular case, for instance, if a system is designed to work under conditions close to those of flooding, the liquid mean velocity $\bar{u}_L$ (or the flow rate Q_L') is reduced, hence requiring larger contactors and subsequently higher auxiliary fan power to insure the desired heat and mass transfer. Due to the associated lower heat and mass transfer characteristics, similar requirements will also result if smaller gas velocities are used. As a consequence, in lieu of the theoretical flooding limit, which should not in any case be reached, and is too complex to be put into a convenient form, it is more practical to introduce a more restrictive but realistic criterion for design purposes. The simplest and most reasonable criterion is the non-entrainment limit, which is illustrated in Figure 3-2b and corresponds to $u = 0$ at $y' = \delta_L$.

When the non-entrainment condition is applied in Equation (3-39) a maximum allowable design film thickness is deduced

$$\delta_{L,max} = \frac{2\tau}{g\rho} \qquad (3\text{-}43)$$

which, when substituted for δ_L into Equation (3-41) gives

$$Q_L' = \frac{2}{3} \frac{\tau_{max}^{3}}{\nu\, g^{2}\, \rho^{3}} \qquad (3\text{-}44)$$

or

$$\tau_{max} = (\frac{3}{2} Q_L' \nu g^2 \rho^3)^{1/3} \qquad (3\text{-}45)$$

where τ is replaced by τ_{max} to refer to the maximum allowable design condition.

If the correlation between the shear stress τ and the gas velocity is known, then Equation (3-45) can be solved for the non-entrainment gas velocity limit for a specified liquid flow rate.

As long as the liquid mean velocity is much smaller than that of the gas, which is the case in the falling film, the interface shear stress can be easily related to the bulk gas velocity. If the liquid film is assumed to be still, then the problem is reduced to the flow of a gas through a rectangular conduit. As a consequence of those assumptions, the Moody charts or their associated relations can be used in conjunction with the hydraulic radius concept. Furthermore, if the interface gas liquid surface is assumed smooth, then the friction coefficient can be related to the Reynold number by Blasius' empirical relation, and the wall shear stress for a turbulent flow in a conduit can be expressed [55] by

$$\tau = 0.03325 \rho \overline{U}^{7/4} (\frac{\nu}{R_h})^{1/4} \qquad (3\text{-}46)$$

where R_h is the hydraulic radius defined as

$$R_h = \frac{A}{P} \tag{3-47}$$

and U is the mean velocity, A denotes the cross section, while P refers to the wetted perimeter. In the case of a thin duct, of thickness 2t, much smaller than the width w, the hydraulic radius can be approximated by

$$R_h = \frac{\omega\ t}{(w + 2t)} \cong t \tag{3-48}$$

By combining Equations (3-45), (3-46) and (3-48), it is possible to determine the maximum gas velocity, before entrainment takes place in a thin conduit, from

$$\overline{U}_{G,max} = \left(34.4275\ (Q_L'\ \nu_L\ g^2)^{1/3}\ \left(\frac{\rho_L}{\rho_G}\right)\ \left(\frac{\nu_g}{t}\right)^{1/4}\right)^{4/7} \tag{3-49}$$

where subscripts G and L are added to distinguish between the gas and liquid properties, respectively. This relation will be used later, during the design of the analysis and design of the desiccant system, to check for non-entrainment once the flow rates and dimensions are chosen.

3.5. Non-Adiabatic Packed Tower Analysis

3.5.1. Generalized Differential Analysis

Since the ultimate objective of this work is the analysis of moisture transfer between moist air and liquid desiccants, the following theoretical development will only deal with the case of mass transfer of a solute A between two non-transferrable solvents, a liquid and a gas. The analysis will be general and could be used for both absorption and regeneration (desorption or stripping) processes. The direction of the mass transfer, corresponding to either of the two processes, is mainly controlled by the local temperatures, which subsequently monitor the equilibrium concentrations and hence the rate and orientation of mass transfer.

Consider the column, packed with a stack of horizontal finned-tube heat exchangers, as shown in Figure 3-3. A gas mixture, of a solvent mass flow rate $\dot{G}_s$, a solute to solvent mass ratio Y_1', and at a temperature T_{G1}, is blown upwards through the contactor. At the same time, a liquid solution, of a solvent mass flow rate $\dot{L}_s$ and a mass ratio X_2', enters at the top at a temperature $T_{L,in}$. The solution is sprayed on the outer surface of the heat exchangers, and trickles down in the form of a thin falling film, coutercurrent to the rising gas. To control the temperature inside the tower, process water at a temperature T_{W2} and a flow rate $\dot{M}_W$ is simultaneously pumped

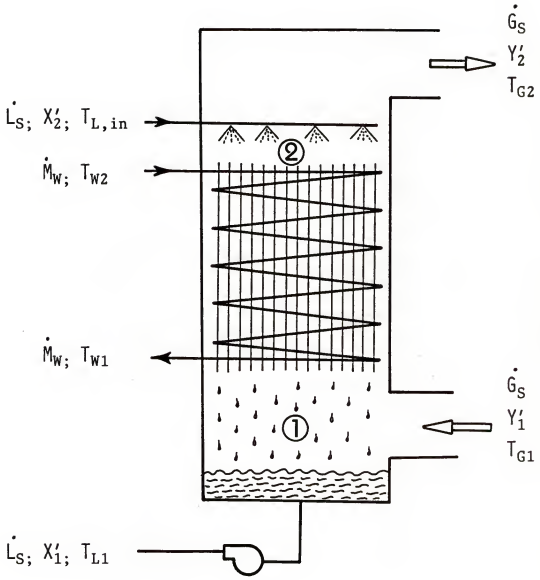

Figure 3-3: Non-Adiabatic Packed Tower.

through the finned tubes to exchange thermal energy with both gas and liquid phases. At any section of the contactor, boundary layers are developed, and simultaneous heat and mass transfers take place. As a result, the gas leaves at a mass ratio Y_2' and temperature T_{G2}, while the liquid drains to the bottom of the contactor at a composition Y_1' and a temperature T_{L1}, and the process water flows out at a temperature T_{w1}.

Note that for the case of liquid desiccant air conditioning systems, the solute corresponds to the moisture while the liquid and gas solvents represent the desiccant and air, respectively.

Before getting involved in lengthy derivations to model this complex non-adiabatic simultaneous heat and mass transfer, it is beneficial, at this point, to make the following appropriate assumptions that will help in simplifying the problem:

1. In practice, most systems are designed to operate in a continuous manner with constant flow rates. Therefore, a steady state is assumed.
2. Although process water circulation through the tubes can be achieved in many different ways, the circuiting is usually such that counterflow will be approached; besides, if the tower is tall a large number of tube rows is required.

Therefore, the process water can be considered flowing in a pure counterflow manner to the gas phase, and cocurrent to the falling film.

3. Along with assumption 2, the wall effects that might influence the gas and liquid flow patterns as well as temperature and concentration distributions are ignored. Hence, all variables are uniform at any cross section of the contactor.
4. All heat and mass transfer takes place in the part of the column packed with finned tube coils. Furthermore, there is neither heat transfer with the surroundings through the outside walls, nor axial thermal or mass diffusion between adjacent cross sections.
5. At the liquid/gas interface, the gas mixture is in equilibrium with the liquid solution at the local temperature and concentration.
6. Because the changes in temperatures and concentrations are moderate in actual working systems, heat and mass transfer coefficients as well as all thermophysical properties are considered constant throughout the contactor and average values are used.

7. The thermal resistances in the liquid film, fins, and tube walls are negligible when compared to the gas side and process water side. Thus, the local temperature is uniform throughout the liquid film and wall thicknesses. Also, the heat transfer between the gas stream and the falling solution as well as the packing is gas phase controlled.
8. Owing to the relatively small working range of concentrations, the equilibrium curves could be considered linear, and subsequently the overall mass transfer coefficients may be used. Furthermore, since the water vapor is highly soluble in liquid desiccants, the mass transfer will be assumed as gas phase controlled ($K_y = k_y$).

Other assumptions will be introduced as needed during the rest of the analysis. Assumptions 2, 3, and 4 permit the analysis of the simultaneous heat and mass transfer rates on a differential volume of cross-section A_c and height dz. Figure 3-4 illustrates the differential element with all rates expressed in differential form. It shows the liquid, gas and process water flowing in their respective directions, separated by the tube wall and the gas-liquid interface. It also displays the temperatures and mass ratio profiles for an absorption case, along with their corresponding boundary layers. The superscript prime

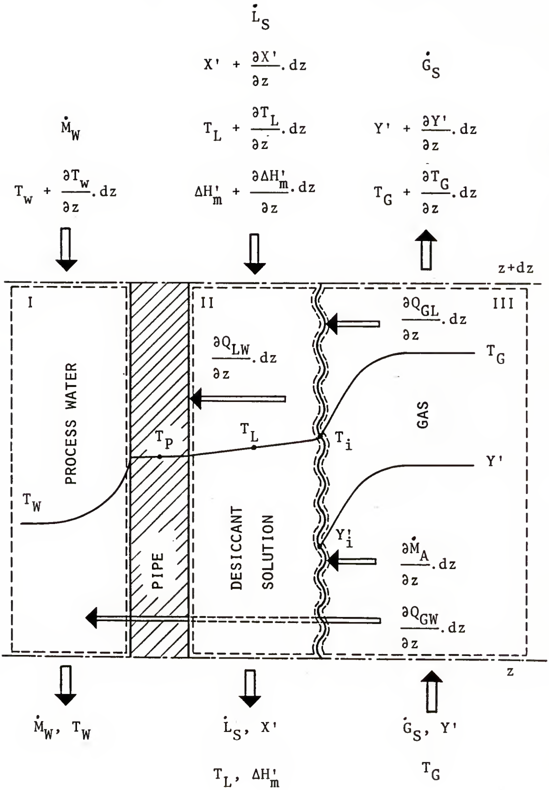
$\dot{L}_S$
$X' + \frac{\partial X'}{\partial z}.dz$
$\dot{G}_S$
$\dot{M}_W$
$T_L + \frac{\partial T_L}{\partial z}.dz$
$Y' + \frac{\partial Y'}{\partial z}.dz$
$T_w + \frac{\partial T_w}{\partial z}.dz$
$\Delta H'_m + \frac{\partial \Delta H'_m}{\partial z}.dz$
$T_G + \frac{\partial T_G}{\partial z}.dz$
z+dz
I
II
III
$\frac{\partial Q_{GL}}{\partial z}.dz$
$\frac{\partial Q_{LW}}{\partial z}.dz$
T_G
PROCESS WATER
GAS
T_P
T_L
T_i
Y'
T_W
DESICCANT
SOLUTION
PIPE
Y'_i
$\frac{\partial \dot{M}_A}{\partial z}.dz$
$\frac{\partial Q_{GW}}{\partial z}.dz$
z
$\dot{M}_W$, T_W
$\dot{L}_S$, X'
T_L, $\Delta H'_m$
$\dot{G}_S$, Y'
T_G

Figure 3-4: Heat and Mass Transfer in a Differential Element.

(') denotes that the variable is expressed on a per unit mass solvent basis, whereas the subscripts L, G, w and s refer to liquid, gas, process water and solvent, respectively.

Owing to the difficulty of measuring the contact area between the different fluids and the packing, it is generally more convenient to use surface densities defined as the contact area per unit volume of packing. In the case of finned tube heat exchangers, "a" will denote the fin side surface density and "a_w" will refer to that of the process water side. Furthermore, the falling film does not actually cover the total available packing surface. The wetted portions depend on the liquid distribution system as well as many other parameters, such as geometry, flow rates, surface tensions, surface roughness and viscosities. To bypass this problem of estimating the wetted area, which actually participates in the mass transfer, a wetting factor F is introduced and is defined as the ratio of wetted to dry area. The F can not be predicted analytically and should be determined experimentally for each particular system.

With the previous assumptions and notations in mind, the heat and mass transfer rates between the different fluids can be expressed by the following:

a) Rate of heat transfer from the gas to the liquid film:

$$\frac{\partial \dot{Q}_{G,L}}{\partial z} = h_G\, a\, A_c\, E_h\, F\, (T_G - T_i) \qquad (3\text{-}50)$$

where h_G is the gas phase heat transfer coefficient, E_h is the heat transfer surface effectiveness of the coil, and T_G and T_i are the gas bulk and the gas-liquid interface temperatures, respectively. Note that the order of subscripts, as in $Q_{G,L}$, gives the transfer direction according to the arbitrary representation of Figure 3-4.

b) Rate of heat transfer from the gas to the process water (through the dry surface):

$$\frac{\partial \dot{Q}_{G,w}}{\partial z} = h_G\, a\, A_c\, E_h\, (1 - F)\, (T_G - T_p) \qquad (3\text{-}51)$$

where T_p is the pipe wall temperature, and the gas phase film coefficient h_G as well as the surface effectiveness E_h are assumed the same for both dry and wet surface cases.

c) Rate of heat transfer from the solution liquid film to the process water:

$$\frac{\partial \dot{Q}_{L,w}}{\partial z} = h_{L,w}\, a\, A_c\, E_h\, F\, (T_L - T_w) \qquad (3\text{-}52)$$

where $h_{L,w}$ is the overall heat transfer between the falling film and the process water, T_L and T_w are the bulk temperatures of the solution and water, respectively, and where the same surface effectiveness is considered.

d) Total heat transfer rate to the process water:

$$\frac{\partial \dot{Q}_w}{\partial z} = h_w \, a_w \, A_c \, (T_p - T_w) \tag{3-53}$$

where h_w is the water side heat transfer coefficient. Or, if expressed as the sum of the individual rates given by Equations (3-51) and (3-52), then

$$\frac{\partial \dot{Q}_w}{\partial z} = h_G \, a \, E_h \, A_c \, (1 - F) \, (T_G - T_p) + h_{L,w} \, a \, E_h \, A_c \, F \, (T_L - T_w) \tag{3-53a}$$

e) Rate of mass transfer of solute A from the gas to the liquid film:

$$\frac{\partial \dot{M}_A}{\partial z} = K_Y' \, a \, A_c \, E_m \, F \, (Y' - Y_i'^{*}) \tag{3-54}$$

where K_Y' is the overall mass transfer coefficient based on mass ratios, E_m is the mass transfer surface effectiveness and takes into account the fact that the equilibrium properties on the fins are different from those on the tubes due to the temperature difference, and finally Y' and $Y_i'^*$ are respectively the bulk gas and interface mass ratios.

Before developing the conservation equations, it is appropriate to first present the enthalpy relationships to be used.

a) Enthalpy of solute A in vapor phase:

$$H_{A,v} = C_{A,v}\,(T_G - T_R) + \lambda_R \qquad (3\text{-}55)$$

where λ_R is the latent heat at a reference temperature T_R, and $C_{A,v}$ is the specific heat of solute A in the vapor phase at temperature T_G

b) Enthalpy of a gas vapor mixture:

The enthalpy of a mixture of perfect gases equals the sum of individual partial enthalpies of its components. Hence, the enthalpy of the mixture, relative to a reference state, can be expressed on a per solvent unit mass basis by

$$H_G' = C_{S,G}\,(T_G - T_R) + Y'\,[C_{A,v}\,(T_G - T_R) + \lambda_R] \qquad (3\text{-}56)$$

where the first term is the enthalpy of the solvent of specific heat $C_{S,G}$, and the second term represents the enthalpy of the associated vapor.

c) Enthalpy of a liquid solution:

Similarly, but for a nonideal solution, the enthalpy per unit mass of solvent relative to a reference state can be written as

$$H_L' = (C_{S,L} + C_{A,v} X')(T_L - T_R)$$

$$+ \Delta H_m' (T_{L,X}') \tag{3-57}$$

where the first part illustrates the enthalpies of the liquid components if they were not mixed, while the second gives the deviation from ideality. $C_{S,L}$ and $C_{A,V}$ are respectively the specific heats of liquid solvent and solute A, and $\Delta H_m'$ is the enthalpy of mixing per unit mass solvent and is a function of both temperature T_L and mass ratio X'.

Utilizing Equations (3-50) through (3-57) mass and energy balances are conducted on control volumes I, II and III, pictured in Figure 3-4. After rearrangement and use of the Lewis relation relating the heat and mass transfer coefficients, the following set of differential equations giving the variation of the independent variables is deduced.

$$\frac{\partial Y'}{\partial z} = \frac{- K_Y \, a \, E_m \, A_c \, F}{\dot{G}_S} (Y' - Y_i'^{*}) \tag{3-58}$$

$$\frac{\partial x'}{\partial z} = \frac{-K_Y \, a \, E_m \, A_c \, F}{\dot{L}_S} (Y' - Y_i'^*) \tag{3-59}$$

$$\frac{\partial T_G}{\partial z} = \frac{K_y \, a \, A_c}{\dot{G}_S \, C_G'} [C_{S,V} \, E_m \, F \, (Y' - Y_i'^*)$$

$$- C_G' \, Le^{2/3} \, E_h] \, (T_G - T_i) \tag{3-60}$$

$$\frac{\partial T_L}{\partial z} = \frac{-K_Y \, a \, A_c \, F}{\dot{L}_S \, C_L'} [Le^{2/3} \, C_G' \, E_h \, (T_G - T_i)$$

$$+ E_m \, \lambda_{Ti} \, (Y' - Y_i'^*)] + \frac{h_{L,w} \, a \, E_h \, A_c \, F}{\dot{L}_S \, C_L'}$$

$$(T_L - T_w) - \frac{1}{C_L'} \frac{\partial \Delta H_m'}{\partial z} (X', T \,) \tag{3-61}$$

$$\frac{\partial T_w}{\partial z} = - \frac{h_w \, a_w \, A_c}{\dot{M}_w \, C_w} (T_p - T_w) \tag{3-62}$$

where C_G' and C_L' are the specific heats per unit mass of solvent of the gas mixture and the liquid solution and are respectively defined by

$$C_G' = C_{S,G} + Y' \, C_{A,v} \tag{3-63}$$

$$C_L' = C_{S,L} + X' \, C_{A,L} \quad . \tag{3-64}$$

It is clear that the integration of this system of differential equations over the height of the contactor is complex, especially with the counterflow configuration. However, it is possible to solve the system by numerical methods using a finite difference approach. Peng [56], at the University of Texas at Austin, developed a computer program to integrate a similar system. Because the conditions of one stream must be known before calculations are possible on the other, Peng assumed the temperature and concentration axial distribution on one stream, then, through a complicated iteration scheme, within each finite element, and over the whole tower. Computations are performed until all variables in each control volume converge to a certain limit.

Although such an accurate but complex solution is feasible, the question is whether the increased accuracy is worth the time and effort for certain engineering applications. In the case of air conditioning, in particular, the cooling load depends on the continuously changing weather conditions; besides, systems are conceived for certain design conditions that would happen only for very short operating times, if ever. Also, unless for very special applications, reasonable fluctuations of temperature and humidity are not critical. From the above remarks, one may conclude that there is no need for a high accuracy, and an approximate but much simpler method would certainly be preferred for the design of liquid desiccant air conditioning systems. In the next section, a simplified method is proposed.

3.5.2. Simplified Model for Liquid Desiccant Systems (Nearly Isothermal Processes)

Threlkeld [54] studied the heat and mass transfer in cooling coils with water vapor condensation. With the assumption that over a small range of temperature, the enthalpy of saturated air is a linear function of temperature, he concluded that enthalpy is the driving potential for simultaneous heat and mass transfer to a close approximation, whereas temperature and concentration are the driving potential for sensible heat and mass transfer, respectively. He consequently introduced an overall transfer coefficient, U_w, based upon air enthalpy differences, which enabled him to express the heat $d\dot{Q}_R$ transferred to the refrigerant by

$$d\dot{Q}_R = U_w \ (H - H_{S,R}) \ dA \tag{3-65}$$

where H and $H_{S,R}$ are the enthalpies of moist air at bulk flow conditions and saturated at refrigerant temperatures, respectively. Furthermore, with the help of the previous assumption, it can be shown that a mean air enthalpy difference can be used for a pure counterflow problem. The total heat transferred to the refrigerant is then given by

$$\dot{Q}_R = U_w \ A \ \Delta H_m \tag{3-66}$$

where

$$\Delta H_m = \frac{(H_1 - H_{S,R,1}) - (H_2 - H_{S,R,2})}{\ln\left(\frac{H_1 - H_{S,R,1}}{H_2 - H_{S,R,2}}\right)} \qquad (3\text{-}66a)$$

and subscripts 1 and 2 refer to the inlet and outlet conditions.

Although approximate, this method allows a much easier analysis of heat and mass transfer in wet cooling coils. A similar simplified model will be developed for use with a liquid desiccant film in lieu of water, and for temperatures even higher than the air dew point.

Using Equation (3-62) and assumption 7, which is equivalent to $T_i = T_L = T_P$, Equation (3-61) can then be rearranged in the form

$$\begin{aligned} \dot{L}_S \, C_L' \frac{\partial T_L}{\partial z} + \dot{M}_w \, C_w \frac{\partial T_w}{\partial z} = \\ - K_y \, a \, A_C \left[L_e^{2/3} \, C_G' \, E_h \, (T_G - T_i) \right. \\ \left. + E_m \, F \, (Y' - Y_i^*) \, \lambda_{Ti} \right] - \frac{1}{C_L'} \frac{\partial \Delta H_m'}{\partial z} \end{aligned} \qquad (3\text{-}61a)$$

This relation shows that the change in sensible energy of both process water and liquid film equals the latent energy of the transferred solute, added to the enthalpy of mixing, and the heat transfer with the gas phase. Further simplifications are possible if the following additional assumptions are made:

9. For a small range of concentration and temperature, the enthalpy of mixing could be expressed as a heat of mixing per unit mass of absorbed solute, defined positive for exothermic cases. Furthermore, if the latter is small when compared to the latent, a mean value $\Delta H_{m,A}'$ may be used and therefore

$$\dot{L}_S \frac{\partial \Delta H_m' (X', T_L)}{\partial z} = \dot{G}_S \frac{\partial Y'}{\partial z} \overline{\Delta H}_{mA}' \tag{3-67}$$

10. Since a) the process water and the liquid solution flow in parallel, b) the water side thermal resistance is much smaller than that of the gas side, and finally, c) if the heat capacity of the process water is much larger than that of the solution, which is true for an efficient desiccant system, then the water temperature change closely equals that of the film.

$$\frac{\partial T_w}{\partial z} = \frac{\partial T_L}{\partial z} = \frac{\partial T_P}{\partial z} = \frac{\partial T_i}{\partial z} \tag{3-68}$$

11. For a relatively small range of temperature, the latent energy λ_{Ti} can be considered constant and replaced by a mean value denoted by $\overline{\lambda_A}$.

12. Because both heat and mass surface effectiveness reflect the non-uniformity of temperature in the finned tube packing, they can be assumed equal ($E_m = E_h$).

The use of these assumptions permits us to rewrite Equation (3-61a) in the form

$$(\dot{L}_S\ C_L' + \dot{M}_w\ C_w)dT_L = -K_Y\ a\ A_C\ E\ Le^{2/3}\ [C_G'\ (T_G-T_i)$$

$$+ \frac{F}{Le^{2/3}}\ (Y' - Y_i'^{*})(\bar{\lambda}_A + \overline{\Delta H}_{m,A}')]dz \qquad (3\text{-}61b)$$

where it can be easily noticed that, if the gas specific heat C_G is constant for small rates of mass transport, then the right hand side is the difference of the same enthalpy expression evaluated at bulk and interface conditions. The left hand side represents the change of sensible energy of both liquids, water and solution, and will be referred to as dQ_L. If one imagines that both liquids move as one entity, then dQ_L would be expressed by

$$d\dot{Q}_L = \dot{M}_L\ C_{L,w}\ dT_L \qquad (3\text{-}69)$$

where

$$\dot{M}_L = \dot{L}_S + \dot{M}_w \qquad (3\text{-}69a)$$

$$C_{L,w} = \frac{\dot{L}_S\ C_L' + \dot{M}_w\ C_w}{\dot{L}_S + \dot{M}_w} \qquad (3\text{-}69b)$$

$\dot{M}_L$ is the total liquid mass flow rate, and $C_{L,w}$ is the corresponding mass weighted specific heat. If, in addition, H* is defined by

$$H^* = C_G^{'} \ T + \frac{F}{Le^{2/3}} Y' (\bar{\lambda}_A + \overline{\Delta H}^{'}_{m,A}) \tag{3-70}$$

then Equation (3-61b) becomes

$$d\dot{Q}_L = -K_Y \ a \ A_C \ E_h \ Le^{2/3} \ (H_G^* - H_i^*) dz \tag{3-71}$$

This relation shows that H^* represents the driving potential for the simultaneous heat and mass transfer.

We now need to develop an expression for a mean enthalpy difference, which is expected to be similar to that developed by Threlkeld [54] and used for cooling coils with dehumidification. As concluded in the literature review, for an efficient mass transfer operation, the process should be as cool as possible during the absorption, and conversely, as hot as possible during the stripping. Therefore, a well-designed liquid desiccant system should operate under conditions close to isothermal. This can be insured by the use of the process water with a thermal capacity higher than that of liquid desiccant and air stream, combined. On the other hand, for liquid desiccants, and in particular for triethylene glycol which is used in this work, the enthalpy of mixing is much smaller than the latent heat. As a consequence, the main function of a liquid desiccant contactor becomes the extraction of moisture from either the moist air or the dilute solution, and the energy exchanged with the process water corresponds mostly to the latent heat. With this in mind, it can be shown that, for a small range of working concentration and temperature, the equilibrium mass ratio $Y_i^{'}$ as well as H_i^{*} may be approximated by the following linear functions

$$Y_i^{'} \simeq A\ T_i + B \tag{3-72}$$

or $$Y_i^{'} \simeq A'\ X' + B' \tag{3-72a}$$

and $$H_i^{*} \simeq \alpha\ T_i + \beta \tag{3-73}$$

where α, β, A, A', B and B' are constants. Detailed derivations are presented in Appendix B, but a physical interpretation is best performed on a psychrometric chart. The solution temperature, T_i, and the concentration, X', change throughout the contactor. Therefore, If the equilibrium mass ratio $Y_i(X',T_i)$ is plotted on a psychrometric chart, it would be represented by a curve AB. For a small range of temperature and concentration, however, the curve AB may be approximated by a straight line $\overline{AB}$, and thus resulting in the linearity relations presented above. Furthermore, dry packing is of course completely ineffective for mass transfer, and the liquid distribution (spraying) system should insure a maximum surface wetting. If the wetting factor, F, is assumed to be close to 0.85, then, as shown in Appendix B, the integration of Equation (3-71) is greatly simplified by the linearity approximations and leads to the logarithmic mean enthalpy difference defined by

$$\dot{Q}_L = \dot{M}_L C_{L,w} (T_{L2} - T_{L1})$$

$$= -K_y E A_o \Delta H^*_{\ell,m} \qquad (3\text{-}74)$$

where

$$\Delta H^*_{\ell,m} = \frac{(H^*_{G2} - H^*_{i2}) - (H^*_{G1} - H^*_{i1})}{\ln\left(\frac{H^*_{G2} - H^*_{i2}}{H^*_{G1} - H^*_{i2}}\right)} \qquad (3\text{-}74a)$$

A_o is the total packing area, subscripts 1 and 2 refer to the end points of the contactor, and $E_h \, Le^{2/3}$ is lumped into the effectiveness E.

It should be noted that Equation (3-74) expresses a total heat transfer rate, sensible and latent, and fails to separate the heat and mass transfer. To overcome this problem, another integral relation must be used in conjunction with it. A mean temperature would be inappropriate because of the involved latent energy and enthalpy of mixing; however, the linearity approximation of the interface equilibrium mass ratio, Y_i, made earlier, permits the deduction of this additional relation. The analysis of mass transfer alone is discussed extensively by Treybal [50]. By using the linearity approximation given by equation (3-72a), the integration of equation (3-57) for a pure counter-flow problem becomes possible, and the total amount $\dot{M}_A$ of solute A transferred may be expressed in terms of a logarithmic mean mass ratio difference by

$$\dot{M}_A = \dot{G}_S \, (Y_2' - Y_1') - K_Y A_o \, F \, \Delta Y_{\ell m}' \qquad (3\text{-}75)$$

where

$$\Delta Y_{\ell m}' = \frac{(Y_2' - Y_{i2}') - (Y_1' - Y_{i1}')}{\ell n \left(\dfrac{Y_2' - Y_{i2}'}{Y_1' - Y_{i1}'} \right)} \; . \qquad (3\text{-}75a)$$

Equation 3-75 was experimentally checked by Queiroz et al [57] in an investigation of a similar non-adiabatic liquid-desiccant dehumidifier. The use of the logarithmic mean differences of equations (3-74) and (3-75) requires the knowledge of the temperatures and mass ratios at the end points of the contactor. In order to determine those unknowns, overall energy and mass relations are developed for the system shown in Figure 3-3.

Solute mass balance

$$\dot{L}_S \, (X_2' - X_1') = \dot{G}_S \, (Y_2' - Y_1') \qquad (3\text{-}76)$$

Energy balance

$$\dot{M}_w\ C_w\ (T_{w2} - T_{w1}) + \dot{L}_S\ \bar{C}'_{S,L}\ (T_{L,in} - T_{L1})$$

$$= \dot{G}_S\ [\bar{C}'_G\ \ (T_{G2} - T_{G1})$$

$$+ (Y'_2 - Y'_1)(\bar{\lambda}_A + \overline{\Delta H}'_{m,A})] \qquad (3\text{-}77)$$

where the average specific heats are used, and defined by

$$\bar{C}'_G = C_{S,G} + C_{A,V}\ (\frac{Y'_2 + Y'_1}{2}) \qquad (3\text{-}77a)$$

$$\bar{C}'_{S,L} = C_{S,L} + C_{A,L}\ (\frac{X'_1 + X'_2}{2}) \qquad (3\text{-}77b)$$

Also, recalling assumption 10, one may deduce that the temperature difference, $\Delta T_{L,w}$, between the liquid film and the process water is constant throughout the packing, thus

$$T_{L2} = T_{w2} + \Delta T_{L,w} \qquad (3\text{-}78)$$

$$T_{L1} = T_{w1} + \Delta T_{L,w} \qquad (3\text{-}79)$$

and the total energy exchange with the process water may be expressed by

$$\dot{M}_w\ C_w\ (T_{w2} - T_{w1}) = -\ h_w\ A_w\ \Delta T_{L,W} \qquad (3\text{-}80)$$

where A_w is the total water side area ($A_w = a_w\ A_c\ (Z_2 - Z_1)$).

Equations (3-74) through (3-80) are sufficient to completely analyze the heat and mass transfer in a contactor where the basic assumptions are met. The difficulty of the solution, as well as the procedure, depend however on the specific problem, namely on whether it is a design of a new system or an analysis of an existing one.

CHAPTER IV
COMPONENT MODELS AND NUMERICAL SOLUTION PROCEDURE

In order to perform a computer analysis of a liquid desiccant system, it is necessary to express all variables in algebraic forms. The following sections present the correlations used in this work to model the different components as well as the thermodynamic properties of the selected desiccant. The analysis remains general and could be applied to other configurations and desiccants as long as the appropriate relations are employed.

4.1. Transfer Coefficients and Friction Losses in Finned Tube Heat Exchangers

In view of the considerations discussed in chapter II, finned-tube heat exchangers will be used as packing for both the absorber and regenerator. The Chilton and Colburn analogy discussed in Section 3.3. may be used to determine the mass transfer coefficient from the available heat transfer data. However, recent research showed that the j factor analogy is approximately true only when the surface conditions are identical [58], and that the change of roughness caused by either dropwise or filmwise condensation affects the validity of the analogy [59]. In other words, the heat transfer data available for dry surfaces can not be directly used to deduce the mass transfer coefficient. McQuiston [60] recently conducted an extensive investigation involving finned-tube heat exchangers with and without water condensation. He deduced correlations which account for geometric and hydrodynamic variables, and which relate the dry to the wetted surface problem. Figure 4.1 shows the heat transfer data of dry finned-tube heat exchangers given by several investigators [59,61, 62, 63]. Notice that the results are presented in the form of J factor versus a JP parameter which is defined as

$$JP = Re_D^{-0.4} \left(\frac{A}{A_t}\right)^{-0.15} \qquad (4\text{-}1)$$

where

$$Re_D = \frac{G_c\ D}{\mu} \qquad (4\text{-}1a)$$

A is the total heat transfer area, A_t is the area of the bare tubes without fins, D is the outside tube diameter, μ denotes the air viscosity and G_c is the mass flow rate per unit area of free cross section. The curve J = J(JP) may be well described by the relation

$$J = 2.6144\ 10^2\ JP + 1.3858\ 10^{-3} \qquad (4\text{-}2)$$

The data of Figure 4-1 apply to finned-tube coils with four rows of tubes. The J factor for a coil with a different number of rows N_R can be deduced from the correlation

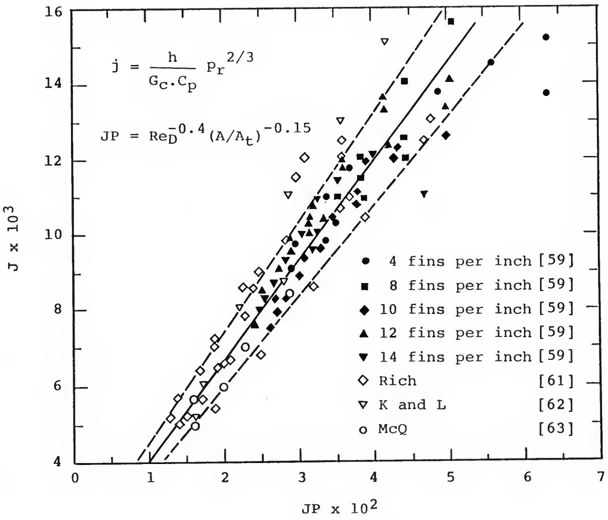

Figure 4-1: Heat Transfer Correlation for Smooth Plate-fin-tube Coils with 4 Rows of Tubes [60].

$$\frac{J_n}{J_4} = \frac{1 - 1280 \quad N_R \; Re_{xb}^{-1.2}}{1 - 5120 \; Re_{xb}^{-1.2}} \tag{4-3}$$

where the subscripts n and 4 refer to the number of tube rows and Re_{xb} is the Reynold number based on the row spacing x_b. Equation (4-3) results from data curve fitting for coils with up to six rows, the generally maximum number for most practical applications. In desiccant systems however, a larger number of rows is required and no information is available for $N_R > 6$. To overcome this problem, the J factor will be extrapolated using equation (4-3) for up to ten rows then kept constant for higher numbers ($J_n = J_{10}$ if $N_R > 10$).

In the same investigation, McQuiston deduced a generalized correlation for friction data. The results are summarized in Figure 4-2, which gives the air side friction factor f for dry finned-tube heat exchanges in terms of a parameter FP defined as

$$FP = Re_D^{-0.25} \cdot \frac{D}{D^*} \quad \left(\frac{X_a - D}{4(S-y)} \right)^{-0.4} \cdot \left(\frac{X_a}{D^*} - 1 \right)^{-0.5} \tag{4-4}$$

where, D^* is the hydraulic diameter given by

$$D^* = \frac{D \; (A/A_t)}{1 + (X_a - D)/S} \tag{4-5}$$

X_a is the distance separating the tubes of a same row, S and y are the fin spacing and thickness, respectively. The curve of Figure 4-2 may be well represented by the equation

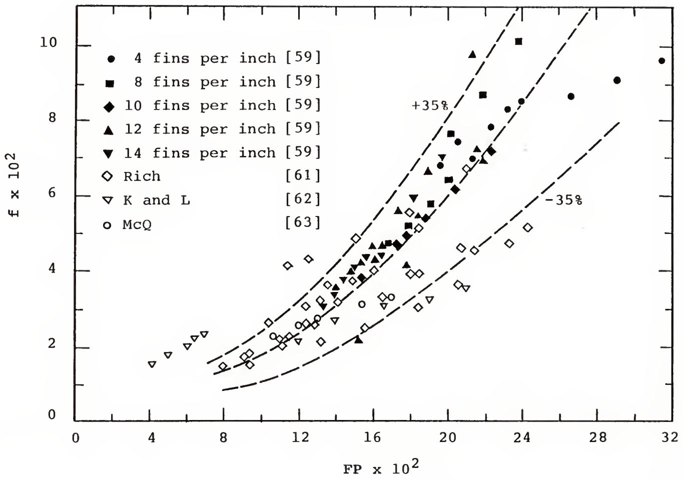

Figure 4-2: Correlation of Friction Data for Smooth Plate-fin-tube Coils [60].

$$f = 0.00691 - 0.03761\ FP + 1.50324\ FP^2 \qquad (4\text{-}6)$$

For film-type wetted surfaces as is the case in liquid desiccant contactors, correction of the dry surface data is performed by transforming the coordinates JP of Figure 4-1 to J(S)·JP, and FP of Figure 4-2 to F(S)·FP, with the parameters J(S) and F(S) defined as follows

$$J(S) = 0.84 + 4.10^{-5}\ Re_S^{1.25} \qquad (4\text{-}7)$$

$$F(S) = \left(1 + Re_S^{-0.4}\right)\left(\frac{S}{S-y}\right)^{1.5} \qquad (4\text{-}8)$$

where Re_S is the Reynold number based on the fin spacing S. The air side pressure drop across the finned-tube configuration can then be determined from the energy equation, if the change of momentum, elevation, and inlet and outlet contractions are neglected.

Forced-convection turbulent flow inside tubes is generally used for better heat transfer performance. The heat transfer coefficient h for this common case can be deduced from the widely used Dittus-Boelter correlation [64]

$$\frac{h\ D_i}{k} = 0.023\ Re_{Di}^{0.8}\ Pr^n \qquad (4\text{-}9)$$

where

$n = 0.4$ for $T_{wall} > T_{Bulk}$

$n = 0.3$ for $T_{wall} < T_{Bulk}$

D_i is the tube inside diameter, k is the fluid thermal conductivity, T_{wall} is the pipe wall temperature, and where all properties are evaluated at the mean bulk temperature of the fluid, T_{Bulk}. The pressure drop for incompressible flow in pipes is easily determined using the friction factor, given in published Moody charts.

4.2. Recovery heat exchangers

The desiccant regeneration is generally achieved by heating either the air stream or the liquid sorbent or both. In all cases, the exhaust humid air is relatively hot, and a considerable amount of energy would be lost if not recovered. Also, in a continuous operation, the regenerated and hot solution is pumped to the absorber carrying non desired heat with it, while the already cooled dilute solution is heated either before or within the regeneration chamber. It is thus obvious that the use of an air-to-air recovery heat exchanger between the inlet and outlet of the regenerator, and the insertion of an intercooler between the hot (concentrated) and cold (dilute) solutions improve the thermal performance of a liquid desiccant air-conditioning system. The heat exchangers may be simply modeled by the constant effectiveness approach, with the effectiveness ε defined by

$$\varepsilon = \frac{\text{Actual heat transfer rate}}{\text{Maximum possible heat transfer rate}}$$

which, if expressed in terms of the specific heats, can be written as

$$\varepsilon = \frac{C_h\,(T_{hi} - T_{ho})}{C_{min}(\,T_{hi} - T_{ci})} \qquad (4\text{-}10)$$

or

$$\varepsilon = \frac{C_c\,(T_{co} - T_{ci})}{C_{min}\,(T_{hi} - T_{ci})} \qquad (4\text{-}10a)$$

where C is the fluid total heat capacity, the subscript h stands for the hot stream, c stands for the cold stream, and min refers to the minimum of the two. If the heat capacities of the hot and cold streams are equal ($C_h = C_c = C_{min}$), then the effectiveness relations reduce to

$$\varepsilon = \frac{T_{hi} - T_{ho}}{T_{hi} - T_{ci}} = \frac{T_{co} - T_{ci}}{T_{hi} - T_{ci}} \qquad (4\text{-}10b)$$

For simplicity, equations (4-10b) are used in the analysis of the liquid desiccant systems, since the flow rates differ only by the small amount of moisture transferred, and constant specific heats may be assumed within the range of working temperatures.

4.3. Evaporative Cooler

The evaporative cooler, used in this work, consists of a chamber where recirculated water is sprayed and brought into direct contact with the dry and warm air coming from the absorber. Water evaporates thus cooling itself and consequently cooling the air in contact with it. The amount of water evaporated equals the increase in moisture of the air and is continuously replaced by make-up water.

The basic relations, governing the direct contact heat and mass transfer processes in an evaporative cooler, have been investigated by several researchers [50,54,65] and are similar to those developed for air washers and cooling towers. The only difference stems from the fact that water is recirculated with no heat exchange other than that with the air stream. The water temperature falls to, and remains equal to, the entering air wet bulb temperature. Meanwhile, the air is cooled and humidified, following the path of the diabatic saturation curve (constant enthalpy line when plotted on a psychrometric chart). This assumes that there is no heat exchange through the chamber walls, and that the make-up water enters the system at the same adiabatic saturation temperature. The second assumption may be justified by the fact that, for most purposes, the amount of evaporated water is so small relative to the total liquid circulation that the sensible energy introduced by the make up water may be ignored.

Depending upon the degree of contact with water, which is function of both the spray quality and the chamber size, the air will approach more closely the adiabatic saturation conditions. The extent to which the leaving air temperature approaches the wet bulb temperature of the entering air is expressed as cooling or saturation efficiency, and is defined [66] as

$$E_c = \frac{T_1 - T_2}{T_1 - T_{WB1}} \qquad (4\text{-}11)$$

where E_c is the saturation efficiency, T_2 is the leaving air temperature, and T_1 and T_{WB1} are the dry and thermodynamic wet bulb temperatures of the entering air, respectively. The evaporative cooler represents the last step in a liquid desiccant air-conditioning system. Its saturation efficiency must be chosen such that the leaving air conditions equal the required supply temperature and humidity in order to meet both sensible and latent loads.

4.4. Liquid Desiccants- Triethylene Glycol

Desiccant systems are mainly based on the fact that sorbents have the property of absorbing moisture upon physical contact, and of being easily regenerated at reasonable temperatures. To meet the efficiency, safety, and economic criteria, liquid desiccants should have the following characteristics [67]:

1. Suitable vapor pressure properties.
2. Cristallisation temperature lower than working temperatures.
3. easily regenerated.
4. non-corrosive and non-inflammable.
5. non-toxic and odorless.
6. stable and do not vaporize in the range of operating temperatures.
7. low viscosity and good heat transfer properties.
8. cheap and abundant.

There are several solutions that have most of these characteristics; the most common, however, are the triethylene glycol as used in the Niagara system, and the aqueous lithum chloride as employed in the Kathabar unit. Lithium chloride solutions are more effective as sorbents but they require higher regenerating temperatures (200°F).

High concentration triethylene glycol is also as effective; and in addition, it has the advantage of lower regenerating temperatures that can be reached by commercial flat-plate collectors (150°F). For the reasons mentioned above, triethylene glycol is selected for this work, but special care must be taken during the design to avoid any loss of material due to evaporation during the regeneration process.

Figures 4-3, 4, 5, 6 give the required thermophysical properties of the chosen desiccant [68]. For simplicity, average specific heats and viscosities are used for each range of temperature. Similarly, since the change of concentration is small, and because the associated heat of mixing is small compared to the latent energy, an average heat of mixing per unit mass of transferred water is deduced to be $\Delta Hm = 24.3$ Btu/Lb. of absorbed water. The equilibrium vapor pressure curves of Figure 4.6 need however to be expressed in an algebraic form in order to perform the computer simulation. Due to unknown reasons, Dow Chemical Corporation, which manufactures the glycols, refused to answer several requests for such information. To overcome this problem, a curve fitting, based on the reference-substance plots technique [50], was performed for the data of Figure 4-5. The detailed procedure is presented in Appendix B, and resulted in the following correlation relating the equilibrium water vapor pressure of aqueous triethylene glycol solutions to both temperature T in °F and concentration by weight C

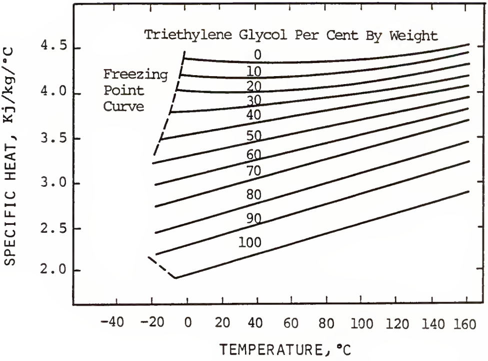

Figure 4-3: Specific Heat of Triethylene Glycol Solutions versus Temperature and Concentration (Dow Chemical Company) [68].

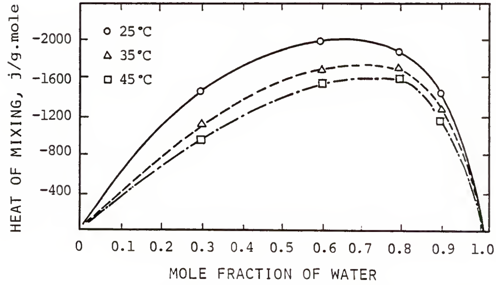

Figure 4-4: Integral Heat of mixing of Triethylene Glycol Solution versus Water Molar Fraction [56].

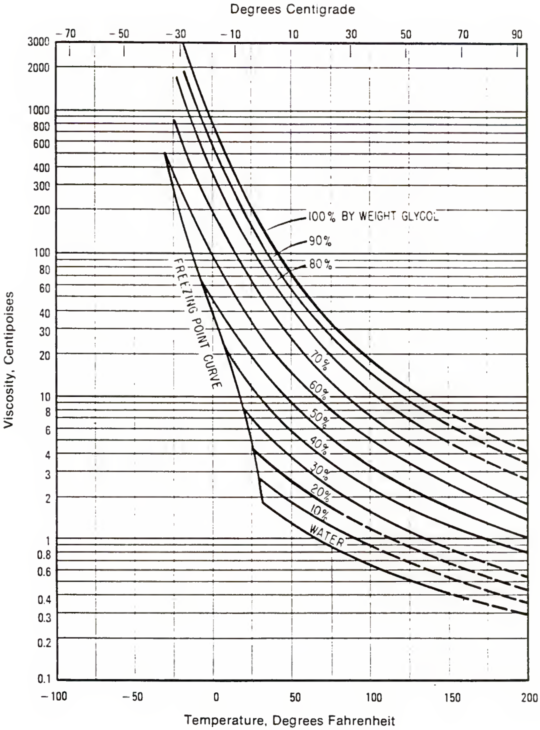

Figure 4-5: Viscosity of Aqueous Triethylene Glycol Solutions (Dow Chemical Company) [68].

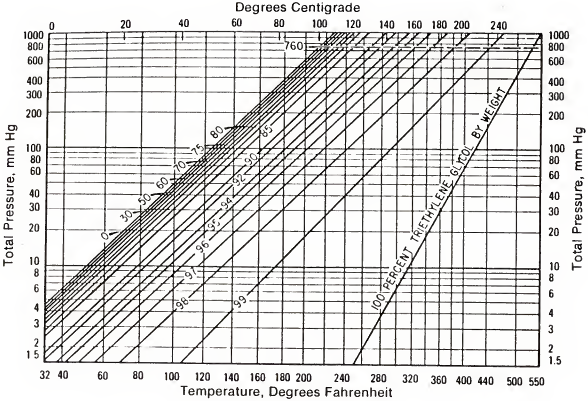

Figure 4-6: Total Pressure over Aqueous Triethylene Glycol Solutions versus Temperature (Dow Chemical Company) [68].

$$Pe = (-3.07443 + 11.44548C - 8.37558C^2)\ [P_{WS}(T)]^{0.972} \qquad (4\text{-}12)$$

where P_{WS} is the water saturation pressure at temperature T, with well known analytical expressions [69], and where both pressures are expressed in millimeter of mercury.

4.5. Numerical Solution Procedure

The simultaneous heat and mass transfer in a desiccant contactor has been discussed in chapter III, where a simplified model was proposed. For a given desiccant contactor with known inlet conditions (temperatures, humidities, concentration and flow rates), equations (3-74) through (3-80) could be solved simultaneously if heat and mass transfer coefficients and themodynamic properties are known. By successive substitutions, the above system of equation can ultimately be reduced to the following system of two non-linear equations with the air outlet humidity and temperature as implicit unknowns

$$f(T_{G2}, Y_2') = 0 = \dot{Q}_L + K_Y\ E\ A_o\ \Delta H^*_{1m} \qquad (4\text{-}13)$$

$$g(T_{G2}, Y_2') = 0 = \dot{G}_s(Y_2' - Y_1') - K_Y\ A_o\ F\ \Delta Y'_{1m} \qquad (4\text{-}14)$$

This system may then be solved using the Newton-Raphson iteration techniques [70], which, if applied to equations

(4-8) and (4-9), gives the relationship between iterations i and i + 1 as:

$$(T_{G2})_{i+1} = (T_{G2})_i + \frac{f_Y^i\, g^i - f^i\, g_Y^i}{f_T^i\, g_Y^i - f_Y^i\, g_T^i} \qquad (4\text{-}15)$$

$$(Y_2')_{i+1} = (Y_2')_i + \frac{f^i\, g_T^i - f_T^i\, g^i}{f_T^i\, g_Y^i - f_Y^i\, g_T^i} \qquad (4\text{-}16)$$

where the subscripts T and Y refer to the partial derivatives with respect to T_2 and Y_2', respectively, and the superscript i denotes that the function is evaluated at $(T_2)_i$ and $(Y_2')_i$.

Because of the complexity of the resulting non-linear equations, a computer program DESCON was written where Newton-Raphson successive iterations are used, and where the partial derivatives are evaluated numerically. Convergence problems were met and were found dependant on the inital guesses. To insure and accelerate the convergence, a variable relaxation factor was introduced, and appropriate inital guesses of the temperature and humidity ratio of air leaving the contactor are internally computed by the program in terms of the given input data. The flow diagram shown in Figure 4-7 summarizes the iteration procedure for the analysis of one contactor, and a detailed computer code is presented in Appendix F. In brief, after specifying the independant variables (dimensions, flow rates, effectivenesses and inlet temperatures and concentration),

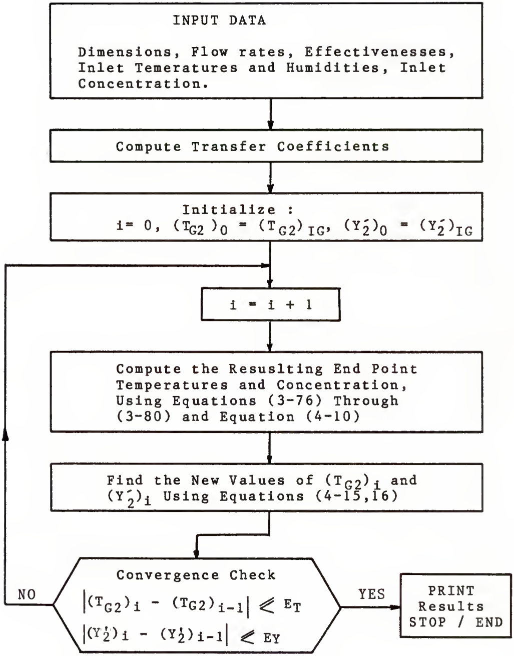
INPUT DATA
Dimensions, Flow rates, Effectivenesses, Inlet Temeratures and Humidities, Inlet Concentration.
Compute Transfer Coefficients
Initialize : i= 0, $(T_{G2})_0 = (T_{G2})_{IG}$, $(Y'_2)_0 = (Y'_2)_{IG}$
i = i + 1
Compute the Resusltíng End Point Temperatures and Concentration, Using Equations (3-76) Through (3-80) and Equation (4-10)
Find the New Values of $(T_{G2})_i$ and $(Y'_2)_i$ Using Equations (4-15,16)
Convergence Check
$|(T_{G2})_i - (T_{G2})_{i-1}| \leqslant E_T$
$|(Y'_2)_i - (Y'_2)_{i-1}| \leqslant E_Y$
NO
YES
PRINT Results STOP / END

Figure 4-7: Flow Diagram of Subroutine DESCON, a Liquid Desiccant Contactor.

the heat and mass transfer coefficients are computed based on average thermophysical properties. The iteration procedure is then started by first guessing the air outlet conditions. All end point temperatures and mass ratios are thereafter deduced and a convergence check is performed. The iterations procedure is allowed to continue until the computed leaving temperature and humidity converge to a certain limit.

The computer code DESCON serves only to analyse one contactor in either regeneration or absorption mode. In an actual desiccant system with continuous operation, as shown in Figure 2-4 with the addition of the recovery heat exchangers, there are interactions between the absorber and regenerator. The inlet desiccant concentration and temperature of one contactor depend on the outlet conditions of the other and on the effectiveness of the intercooler. To analyse the performance of a complete liquid desiccant unit, a computer program DESYST was written to link the absorber and regenerator as illustrated in the algorithm of Figure 4-8 and also detailed in Appendix F. After specifying all independent variables and computing the transport coefficients, the temperature and composition of the desiccant entering the absorber are first guessed and subroutine DESCON is called to compute the corresponding absorber outlet conditions. The resulting dilute solution temperature and concentration are then used to deduce the regenerator inlet conditions after the intercooler, then

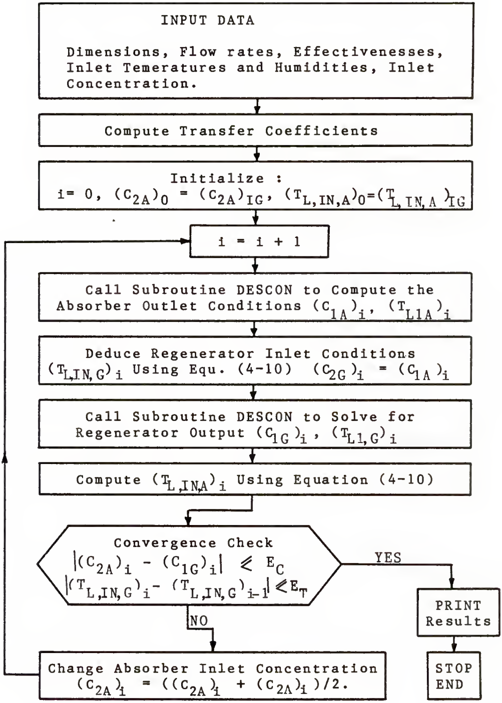
INPUT DATA
Dimensions, Flow rates, Effectivenesses, Inlet Temeratures and Humidities, Inlet Concentration.
Compute Transfer Coefficients
Initialize :
$i = 0$, $(C_{2A})_0 = (C_{2A})_{IG}$, $(T_{L,IN,A})_0 = (T_{L,IN,A})_{IG}$
$i = i + 1$
Call Subroutine DESCON to Compute the Absorber Outlet Conditions $(C_{1A})_i$, $(T_{L1A})_i$
Deduce Regenerator Inlet Conditions $(T_{L,IN,G})_i$ Using Equ. (4-10) $(C_{2G})_i = (C_{1A})_i$
Call Subroutine DESCON to Solve for Regenerator Output $(C_{1G})_i$, $(T_{L1,G})_i$
Compute $(T_{L,IN,A})_i$ Using Equation (4-10)
Convergence Check
$|(C_{2A})_i - (C_{1G})_i| \leqslant E_C$
$|(T_{L,IN,G})_i - (T_{L,IN,G})_{i-1}| \leqslant E_T$
YES
NO
PRINT Results
STOP END
Change Absorber Inlet Concentration
$(C_{2A})_i = ((C_{2A})_i + (C_{2A})_i)/2.$

Figure 4-8: Flow Diagram of the Computer Program DESYST, for the Analysis of a Continuous Liquid Desiccant Air Conditioner.

subroutine DESCON is called again to now calculate the subsequent outlet conditions of the regenerator. An iteration loop is performed by changing the concentration of the desiccant entering the absorber (C_{2A}) to the average of its previous value and that of the regenerator outlet. Iterations proceed until the output of one contactor agrees with the imput of the other to a specified convergence criteria. Computer simulation results are presented and discussed in the theoretical analysis section.

CHAPTER V
THEORETICAL RESULTS AND DISCUSSION

The parametric analysis of both absorber and regenerator was conducted using the computer code DESCON. The performance dependence on various controlling parameters was investigated by allowing one parameter to vary while all other kept constant at some selected values. This is a simplistic approach since the parameters in a real desiccant system are coupled togather by the continuity of the dehumidification and regeneration processes. In the parametric analysis, the continuous interactions between the absorber and the regenerator is simply studied by changing the inlet temperature and concentration of the desiccant solution that links the two contactors. Those interactions are further discussed in Chapter VI where a complete desiccant system is designed and optimized, and are more detailed in Chapter VII where the experimental results are discussed and evaluated.

5.1. Absorber Parametric Analysis

Considering the complex interaction between the numerous controlling parameters, the absorber analysis was conducted on a one square foot cross-section basis. The results could then be used to design systems with specific cooling loads once best operating conditions are determined.

The inlet air conditions of the absorber were taken equal to those of recirculated room air, 78°F dry bulb temperature and 50% relative humidity as suggested for energy conservation. The cooling water was assumed to enter the absorber at 70°F, which is the ground water temperature available in North Florida. The triethylene glycol solution was considered regenerated to a 96% concentration by weight, which is feasible with hot water at 150°F that can be supplied by today's flat-plate collectors. The hot and concentrated desiccant, coming from the regenerator, was assumed precooled to 90°F by a liquid-to-liquid intercooler. The other parameters were selected or allowed to vary within specified ranges, based on both practical and economical considerations.

The finned-tube coils used in this analysis have the same characteristics as those described earlier in Section 4.1. For commonly used coils, the number of fins per inch (fin pitch) varies between 6 to 14. In this work a value of 6 fins/inch was selected in order to allow sufficient surface area for both heat and mass transfer, and sufficient chanel space for both air and desiccant flow without flooding and at reasonable air side pressure drop. Preliminary calculations showed that the fin efficiency is about 0.75 for the finned coils used. In order to have good heat transfer properties on the liquid side, the water flow is chosen to have two passes per row; other flow configurations could be used depending on the flow rate and the tubing size.

In chilled water application with coils up to 8 rows deep, the commonly used air face-velocities vary between 400 to 600 fpm. In a desiccant contactor, however, the larger coil depth required, the additional air flow restriction due to the falling desiccant film, and the flooding possibilities suggest that lower face velocities should be used. A value of 365 fpm (or 1600 pounds dry air per square foot cross section) was therefore chosen to maintain good heat and mass transfer properties at reasonable blower power costs.

From the experimental work, it was deduced that a minimum desiccant flow rate of about 200 Lb/hr. ft^2 (cross-section) is necessary for an effective and even spray. The maximum flow rate is, however, limited by the flooding or non entrainment conditions, which are also controlled by the coil geometry and air flow rates. Flooding checks, using the equations developed in Section 3.4, showed that, for the finned-tube coil used and the selected air flow rate, no entrainment would occur for desiccant flow rates up to about 800 Lb/hr. ft^2.

In order to maintain the absorber as cool as possible for a better mass transfer performance, it is desirable to have the heat capacity of the process water higher than that of both air and desiccant combined. A minimum water flow rate of 1600 Lb/hr. per square foot cross-section was therefore selected; while practical and economical considerations were used to determine the maximum.

Numerous computer runs were performed for the analysis of the absorber, allowing the controlling parameters to vary, one at a time. The results are summarized and discussed in the rest of this section.

5.1.1. Effect of desiccant flow rate and packing depth

Figures 5-1 through 5-11 illustrate the effect of the desiccant flow rate (MD) and the packing depth (NR) on the different output parameters of interest. Figures 5-1 and 5-2 give the leaving air humidity ratio (W2). They show that, for a given desiccant flow rate, there is more dehumidification with deeper packings, due to the larger moist-air/desiccant contact area for mass transfer. They also show that larger desiccant flow rates permit more dehumidification as well because of the resulting higher solution concentration throughout the contractor, and therefore higher capacity of absorbing moisture (lower equilibrium water partial pressure).

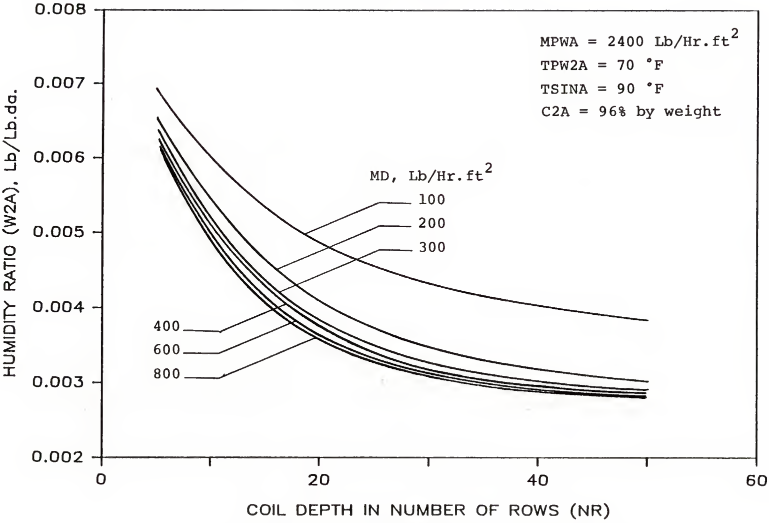

Figure 5-1: Humidity Ratio of Air Leaving the Absorber versus Packing Depth , for different Desiccant Flow Rates.

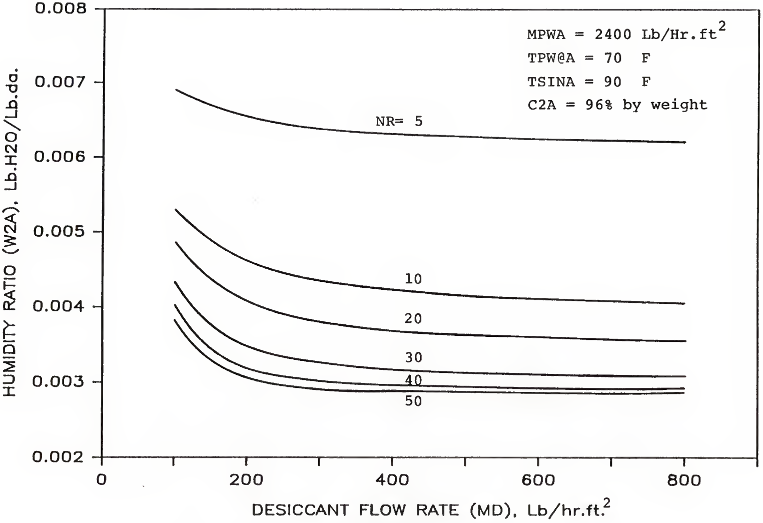

Figure 5-2: Humidity Radio of Air Leaving the Absorber versus Desiccant Flow Rate, for different Packing Depths.

Figures 5-3 and 5-4 illustrate the decrease in the leaving air temperature (TDB2) with larger packing depth since more heat is then rejected to the cooling process water. They also show that higher desiccant flow rates result in higher leaving air temperatures. This can be attributed to the fact that, with more desiccant introduced as 90°F, more sensible heat is added to the process in addition to the larger latent heat rejected by the resulting higher dehumidification.

The combination of the temperature and humidity results give the leaving air enthalpy (H_2) as illustrated by Figures 5-5 and 5-6. The enthalpy curves confirm the complex interaction between the heat and mass transfer mechanisms inherent in the process. As expected, they show that, for a given desiccant flow rate, the leaving air enthalpy decreases with larger packing number of rows because of the larger contact area for both heat and mass transfer. However, for a specified packing depth (NR), the enthalpy (H_2) first decreases to a minimum then starts increasing with larger desiccant flow rates. This behaviour is explained by the fact that larger desiccant flow rates introduce more sensible heat to the process, thus offsetting the advantage of higher solution concentration throughout the packing. Because the equilibrium water partial pressure is function of both concentration and temperature, increasing the desiccant flow rate beyond a certain limit does not cause further noticeable dehumidification as can be

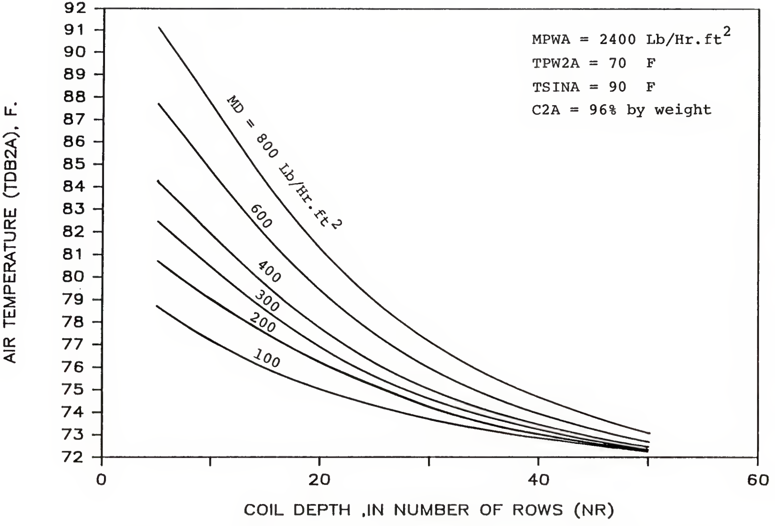

Figure 5-3: Temperature of Air Leaving the Absorber versus Packing Depth, for different Desiccant Flow Rates.

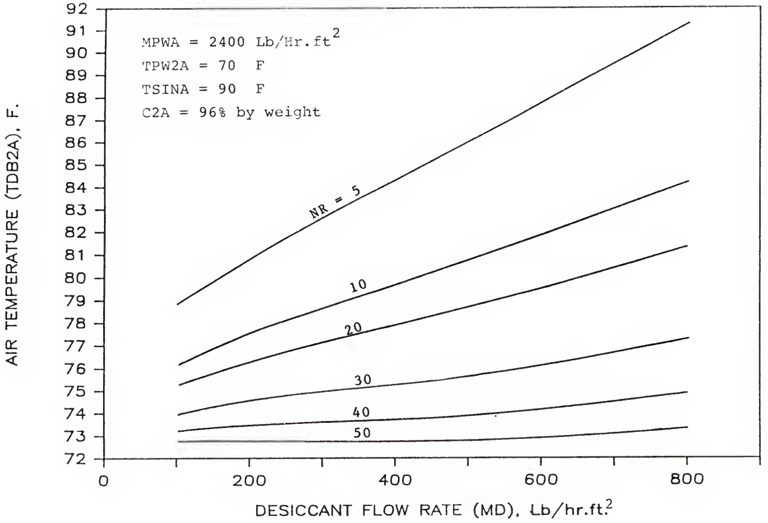

Figure 5-4: Temperature of Air Leaving the Absorber versus Desiccant Flow Rate, for Different Packing Depths

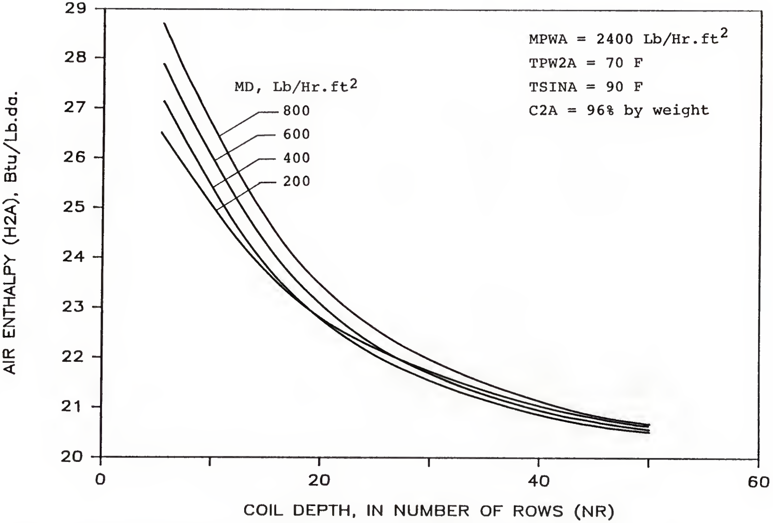

Figure 5-5: Enthalpy of Air Leaving the Absorber versus Packing Depth, for different Desiccant Flow Rates.

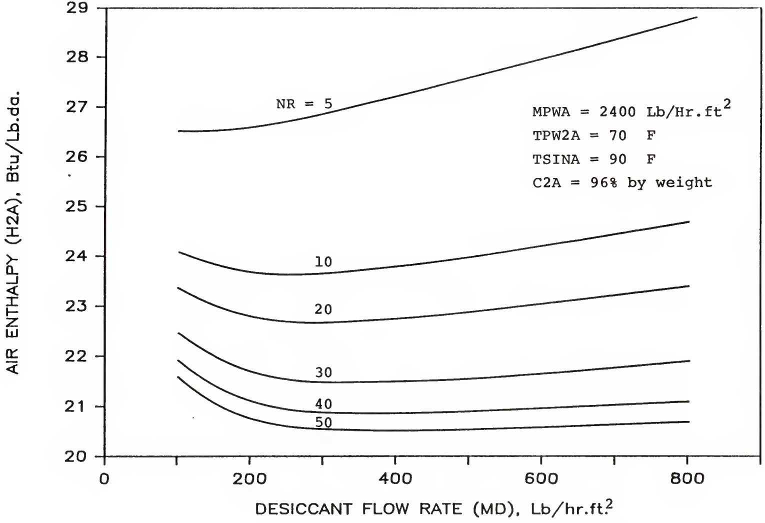

Figure 5-6: Enthalpy of Air Leaving the Absorber versus Desiccant Flow Rate, for different Packing Depths.

seen in Figure 5-2, but introduces enough heat to make the dehumidification process warmer as illustrated by the higher air temperatures of Figure 5-4. The increase of air temperature offsetts the small gain in dehumidification and results in the higher air enthalpies. This also explains why the enthalpy curves of Figure 5-5 intersect in a non-predictable pattern.

Figures 5-7 and 5-8 picture the variation of the outlet water temperature (TPW1). They confirm that larger amounts of heat are rejected to the cooling water with larger desiccant flow and/or deeper packing coils.

The dependence of the weak solution concentration (C1A), leaving the absorber, on both packing depth and desiccant flow rate is illustrated by Figure 5-9. As the desiccant flow rate increases, more solution is available to absorb the moisture from the air stream. As a result, the solution leaves the contactor at a higher concentration, in spite of the larger dehumidification due to the consequent higher mass transfer driving potential. It is also obvious that, with deeper packing, more contact area between the falling desiccant film and the countercurrent air stream is available for mass transfer, and therefore results in lower weak solution concentrations leaving the absorber. Figures 5-10 and 5-11 picture the mass transfer driving potential at the inlet and outlet of the absorber. They give the difference between the humidity ratio of moist air (W) and that of equilibrium conditions (We) of the desiccant

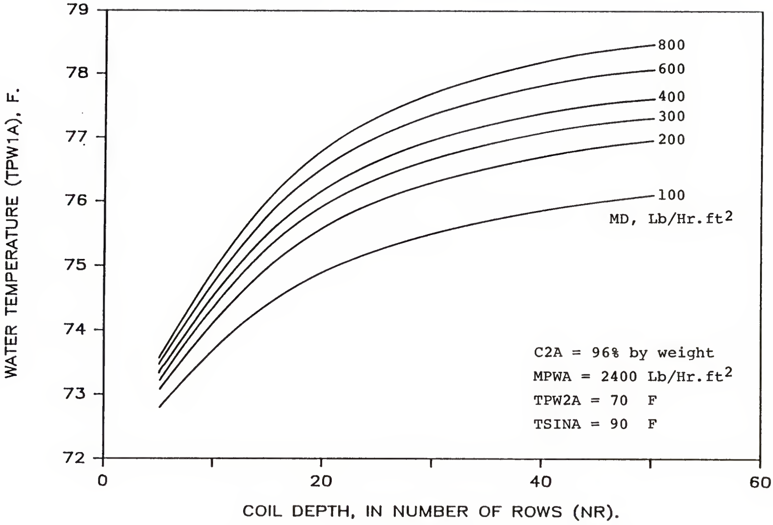

Figure 5-7: Outlet Temperature of Cooling Waterversus Packing Depth, for differnt Desiccant Flow Rates.

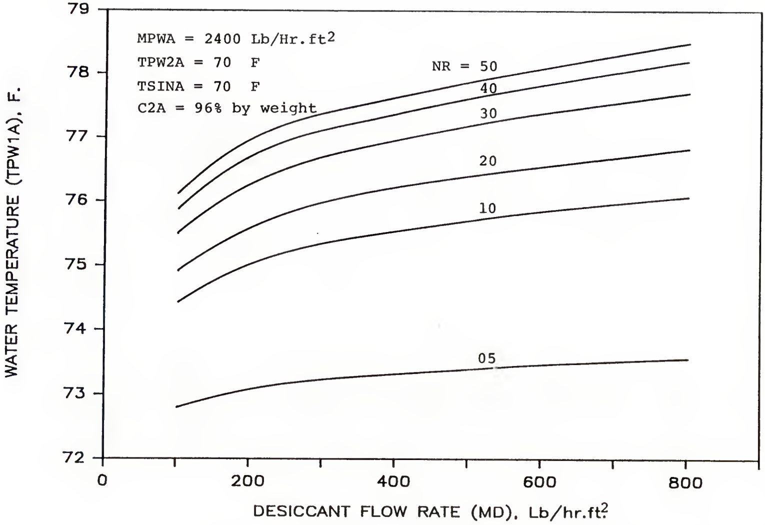

Figure 5-8: Outlet Temperature of Cooling Water versus Desiccant Flow Rate for different Packing Depths.

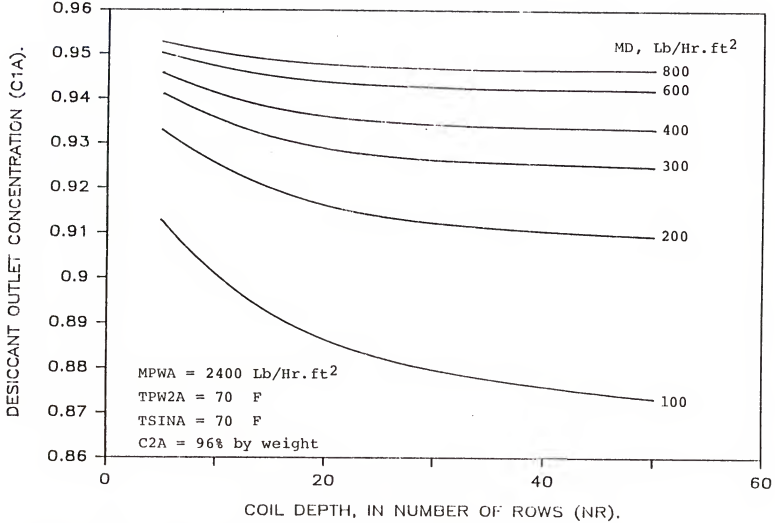

Figure 5-9: Concentration by Weight of the Desiccant Solution Leaving the Absorber versus Packing Depth, for different Desiccant Flow Rates

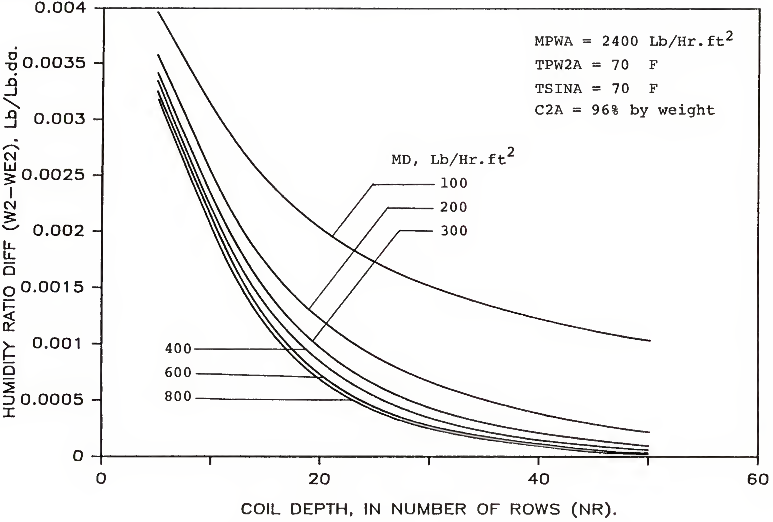

Figure 5-10: Mass Transfer Driving Potential at top of Absorber versus Coil Depth, for different Desiccant Flow Rates.

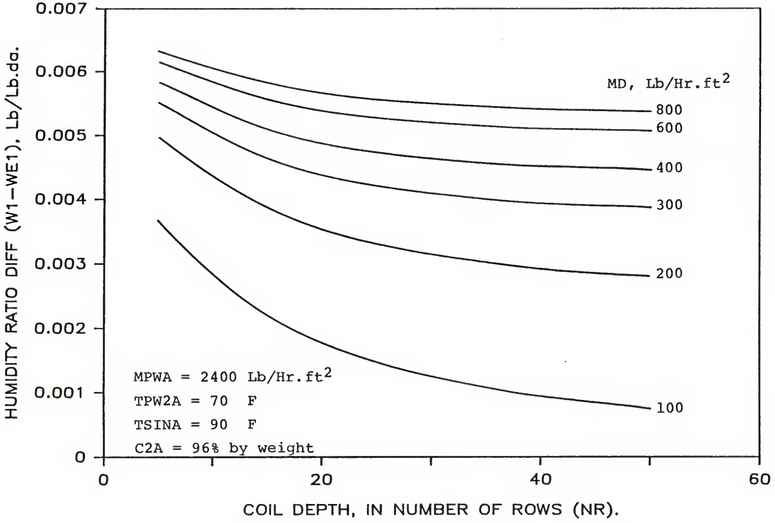

Figure 5-11: Mass Transfer Driving Potential at the Bottom of the Absorber versus Packing Depth, for different Desiccant Flow Rates.

solution at the local concentration and temperature. The inspection of those figures reveals that the driving potential for mass transfer is minimum a the bottom of the absorber for low desiccant flow rates, and is minimum at the top for larger flow rates. Less desiccant means lower solution concentration at the bottom of the contactor with less moisture absorbed. As a consequence, the water vapor pressure in the weak solution approaches that of the entering air; while, since less dehumidification occured, a larger mass transfer driving potential persists at the top of the absorber. Inversely, for larger desiccant flow rates, more dehumidification takes place and therefore the humidity ratio (W2) of air leaving the absorber approaches that of the entering solution (We_2), in equilibrium at the local inlet concentration and temperature. Meanwhile, although more moisture is absorbed, there is enough desiccant available that the solution leaves the absorber at a higher concentration, thus maintaining a larger mass transfer driving potential at the bottom of the contactor.

At this point of the analysis, one must recognize that the theoretical model, which is based on the inlet and outlet conditions, fails to describe the process conditions throughout the packing depth. This could present some problems if the operating conditions are such that the mass transfer driving potential is zero for the lower or upper part of the packing. An example for that would be the case with small desiccant flow rate, large packing depth, and small cooling water flow rate. Under such conditions, most mass transfer would take place in the upper part of the contactor; after which, the desiccant solution is both warm and dilute such that its equilibrium water partial pressure becomes too close or equal to the inlet air vapor pressure, and hence no further mass transfer occurs in the remaining lower part of the packing. The theoretical model, developed and used in this investigation, ignores that and considers that all the packing area participates evenly in the mass transfer operation. As a consequence, the accuracy as well as the validity of the model become questionable under those conditions.

In view of the discussion above, special care must be taken in recognizing the cases where the mass transfer occurs only in a part of the packing. The validity of the theoretical model is questionable under all conditions that yield such cases, which anyway correspond to less efficient designs and should be avoided. The presence of such conditions may be recognized: a) if the theoretical model does not converge or requires an unreasonably large number of iterations for convergence, b) by checking how close the mass transfer is from its asymptotic maximum as the packing depth is changed.

5.1.2. Effect of cooling water flow rate and inlet temperature

Figures 5-12 through 5-14 represent the air conditions

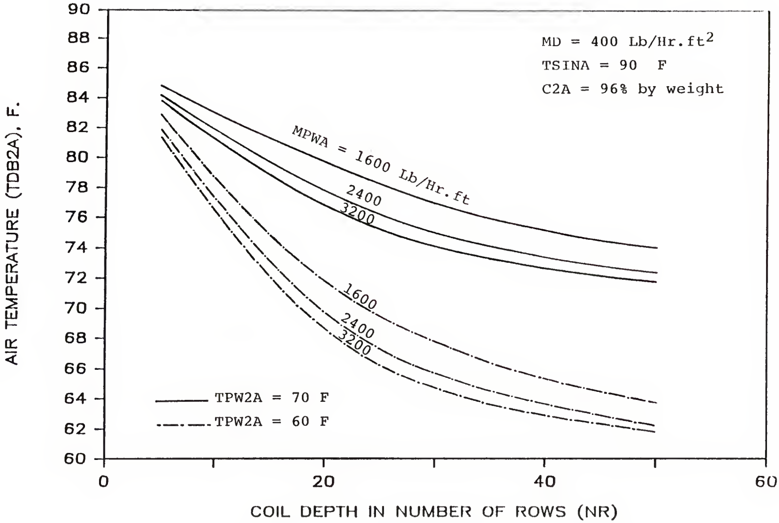

Figure 5-12: Temperature of Air Leaving the Absorber versus Coil Depth, for different Cooling Water Flow Rates and Inlet Temperatures.

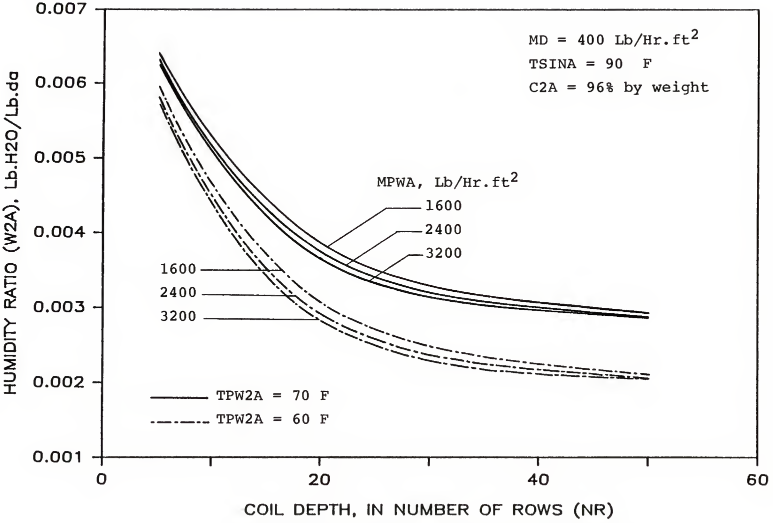

Figure 5-13: Humidity Ratio of Air Leaving the Absorber versus Coil Depth, for different Cooling Water Flow Rates and Inlet Temperatures.

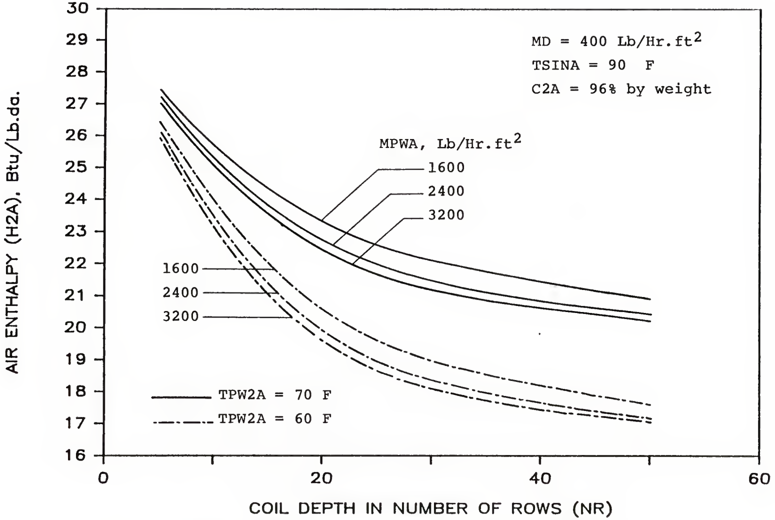

Figure 5-14: Enthalpy of Air Leaving the Absorber versus Coil Depth, for different Cooling Water Flow Rates and Inlet Temperatures.

leaving the absorber versus the coil depth and for different cooling water flow rates and inlet temperatures. The cross examination of the curves shows that larger cooling water flow rates result in dryer and cooler air leaving the absorber. More cooling water means larger heat capacity, which permits keeping the desiccant cooler throughout the packing, and thus enhances the mass transfer by lowering the equilibrium water partial pressure in the desiccant solution. In addition, the resulting larger air-to-water temperature differential and higher liquid side heat transfer coefficient lead to a better cooling of the air stream. At large flow rates and large coil depths, the curves approach certain asymptotic limits. Those limits correspond to the inlet water temperature (TPW2) and to the vapor pressure of water in the desiccant solution at the inlet temperature and concentration.

The comparison of the curves corresponding to different water inlet temperatures (same figures), shows that cooler cooling water results in the same effects as those of larger water flow rates. That is as expected since both cases lead to lower operating temperatures.

The results, discussed above, emphasize the advantage of non adiabatic contactors; namely, more efficient mass transfer. The equilibrium water partial pressure is lowered by cooling the desiccant instead of using higher concentrations, which would require higher regenerating temperatures and consequently less efficient or more expensive solar collectors.

5.1.3. Effect of the solution inlet concentration and temperature

The effect of the solution inlet conditions on the absorber performance are illustrated in Figures 5-15 through 5-18. For a given inlet concentration, warmer desiccant introduces more sensible heat to the process. As a result the air leaves the absorber at a higher temperature (Figure 5-15); and since the desiccant is then slightly warmer throughout the contactor, less dehumidification takes place (Figure 5-16) due to the resulting higher equilibrium water partial pressure in the aqueous solution. This shows the importance of precooling the desiccant, which can easily be done by a solution-to-solution intercooler.

As the inlet concentration is decreased, the desiccant solution becomes less capable of absorbing moisture as clearly seen in Figure 5-18. A minimum concentration is however required if any dehumidification is to occur. At that minimum, which is 84% by weight for the set of conditions of Figure 5-18, the equilibrium water partial pressure in the desiccant solution equals that of inlet moist air and the mass transfer driving potential becomes zero. Under those conditions, there is no dehumidification regardless of the packing depth, and the process reduces to a simple heat transfer problem. If the inlet concentration

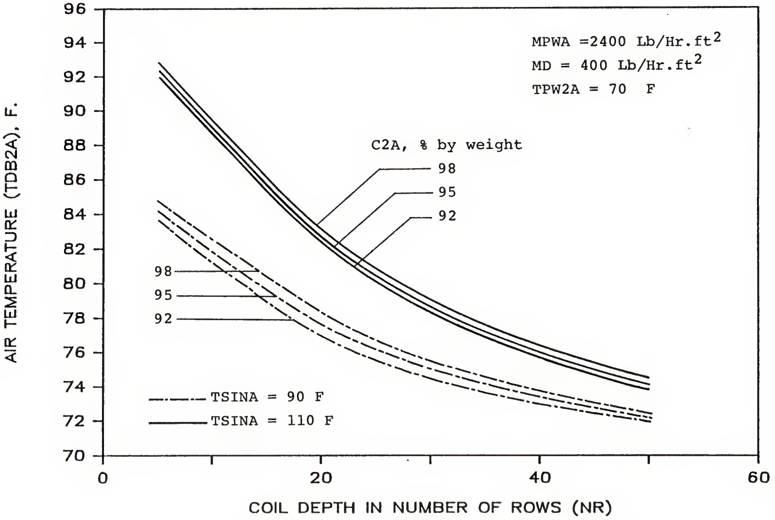

Figure 5-15: Temperature of Air Leaving the Absorber versus Coil Depth, for different Desiccant Solution Inlet Concentrations and Temperatures.

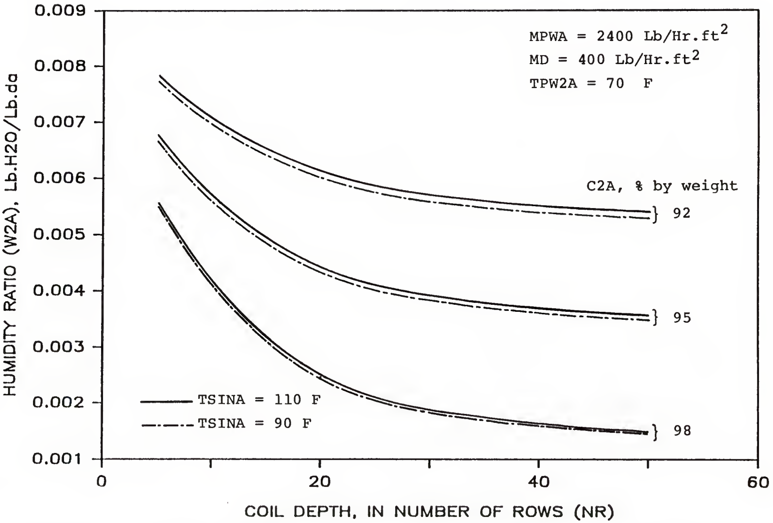

Figure 5-16: Humidity Ratio of Air Leaving the Absorber versus Coil Depth, for Different Desiccant Solutions Inlet Concentrations and Temperatures.

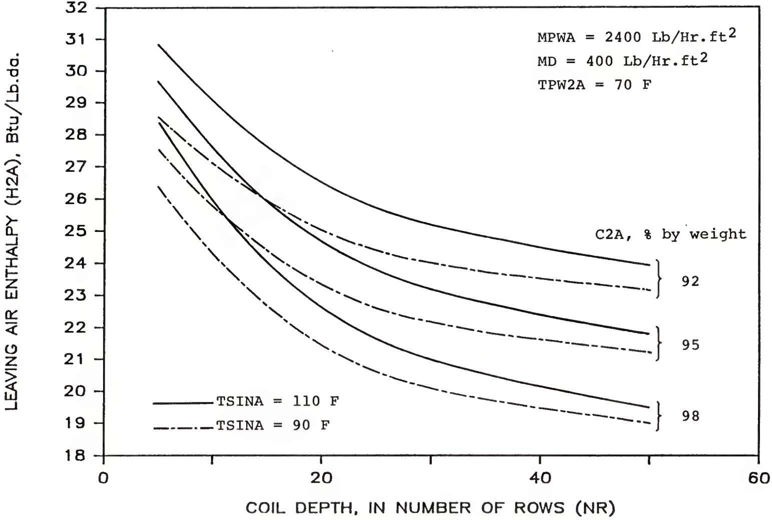

Figure 5-17: Enthalpy of Air Leaving the Absorber versus Coil Depth, for different Desiccant Solution Inlet Concentrations and Temperatures.

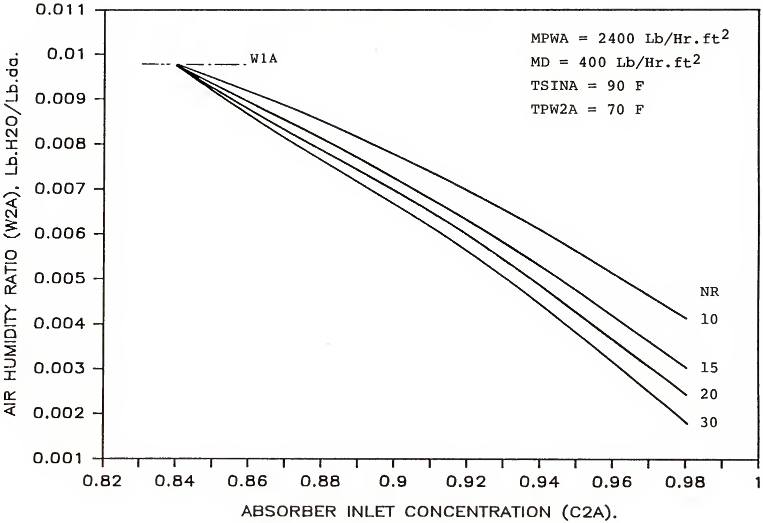

Figure 5-18: Humidity Ratio of Air Leaving the Absorber versus Desiccant Solution Inlet Concentrations, for different Coil Depths.

was further reduced, the process would be reversed and water would be removed from the dilute desiccant solution.

By analogy to the above conclusions, it can be deduced that, for each desired degree of dehumidification, there is a minimum solution concentration required. If sufficient packing is available for mass transfer, then the water vapor pressure of moist air, leaving the absorber, approaches that of water in the desiccant solution in equilibrium at that minimum concentration and local temperature.

5.2. Regenerator Parametric Analysis

The regenerator considered in this work consists of a contactor packed with finned-tube coils, and exactly similar to the absorber. The interacting heat and mass transfer operations are governed by the same equations. The only difference between the regenerator and absorber resides in the operating temperatures, which control the direction of mass transfer. When the process is cooled, the water partial pressure in the desiccant solution is lower than that of the moist air and hence causing the dehumidification. Inversely, when the desiccant solution is heated, its water partial pressure becomes higher than that of the moist air, therefore reversing the mass transfer driving potential and causing the water removal from the solution.

The above comparison between the regeneration and dehumidification processes shows that one is the inverse of the other. For that reason, the effects of the different controlling parameters are expected to be reversed too, and therefore a detailed qualitative analysis of the regenerator is judged unnecessary. In the following, only the effects of certain key parameters are investigated in order to gain a quantitative feeling of the regeneration process, and to deduce its requirements and limitations such as regenerating temperature and maximum obtainable concentration.

As done with the absorber, the regenerator analysis was performed on a one square foot cross-section basis. The same air flow rate of 1600 Lb/hr.ft^2 of dry air and similar finned-tube configuration were also used. Hot and humid outside air (93°F dry bulb and 55% relative humidity, a typical summer weather conditions for Gainesville, Florida) was used for the desiccant regeneration. The regenerator was assumed to be coupled to a 30 rows deep absorber, operating with a desiccant flow rate of 400 Lb/hr. ft^2, and cooled with available water which is at 70°F. An air-to-air heat exchanger (heat pipes), with a recovery efficiency of 60% [71], was inserted to recuperate the energy carried by the exhaust air, otherwise rejected into the environment. The liquid desiccant was pumped through a solution-to-solution intercooler, with an effectiveness taken as 80%, before entering the regenerator.

The effects of the packing depth and of the hot water flow rate and temperature on the regeneration process were investigated in order to determine the design requirements

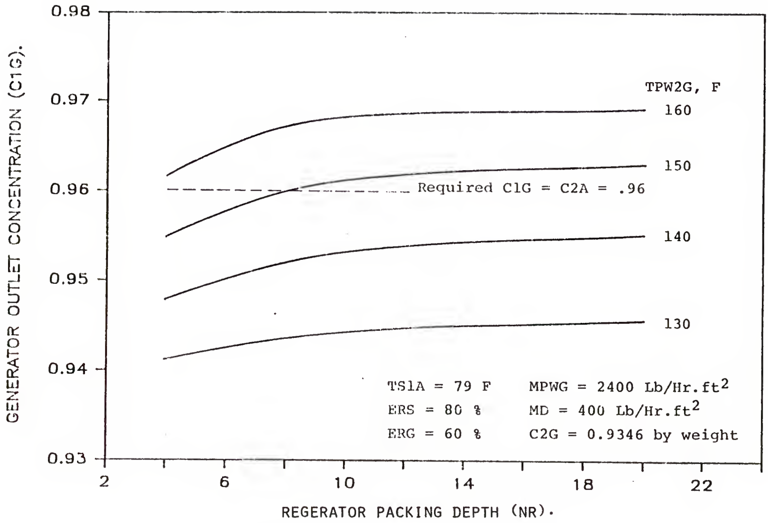

Figure 5-19: Desiccant Outlet Concentration (by weight) versus Packing Depth, for different Hot Water Inlet Temperatures.

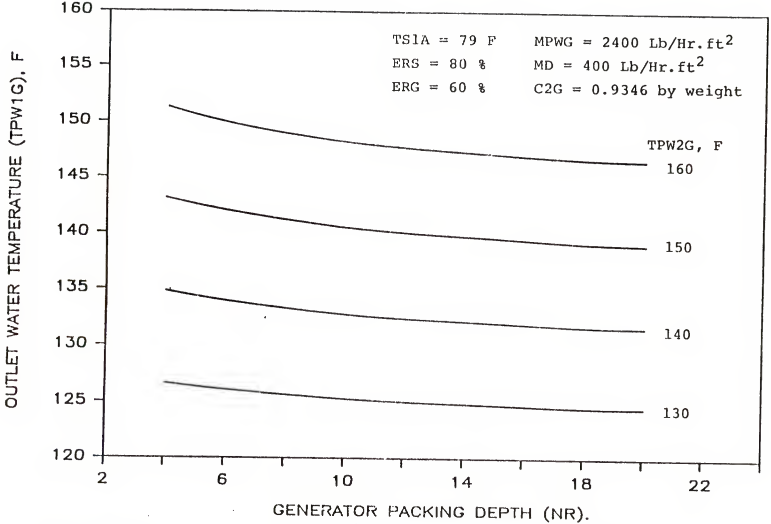

Figure 5-20: Hot Water Outlet Temperature versus Packing Depth, for different Inlet Water Temperatures.

to reactivate a dilute desiccant solution to a given concentration. Figures 5-19 and 5-20 show the outlet desiccant concentration (C1) and the process water temperature (TPW1) in terms of the packing depth, and for different regenerating temperatures and a constant heating water flow rate of 2400 Lb/hr. ft^2. The desiccant solution was assumed to come from the absorber at a 93.46% concentration by weight and at 79°F, conditions that would result if a 96% strong solution was used in the dehumidification process. It can be observed from those figures that higher hot water inlet temperatures and/or larger packing depths result in warmer and more concentrated desiccant solutions leaving the regenerator. For each inlet temperature, there is a maximum obtainable concentration. That maximum corresponds to the limit where the leaving desiccant temperature and concentration are such that the solution equilibrium water partial pressure approaches that of the entering air. For illustration, it can be deduced from Figure 5-19 that at least an inlet hot water temperature about 147°F is required to reactivate the desiccant solution to a concentration of 96% by weight.

Figures 5-21 and 5-22 represent the same parameters but for a different water flow rate of 1600 Lb/hr. ft^2. The cross examination of the results for the two flow rates considered permits the conclusion that, for a given regenerating temperature, larger water flow rates result in more regeneration and higher attainable maximum

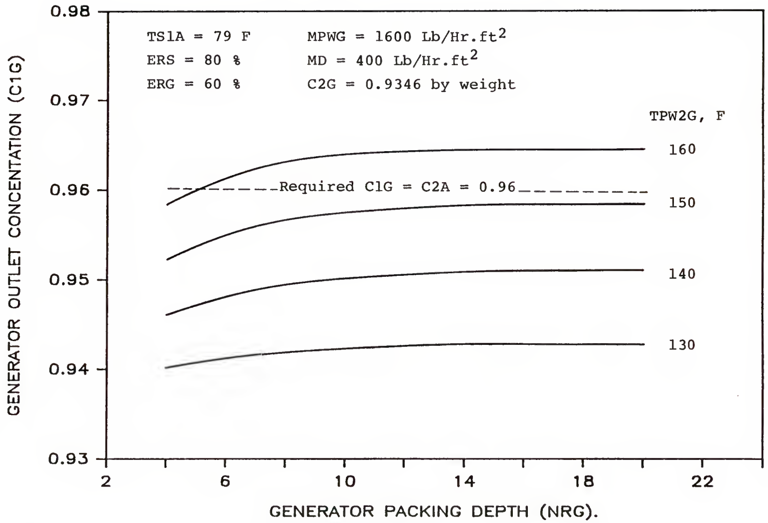

Figure 5-21: Desiccant Outlet Concentration (by weight) versus Packing Depth, for different Inlet Water Temperatures.

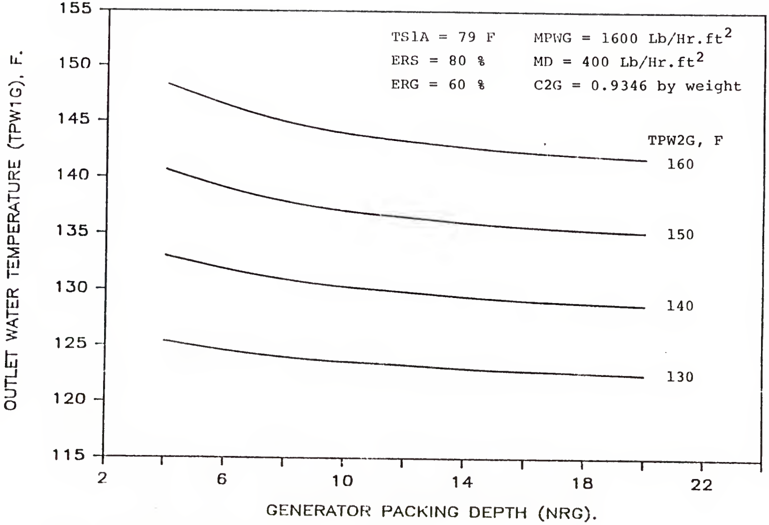

Figure 5-22: Hot Water Outlet Temperature versus Packing Depth, for different Inlet Water Temperatures.

concentrations. Larger heating water flow rates permit to maintain the process at a higher temperature due to their larger heat capacities. The desiccant solution is therefore warmer throughout the contactor and particularly at the bottom, where the solution concentration must be higher for the equilibrium water partial pressure to approach the same inlet air vapor pressure. Those effects of the heating water flow rate are better visualized in Figure 5-23, which also shows that, for a given regenerator size, there is a combination of minimum water flow rate and inlet temperature required for the regeneration of the desiccant to a specified concentration.

Although deeper packings and higher hot water inlet temperatures and flow rates result in a more concentrated solution, which in turn permits more dehumidification, they also increase the heat transfer driving force between the air stream and the finned-tube arrangement. The humid regeneration air is then exhausted at higher temperatures. Unless appropriate measures are taken to recover the sensible energy, otherwise rejected in the environment by the warmer exhaust air, the advantage of the resulting higher concentration available for the dehumidification process may be offset by the larger exhaust thermal losses. This shows the importance of the air-to-air recovery heat exchangers inserted in this desiccant system.

A similar analysis was performed for the regeneration of a 91.23% concentration by weight solution, that would

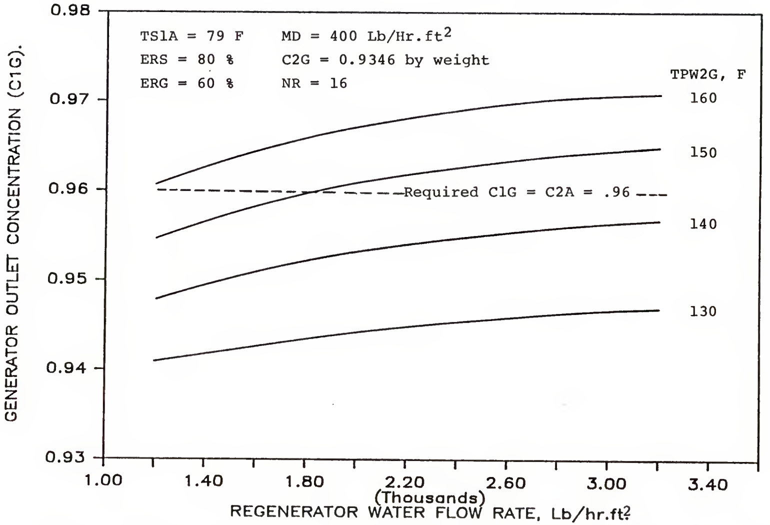

Figure 5-23: Desiccant Outlet Concentration (by weight) versus Process Water Flow Rate, for different Regenerating Temperatures.

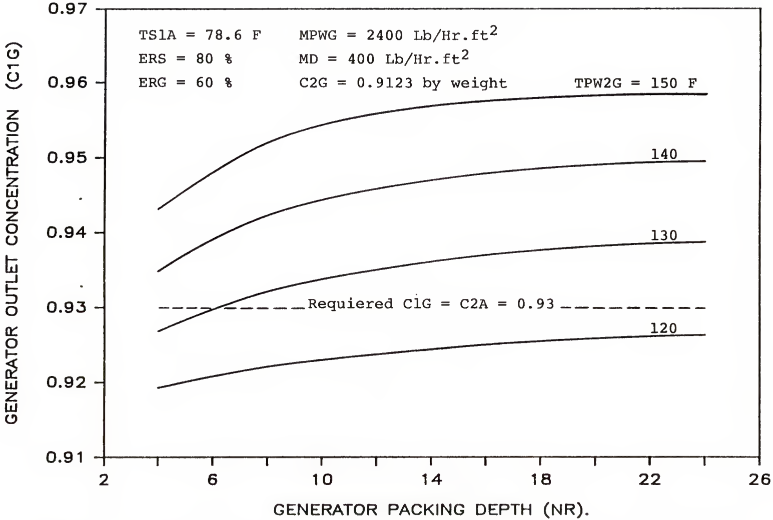

Figure 5-24: Desiccant Outlet Concentration (by weight) versus Packing Depth, for different Regenerating Temperatures.

result if a 93% strong solution was used in the absorber. The results showed the same parametric variation trends, and Figure 5-24 pictures some of them for comparison purposes.

The cross examination of Figures 5-19 and 5-24 confirms that, with larger working concentrations, the regeneration becomes more difficult and requires higher regenerating water temperatures and/or flow rates. Obvious consequences are the lower efficiency of the solar collectors and the larger energy losses carried by the exhaust air in the form of sensible heat. This emphasizes again the advantage of cooling the desiccant during the dehumidification process. As previously discussed, cooled absorbers require less concentrated solutions to dry moist air to a given humidity ratio. Those lower concentration requirements were the result of lowering the equilibrium water partial pressure by cooling the desiccant solution instead of using higher concentrations.

CHAPTER VI
SYSTEM DESIGN AND OPTIMIZATION

In the previous chapter, the absorber and regenerator were analyzed separately and on a one square foot cross section basis. In this chapter, they are coupled together for a continuous operation, and sized to produce a given design cooling load. The computer code DESYST, discussed in Chapter IV, is used to link dehumidification and regeneration processes and to optimize the key controlling parameters based on economic criteria.

6.1. Liquid Desiccant Air-Conditioner Design Procedure

In this desiccant air-conditioner, moist air is first simultaneously dehumidified and sensibly cooled, then evaporatively cooled to a temperature and humidity that satisfy both sensible and latent design loads.

Since heat losses through exterior walls and heat added by the water recirculation pump are small and may be ignored, then the evaporative cooling may be considered as a constant enthalphy process. As a consequence, the cooling effect of a desiccant air-conditioner may be expressed as

$$Q_T = \dot{M}_{a,A} (H_R - H_{2A}) \tag{6-1}$$

where Q_T is the total cooling load, latent and sensible, $M_{a,A}$ is the absorber dry air low rate, H_R and H_{2A} are the moist air enthalpies at room conditions and leaving the absorber, respectively. The sensible portion of the total load is controlled by the saturation efficiency of the evaporative cooler and may be given by

$$Q_S = \dot{M}_{a,A} \cdot Cp_a (T_R - T_{EEC}) \tag{6-2}$$

where T_R and T_{EEC} are the dry bulb temperatures at room conditions and at the exit of the evaporative cooler, respectively, and Cp_a is the moist-air specific heat. Equation 6.2 may be rearranged to give the required absorber air flow rate if the other parameters are specified

$$\dot{M}_{a,A} = \frac{Q_s}{Cp_a (T_R - T_{EEC})} \tag{6-3}$$

Since the analysis of both absorber and regenerator was based on a square foot cross-section, then for a desiccant air-conditioner with a specified design load (sensible and latent) the actual contactors cross-sction A_{cs} should be

$$A_{cs} = \frac{\dot{M}_{a,A}}{\dot{M}''_{a,A}} \qquad (6\text{-}4)$$

where $\dot{M}''_{aA}$ is the dry air flow rate per square foot cross-section used in the parametric analysis; in this work a value of 1600 Lb/hr. ft^2 was selected. All other flow rates per square foot cross-section, namely that of process water and desiccant, are accordingly multiplied by A_{cs} to give the total requirements.

In air conditioning applications, the supply air temperature is preferred to be as low as possible in order to minimize the air flow rate and consequently reduce the fan power costs. Because of condensation problems, however, that temperature must be larger than the room air dew point ($T_{dp,R}$), generally by at least 3°F. This practical limitation creates an extra constraint to consider in the design of a desiccant air-conditioner as follows.

As a reference, consider the case where the supply air conditions are such that $T_s = T_{dp,R} + 3°F$. The supply air mass flow rate ($\dot{M}_{a,s}$) and enthalpy (H_s) are then given by

$$\dot{M}_{a,s} = \frac{Q_S}{Cpa\ (T_R - T_S)} \qquad (6\text{-}5)$$

$$H_S = H_R - \frac{Q_T}{\dot{M}_{a,s}} \qquad (6\text{-}6)$$

Depending on the enthalpy H_{2A} of the moist air leaving the absorber, three design possibilities rise:

1. IF $H_{2A} = H_S$, the supply conditions may be directly obtained by evaporative cooling with appropriate saturation efficiency.

2. IF $H_R > H_{2A} > H_S$, the supply conditions H_S and T_S can not be obtained by evaporative cooling. However, although it might not be economical, the cooling load may still be achieved with a larger air flow rate that is then given by

$$\dot{M}_{a,A1} = \frac{Q_T}{H_R - H_{2A}} \tag{6-7}$$

and the corresponding new supply temperature, that should be obtained by evaporative cooling, becomes:

$$T_{S1} = T_{EEC} = T_R - \frac{H_R - H_{2A}}{Cp_a} \cdot \frac{Q_S}{Q_T} \tag{6-8}$$

3. If $H_{2A} < H_s$, then a room-air bypass is necessary to meet both sensible and latent loads without condensation problems. The adiabatic mixing of moist air leaving the absorber and the bypassed room-air, such that the final conditions are H_s and T_s, may be described by

$$(\dot{M}_{a,A} + M_{a,Bp})\ H_s = \dot{M}_{a,A}\ H_{2A} + \dot{M}_{a,Bp}\ H_R \tag{6-9}$$

$$(M_{a,A} + \dot{M}_{a,Bp})\ C_{pa}\ (T_R - T_S) = Q_s \tag{6-10}$$

where $\dot{M}_{a,Bp}$ is the dry air flow rate of the room-air bypass. Simultaneous solution of the above equations permits the deductuiion of the individual flow rates as

$$\dot{M}_{a,A} = \frac{Q_s}{C_{pa}\ (T_R - T_s)} \left(\frac{H_R - H_s}{H_R - H_{2A}}\right) \tag{6-11}$$

$$\dot{M}_{a,Bp} = \frac{Q_s}{C_{pa}\ (T_R - T_s)} - M_{a,A} \tag{6-12}$$

The corresponding required temperature of air leaving the evaporative cooler may be determined either graphically from a psychrometric chart or from the relation

$$T_{EEC} = T_R - \frac{Q_s}{\dot{M}_{a,A}\ Cp_a} \tag{6-13}$$

For each of the above cases, the evaporative cooler must have a saturation effectiveness that gives the required exit air conditions.

In order to fully operate the desiccant air-conditioner by solar energy, the solar collectors and the energy storage system must be sized according to the local climatic conditions, and such that they provide enough energy to operate the cooling system as needed. For Gainesville, Florida, based on previous work and on a sequence of two successive overcast days at worse, the collectors and the storage system are sized such that a) the daily solar collection equals the daily energy requirement, and b) the stored energy equals the energy requirements for a period of 2 days.

The daily energy requirement (Q_D) of a cooling system may be estimated by

$$Q_D = \frac{Q_T \cdot \mathrm{DFLEOH}}{\mathrm{COP}} \tag{6-14}$$

where DFLEOH is the daily full load equivalent operating hours, taken in this work as 10 hours/day, and COP is the systems coefficient of performance. The area (Ac) of the solar collectors is then determined from

$$Ac = \frac{Q_D}{Q_D''} \tag{6-15}$$

where Q_D'' denotes the average daily solar collection per unit area, 1000 Btu/ft^2 day for Gainesville, Florida. Finally, if water is used as storage means with a temperature drop of 50°F, then the storage capacity can be directly related to the collector area as 4 gallons per ft^2.

From the above design discussion and the results of the parametric analysis, it is obvious that the performance of a liquid desiccant air-conditioner, as well as its cost and operating power requirements, are strongly dependent on several controlling parameters. An optimization is therefore necessary to give the best design configuration.

6.2. Optimization Procedure

Depending on the use of equipment, different criteria could be used as a basis for optimization of cooling systems; namely: performance, initial cost, operating cost, and life cost. Since in most cases the user buys and operates the system, the life cycle criterion is selected for the optimization of the liquid desiccant air-conditioner.

The results of the optimization analysis presented here are based on a 3 ton unit, fully powered by solar energy and designed to operate in Gainesville, Florida. A generator temperature of 140°F, which is easily obtainable by available flat-plate collectors, is selected. All parameters, of which optimization was not required, are the same as specified or selected earlier in the parametric analysis and are summarized at the end of this section for convenience. Instead of using a constant effectiveness for the countercurrent air-to-air recovery heat exchanger and the solution-to-solution intercooler, a constant temperature difference between the fluids involved was imposed at each end of the recovery unit. That is more realistic since it permits to size and price the recovery heat exchangers in terms of the available temperature differentials instead of maximum recoverable energy. The remaining parameters that need optimization are:

1) Cooling water flow rate, MPWA
2) Heating water flow rate, MPWG
3) Desiccant flow rate, MD
4) Absorber packing depth or coil number of rows, NR_A
5) Regenerator packing depth or coil number of rows, NR_G

The objective of the optimization analysis is to determine the combination of the above five parameter that yield the minimum present worth value, calculated over a given project life. It must however be kept in mind that the range of variation of each of the above variables is bounded by practical limitations such as availability, feasibility and noise control. Because of the complex interaction between the different variables, the following successive iteration method was used:

a) To begin the iterative approach, initial values were assumed for each parameter. In order to minimize the number of iterations required to achieve convergence, those initial values were selected, based on experience, to represent conditions that approached maximum mass transfer.

b) In this iterative technique, a new optimized value is generated while holding the other four values constant. This optimum value is determined graphically based on a minimum present worth value. As a new optimized value is created, it replaces the old one. Each of the five parameters is considered in sequence until no significant changes occur in any of the five values. The most recent combination represents the desired solution of the optimization problem.

The present worth calculations are detailed in Appendix C, which also includes initial and operating cost estimations as well as seasonal energy requirements. Since the solar collectors and storage system can also be used for heating and domestic hot water purposes, only a fraction of their cost was charged to the cooling system. That fraction was determined as the ratio of seasonal energy requirements for cooling to the annual energy requirements for heating, domestic hot water and cooling, see Appendix C.

The above iterative procedure was applied to a system with a design cooling load of 3 tons, based on a project life of 20 years, a cost of money of 10%, and an electricity exalation rate of 8%. The results of the last iteration are summarized in Figures 6-1 through 6-5, which show the present worth values as well as the initial and operating costs versus the parameters optimized.

No minimum present worth value was found as the cooling and heating water flow rates were changed, and noise criteria into the pipes were used to limit the maximum water flow rate to 3200 Lb/hr. ft^2, refer to Figures 6-1 and 6-2. Higher water flow rates improve the thermal performance of the system, and result in a smaller system size and therefore in lower initial cost and lower present worth as long as the operating costs do not become excessive. In this case, although the water pumping cost increases with higher water flow rate per unit cross-section area, the overall operating cost decreases because of the savings made in the electric requirements of blowers and desiccant pumps. That results from the lower contactor cross section and hence lower desiccant and air flow rates required to handle the same cooling load. The operating costs could become important if cooling water was pumped from a deep well instead of the shallow one considered here, and would then lead to a minimum present worth value and an optimum cooling water flow rate.

As the desiccant flow rate increases, the concentration remains higher throughout the absorber and therefore results in more dehumidification and consequently in better thermal performance, lower present worth and lower initial and operating costs. However, after a certain optimum value, the larger sensible heat introduced by the desiccant offsets the advantage of higher working concentrations and hence

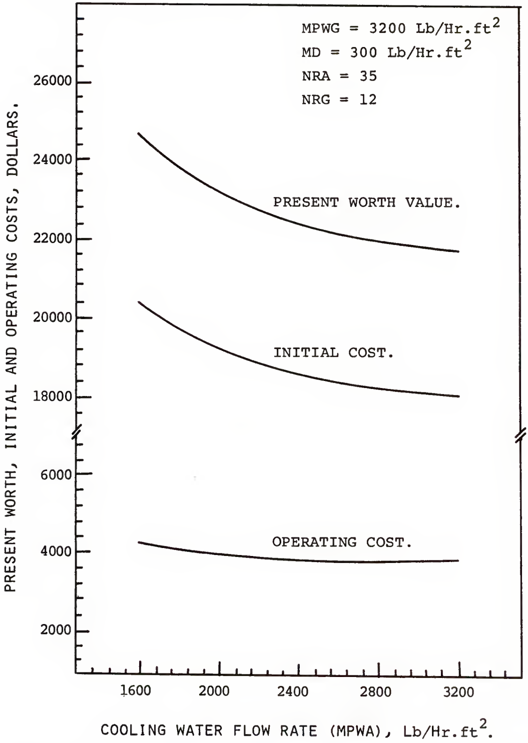

Figure 6-1: Present Worth, Initial, and Operating Costs versus Absorber Process.

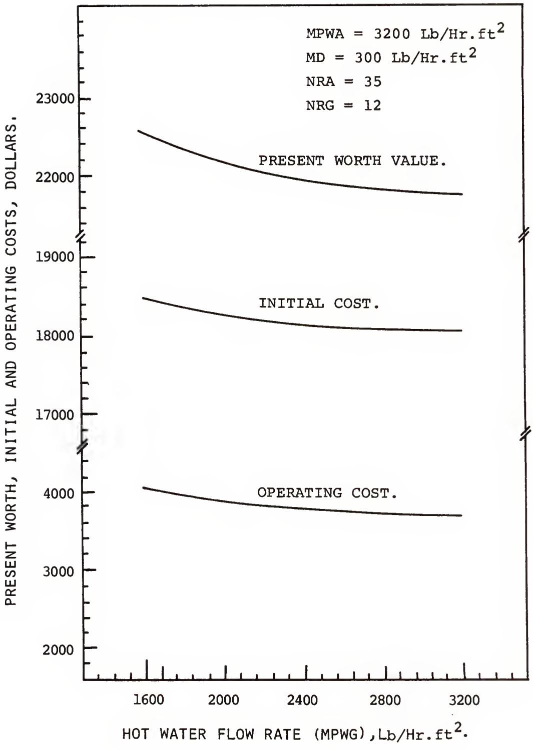

Figure 6-2: Present Worth, Initial, and Operating Costs versus Regenerator Process Water Flow Rate.

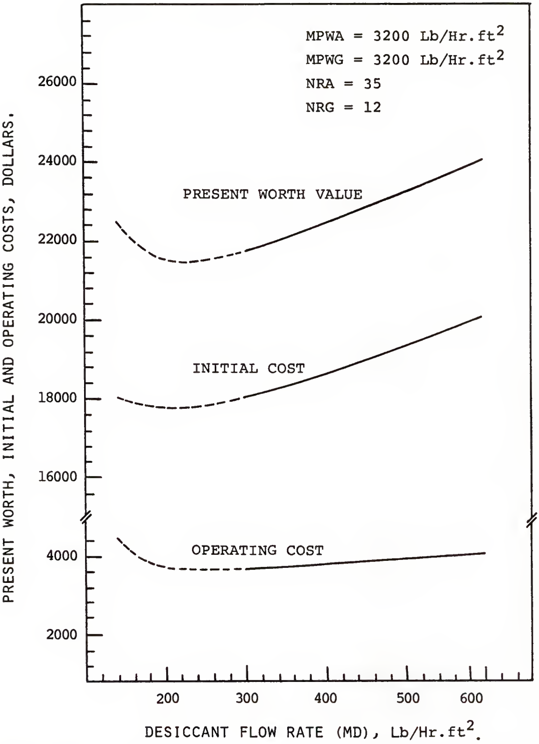

Figure 6-3: Present Worth, Initial, and Operating Costs versus Desiccant Flow Rate.

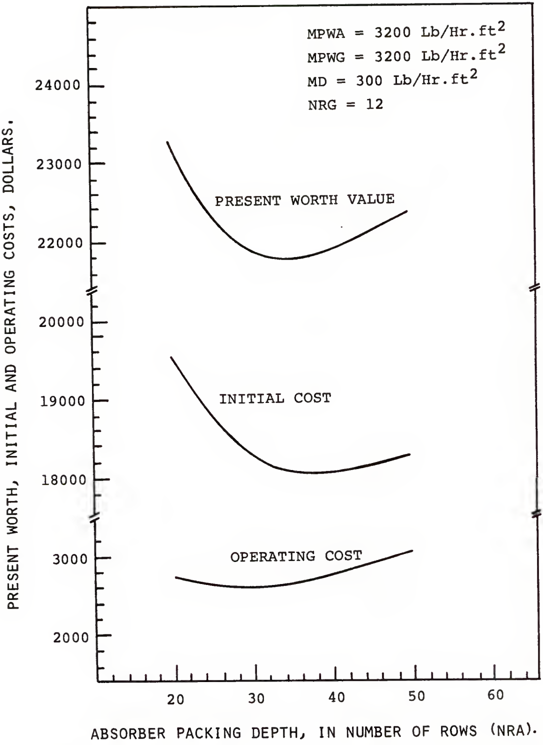

Figure 6-4: Present Worth, Initial, and Operating Costs versus Absorber Packing Height.

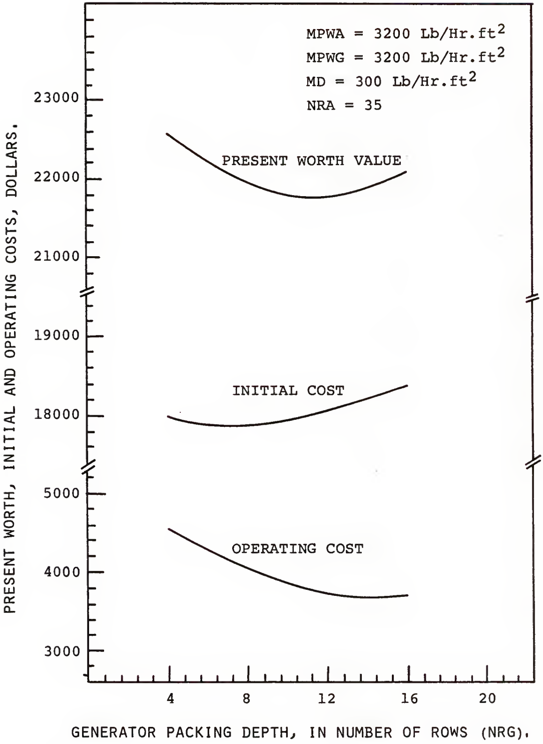

Figure 6-5: Present Worth, Initial, and Operating Costs versus Regenerator Packing Height.

leads to higher costs. That optimum desiccant flow rate was found to be around 200 LB/hr. ft^2 (Figure 6-3); but, based on the experimental work and due to the high desiccant viscosity, a minimum value of 300 Lb/hr. ft^2 was selected to insure an efficient and uniform spray, especially at the absorber where the desiccant enters cool and therefore more viscous.

As the depth of the finned-tube heat exchangers in the absorber is increased, more dehumidification and cooling of moist air are achieved. That improves the performance of the desiccant air-conditioner and therefore reduces the contactors cross-section area and hence the mass flow rates required to handle the same cooling load. Although more money is invested in the finned-tube coils, the savings from the smaller cross-section size are greater and yield a lower overall initial cost as illustrated in Figure 6-4. Similarly, with lower contactor cross-section, less overall flow rates are required and hence the total savings in operating costs offset the higher flow resistance met in the deeper packing and lead to lower operating costs, refer to the same figure. However, after a certain optimum value, further increase in coil depth improves slightly the thermal performance of the system, but the additional initial investment and operating costs become large enough to offset it. The sum of the operating and initial costs give the present worth values, which present a minimum at an optimum coil depth of 35 rows as illustrated by Figure 6-4.

Deeper packing in the regenerator permits more desiccant reactivation and therefore improves the performance of the system and makes it more economic as long as the additional initial investment and operating cost are not excessive. The results of the economic analysis for different regenerator packing depths are, as expected, qualitatively similar to those found with different packing depths in the absorber, as shown by figure 6-5. The major quantitative difference is noticed in the smoother variation of the initial cost at low coil depths. That is attributed to the fact that the smaller and much less expensive air-to-air recovery heat exchanger, used to recuperate energy from the resulting cooler exhaust air, compensates for the cost increase due to the larger contactor cross-section required.

The final dimensions, flow rates, concentrations, temperatures and humidities of the optimized desiccant air-conditioning system are summarized in Tables 6-1 and 6-2. It is nevertheless worth noting that different optimum conditions would result if the optimization was based on other criteria such as minimum initial or operating costs, which would be desired if one had to pay only for either the initial or the operating costs, respectively.

Table 6-1. Characteristics of the Optimized Liquid Desiccant Air Contactors

Parameter	Absorber	Regenerator
Coil depth, in number rows	35	12
Packing cross section area, ft^2	2.58	2.58
Finned tube surface effectiveness	0.75	0.75
Wetting factor	0.5	0.5
Air flow rate, Lb.da/hr	4128	4128
Air inlet temperature, °F	78	117.9
Air inlet humidity Lb H_2O/Lb.da	0.0103	0.0183
Air outlet temperature, °F	72.8	133.9
Air outlet humidity, Lb.H_2O/Lb.da	0.00349	0.0251
Process water flow rate, Lb/hr	8256	8256
Inlet water temperature, °F	70	140
Outlet water temperature, °F	75.0	133.5
Desiccant flow rate Lb/hr.	774	774
Desiccant inlet temperature, °F	85.6	121.9
Desiccant inlet concentration	0.9558	0.9238
Desiccant outlet concentration	0.9238	0.9558

Table 6-2. Overall Design Characteristics of the Optimized Liquid-Desiccant Air-Conditioning system.

Outside design conditions:	$T_{db} = 93°F$, $T_{WB} = 76°F$
Room design conditions:	$T_{db} = 78°F$, $T_{WB} = 65°F$
Supply air conditions:	$T_{db} = 61°F$, T_{WB}
Air conditions at exit of evaporative cooler:	$T_{db} = 54.5°F$, $T_{WB} = 53°F$
Room air bypass flow rate:	2549 Lb da/hr.
Coefficient of performance:	67.47%
Solar collector area:	640 ft^2
Storage capacity:	2560 gallons
Solution intercooler effectiveness:	0.822
Air-to-air recovery heat exchanger effectiveness:	0.602

The air side pressure drops through the finned-tube packings of the optimized system were computed using the relations presented in Section 4.1. An air pressure drop of 2.4 inches of water was found in the absorber and 0.77 inches of water in the regenerator. All other pressure drops through the system components are summarized in

Appendix C for the three working fluids (air, desiccant and water). Assuming a 70% total efficiency for the blowers and pumps, the total electric energy used by the system was then computed as 1.3 Kw. This is considerably lower that required by a comparable solid desiccant unit, which provides only 2 tons of cooling [14].

After taking into account the total electrical energy use and the efficiency of the solar collectors, which was assumed equal to 50%, the overall coefficient of performance of the liquid desiccant system was determined as 31.2%. The system requires a solar collector area of 640 ft^2, based on a daily average solar collection of 1000 Btu/ft^2 day.

6.3. System Performance at Other than Design Regenerating Temperature

The storage water temperature fluctuates depending on both solar collection and amount of energy used to run the air-conditioner and for domestic hot water purposes. Table 6-3 below gives the coefficient of performance of the optimized desiccant system and the ratio of its cooling capacity to the design cooling load for different regenerating inlet water temperatures.

As opposed to their absorption counterparts, liquid desiccant systems can operate at regenerating temperatures far below the design value. In fact they have higher C.O.P.

at such lower regenerating temperatures and provide a partial cooling capacity, thus adjusting to the cooling requirements which are in phase with the solar radiation.

The decline in the C.O.P. at higher regenerating temperatures is attributed to the fact that a) more energy is lost with the exhaust air which leaves at higher temperatures, and b) more sensible heat is introduced in the absorber by the resulting warmer desiccant solution. The C.O.P. of the system would increase with higher regenerating temperatures if appropriate sizes of the recovery heat exchangers were used.

Table 6-3. System Performance at Other than Design Regenerating Temperature

TPW2G °F	Cooling capacity Design cooling load	C.O.P.
160	1.12	0.561
150	1.07	0.614
140	1.00	0.675
130	0.91	0.739
120	0.78	0.819
110	0.63	0.941

CHAPTER VII
EXPERIMENTAL ANALYSIS, RESULTS AND DISCUSSION

7.1. Description of the Experimental Apparatus

A liquid desiccant air conditioning prototype was designed and constructed from available equipment at the Mechanical Engineering Department, University of Florida. The experimental apparatus consists basically of · a) absorber, b) regenerator, c) evaporative cooler, d) desiccant intercooler, e) air duct heater, f) electric water heater, and j) various instrumentation. A schematic diagram and an overall photograph of the experimental set-up are shown in Figures 7-1 and 7-2, respectively.

Both contactors, absorber and regenerator, have approximately one square foot cross-section, and are constructed of galvanized sheet. They are insulated with one inch thick styrofoam, and packed with two finned-tube heat exchangers which are horizontally stacked on each other. The detailed dimensions of the finned coils are presented in Table 7-1.

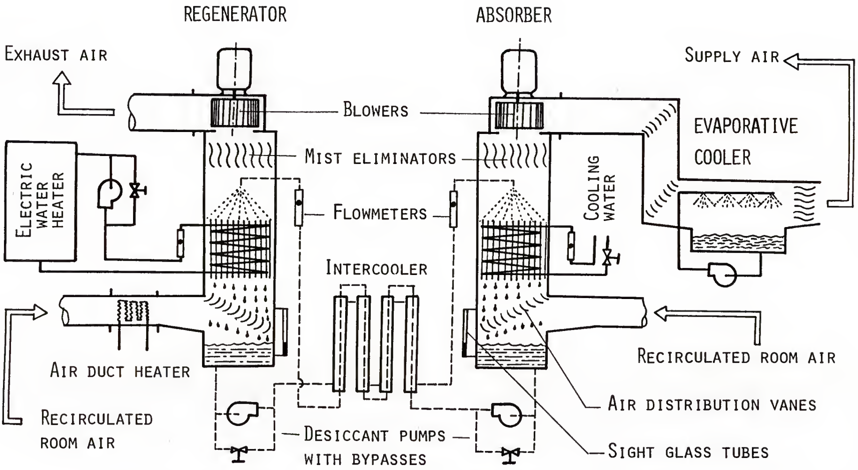

Figure 7-1: Schematic Diagram of the Experimental Liquid Desiccant Air Conditioner

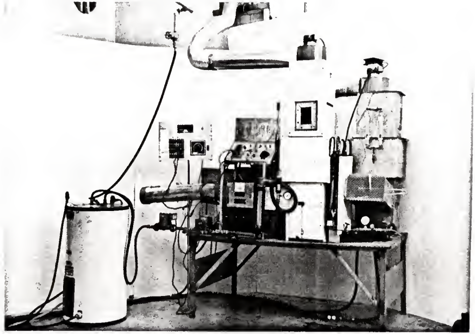

Figure 7-2: Overall View of The Experimental Liquid Desiccant Air Conditioner

Table 7-1: Dimensions of the Finned-Tube Heat Exchangers Used in the Experimental Prototype.

Variable	Absorber	Regenerator
Number of coils	2	2
Face area (inch x inch)	10 x 11	11 x 12
Total number of rows	11	10
Number of tubes per row	10	11
Tube length (inch)	10	11
Pipe outside diameter (inch)	0.525	0.525
Pipe inside diameter (inch)	0.487	0.487
Distant between tubes (inch)	1.25	1.25
Distance between rows (inch)	1.25	1.25
Number of fins per inch ($inch^{-1}$)	11	6.0
Number of tubes fed	2	1
Aluminum fin thickness (inch)	0.006	0.006

The air circulation is insured by a blower mounted on the top of each contactor. This permits the reation of a vacuum in the contactor and therefore reduces possible leak problems of liquid desiccant. To have an even air flow distribution through the finned-tube packings and the evaporative cooler, vanes were installed in all sharp corner of the air flow path.

A single full-jet nozzle, located about one foot above the coils, was used to spray the liquid desiccant over the packing. A screen was also inserted to further break the desiccant drops and improve the spray for a better liquid distribution. Mist eliminators are installed at the top of each contactor to minimize the loss of desiccant by entrainment. The desiccant drains down through the packing in the form of a falling thin-film, and is simply collected at the bottom of the contactors where sight glasses indicate the liquid levels.

To insure the continuity of the operation, two pumps are used to circulate the desiccant between the absorber and regenerator, with bypasses for flow rate adjustments. The desiccant solutions are pumped through a counterflow dual-pipe intercooler to preheat and precool the used and regenerated desiccants before they are sprayed, respectively. As a result, a warm solution reaches the nozzles in both absorber and regenerator where a better spray is obtained due to the consequent lower viscosity of the desiccant.

The evaporative cooler is basically a 1 ft x 3 ft x 1.5 ft spray chamber, with recirculated water. The water is sprayed through eight full-jet nozzles and mist entrainment is reduced by means of mist eliminators. A bypass around the water pump is used to adjust the flow rate and therefore control the saturation efficiency of the evaporative cooler.

An air duct heater is mounted at the regenerator air inlet, and preheats the recirculated room air to a temperature of 103°F. It is used to simulate the air-to-air recovery heat exchanger, which is supposed to reclaim the energy from the hot and humid exhaust air otherwise rejected into the environment.

City water at 74°F, available in the site where tests are conducted, is used as cooling process water; while an electric water heater simulates the solar collectors and supplies the hot water to the regenerator. A pump circulates the hot water in a closed loop between the heater and the regenerator. The water flow rate is controlled by means of a bypass, while the temperature is adjusted by varying the electric imput to the heating element through a variac.

The apparatus is also equipped with flowmeters to measure the water and desiccant flow rates, and with dry and wet-bulb temperature sensors to record the different steps of the process.

7.2. Experimental Procedure and Data Collection

In order to obtain meaningful and comparable data, it is necessary to perform an indoor or laboratory experiment. This permits the control and reproduction of the input conditions such as temperatures and humidities, which would otherwise fluctuate with weather conditions. In this experimental analysis, the liquid desiccant system was operated in a conditioned space, with the regenerator hot and humid exhaust air rejected to the environment. In this manner, both regenerator and absorber have the same air inlet temperature and humidity, which are relatively constant and controllable within the large conditioned laboratory.

After the system is turned on, the flow rates of the strong and weak solutions are adjusted until they are equal, therefore insuring the continuity of the operation. The system is then kept running until equilibrium conditions are reached, then data are collected. The dry and wet-bulb temperatures are measured with copper-constantan thermocouples and double checked with mercury thermometers. To keep the dry bulb temperature sensor at the exit of the evaporative cooler dry, a fine screen was mounted around the sensor to trap the mist entrained by the air stream. For wet-bulb temperature measurements, sensors are covered with gauze which is kept continuously wet by means of a wick connected to a small water container. The air flow rates are deduced from the measurement of area-weighed average air velocities, using a pitot tube velometer (Almor series 6000-P velometer). They are also double checked with a water-air sensible energy balance performed on the system with no desiccant flow ($M_W\ Cp_W\ \Delta T_W = M_a\ Cp_a\ \Delta T_a$). The liquid flow rates are recorded from the flowmeters readings and checked by timing the flow in a container of known volume. Desiccant samples are drawn and stored in sealed containers. They are later weighed on a high accuracy scale

(Mettler Balance H33AR) to determine their specific gravity and hence deduce their concentration. If the volume of the solution is assumed equal to the sum of its individual components (ideal solution), then the triethylene glycol concentration by weight may be deduced from the relation

$$C = \frac{\rho_D M - \rho_D \rho_W V}{M (\rho_D - \rho_W)} \tag{7-1}$$

where C denotes the concentration by weight (mass of desiccant per unit mass of solution), M is the mass of the sample, V is the volume of the sample, and ρ_D and ρ_W are respectively the densities of water and desiccant, evaluated at the room temperature at which the masses were measured.

For a check of the correlation used in the computer simulation to determine the heat transfer coefficient, the later is experimentally approximated with the log-mean temperature difference approach, applied to the system operating with no desiccant circulation.

The experimental results are presented, evaluated, and compared to the theoretical predictions in the following sections.

7.3. Discussion and Evaluation of Experimental Results

In order to analyze the effects of certain parameters on the desiccant system operation and to check the theoretical model, several experimental runs were performed by changing the cooling and heating water flow rates and the regenerator inlet water temperature.

The maximum regenerator water flow rate was fixed by the pump to 1077 pounds/hour. Meanwhile, the hot water temperature was limited to a maximum of 144 °F by the water heater capacity (Electric input to heater = Regenerator energy input), and to a minimum of about 125 °F by the difficulty of spraying the desiccant due to its higher viscosities at lower temperatures. Because of the loss of spray at low flow rates, the desiccant flow rate was however kept constant at its maximum of 203 Lb/hr during all experiments. Available city water at about 74°F was used to cool the absorber. The water flow rate was allowed to vary in the range of 400 to 1700 Lb/hr.

The experimental data and results, corresponding to the three series of tests conducted in this investigation, are summarized in Tables D-1, 2, and 3 of Appendix D. All measured output variables are also plotted in Figure 7-3 through 7-20 and are discussed and evaluated below.

7.3.1. Effect of Cooling Water Flow Rate

Upon examining Figures 7-3 through 7-8, it can be concluded that the use of larger cooling water flow rates has several effects on the desiccant system. Those effects are interelated in a complex manner and are tentatively summarized as follows:

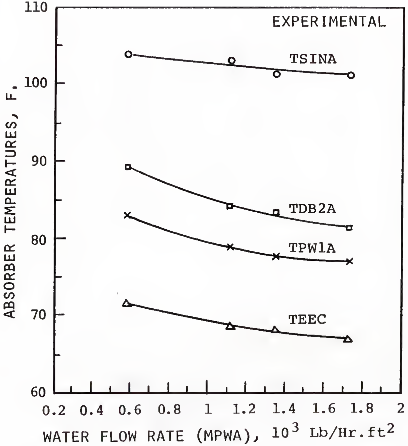

Figure 7-3: Absorber Outlet Air and Water, Inlet Solution, and Exit of Evaporative Cooler Temperatures versus Cooling Water Flow Rate.

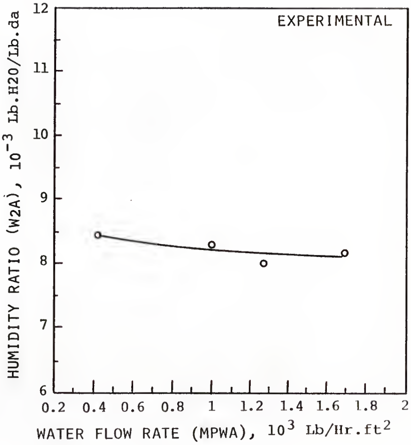

Figure 7-4: Humidity Ratio of Dried Air Leaving the Absorber versus Cooling Water Flow Rate.

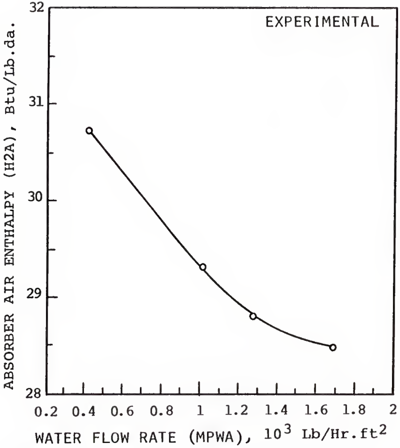

Figure 7-5: Enthalpy of Air Leaving the Absorber versus Cooling Water Flow Rate.

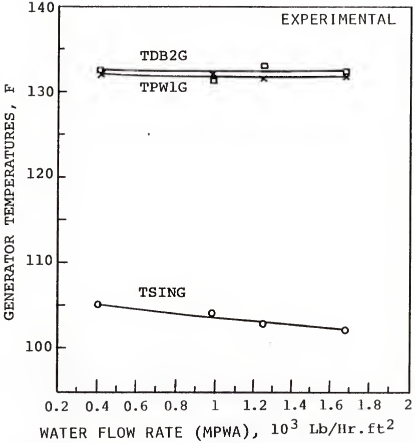

Figure 7-6: Generator Outlet Air and Water, and Inlet Solution Temperatures versus Cooling Water Flow Rate.

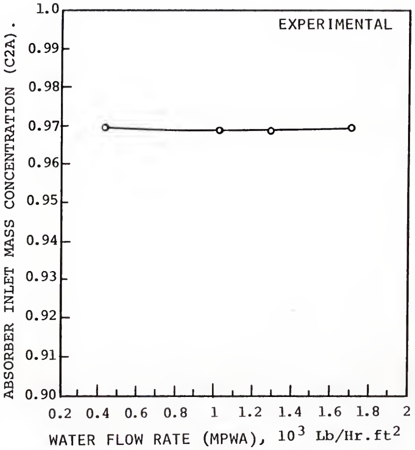

Figure 7-7: Strong Solution Concentration versus Cooling Water Flow Rate.

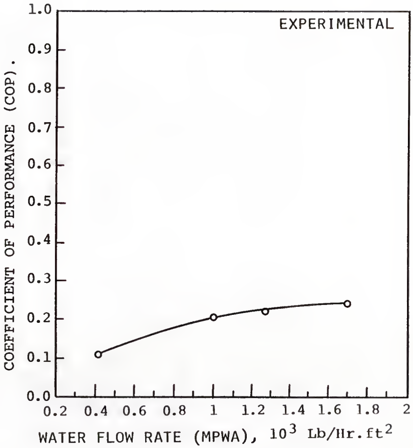

Figure 7-8: System's coefficient of Performance versus Cooling Water Flow Rate.

a) Because of their higher heat capacities, larger water flow rates permit to maintain lower temperatures throughout the absorber, as seen by the decrease in water outlet temperature (TPW1A, Figure 7-3). This results in cooler air leaving the absorber (lower TDB2A, Figure 7-3) and more dehumidification (lower W2A, Figure 7-4) due to the lower partial pressure of water in the cooler desiccant solution. The combination of the two effects yields the decrease in the leaving air enthalpy (H2A, Figure 7-5), which is equivalent to lower wet-bulb temperature and therefore results in lower supply temperatures after evaporative cooling (TEEC, Figure 7-3).

b) Because of the better heat rejection with larger cooling water flow rates, the dilute desiccant solution leaves the absorber at a lower temperature. This permits further precooling of the hot and strong solution, coming from the regenerator and through the intercooler, and therefore results in cooler solution entering the absorber (TSINA, Figure 7-1), with less non desired heat introduced with it..

c) Although preheated by the intercooler, the dilute solution reaches the regenerator at lower temperatures when higher cooling water flow rates are used in the absorber. The lower inlet solution temperature, in addition to the higher latent heat required for the removal of a larger amount of water from the solution, causes the cooling of the regeneration process as illustrated by the decrease in the regenerator air and water outlet temperatures (TDB2G and TPW1G, respectively Figure 7-6). The effect remains however small due to the small heat capacity of the desiccant and small additional amount of water to be removed from the solution.

d) Despite the larger dehumidification achieved, the strong-solution concentration decreases with larger cooling water flow rates (Figure 7-7). The lower concentration results from the fact that the regeneration process is slightly cooler; while the higher dehumidification is attributed to the larger mass-transfer driving-potential in the absorber, resulting from the lower equilibrium water partial-pressures at lower desiccant solution temperatures. This confirms the advantage of cooled dehumidifiers as compared to adiabatic processes, namely in reducing the concentration requirements and associated regenerating temperatures.

e) The coefficient of performance (C.O.P.) of the system increases as the cooling water flow rate is increased (Figure 7-8). This is obvious since more heat rejection is then achieved, resulting in cooler air and enhancing the mass transfer for more dehumidification. Another reason for the performance improvement is the reduction of energy losses carried out by the exhaust air, which leaves at lower temperatures.

Although it was not experimentally investigated in this work, it is reasonable to expect that lower cooling water temperatures would have the same effects as larger water flow rates. Both methods maintain the absorber at lower temperatures and should therefore lead to the same qualitative results.

7.3.2. Effect of the regenerator water flow rate

The effects of increasing the hot water flow rates on the performance of a liquid desiccant air-conditioner are illustrated in Figures 7-9 through 7-14. Those effects are summarized as follows:

a) At large heating water flow rates, the regenerator is kept warmer as shown by the increase in both outlet air and water temperatures (Figure 7-9). The desiccant film, which is directly heated by the hot water through the finned-tube arrangement, is then at higher temperature and consequently more water is stripped from the solution. A higher concentration is therefore obtained as pictured by Figure 7-10.

b) The interaction between the regenerator and absorber is insured by the continuous circulation of the desiccant solution. In addition to transferring moisture, the desiccant solution also carries sensible energies between the two contactors. At higher hot water flow rates, warmer solution leaves the regenerator and that energy exchange is increased as illustrated by the higher solution inlet temperatures (TSING, Figure 7-9 and TSINA, Figure 7-12).

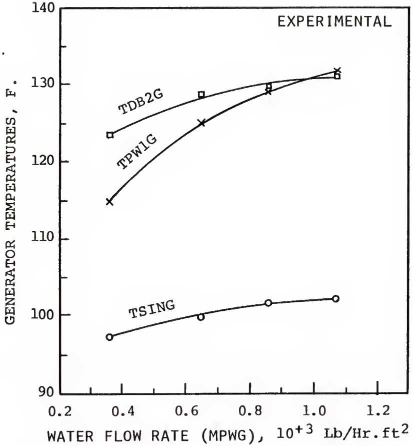

Figure 7-9: Outlet Air and Water, and Inlet Solution Temperatures versus Hot Water Flow Rate.

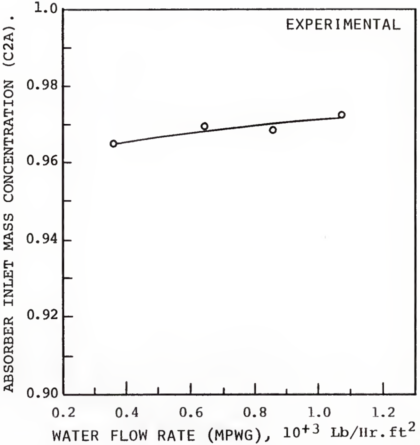

Figure 7-10: Strong Solution Concentration versus Hot Water Flow Rate.

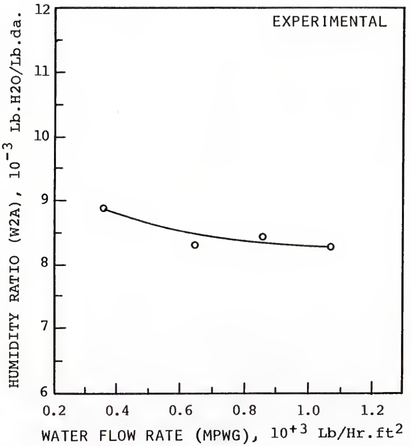

Figure 7-11: Humidity Ratio of Dried Air Leaving the Absorber versus Hot Water Flow Rate.

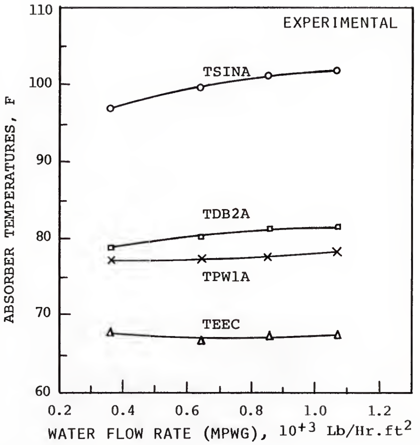

Figure 7-12: Outlet Air and Water, Inlet Solution, and Exit of Evaporative Cooler Air Temperatures versus Hot Water Flow Rate.

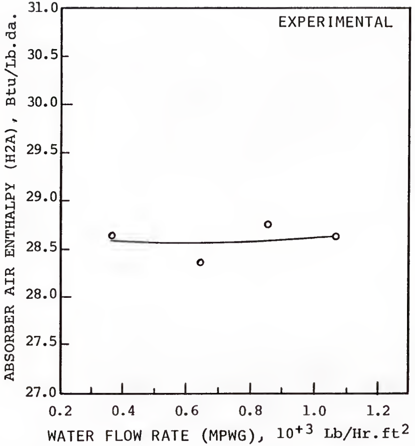

Figure 7-13: Enthalpy of Air Leaving the Absorber versus Hot Water Flow Rate.

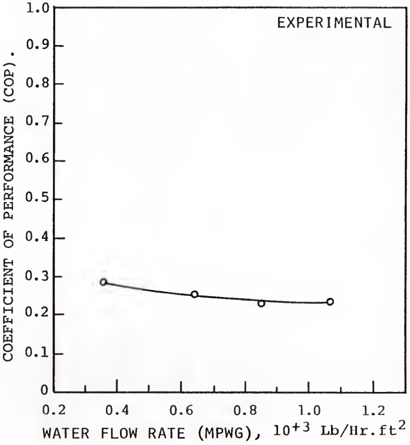

Figure 7-14: System's Coefficient of Performance versus Hot Water Flow Rate.

c) In the absorber, the stronger inlet desiccant solution insures more dehumidification which results in lower leaving air humidity ratio (W2A, Figure 7-11). Meanwhile, the associated latent heat of the absorbed water and the additional sensible heat, introduced by the warmer solution, cause the absorber operating temperature to rise as shown by the increase in outlet air and water temperatures (TDB2A and TPW1A, Figure 7-12). The net effect, under the given conditions, is an almost constant leaving air enthalpy (H2A, Figure 7-13), which explains the similar variation of the supply air temperature at the exit of the evaporative cooler (TEEL, Figure 7-12). The above effects remain small because of the small heat capacity of the desiccant as compared to that of cooling water and due to the fact that the warmer temperatures offset some of the advantages of the higher concentration in the dehumidification process.

d) It is observed that the coefficient of performance (COP) of the system declines as the hot water flow rate increases (Figure 7-14). This result is not unreasonable since the absorber leaving air enthalpy remains almost constant, as discussed in (c), but a larger amount of energy is lost to the environment by the warmer exhaust air.

7.3.3. Effects of Regenerator Hot Water Inlet Temperature

As expected, increasing the hot water inlet temperature permits to maintain the regenerator warmer, and therefore would have similar effects on the system's operation as those resulting from an increase of hot water flow rate. Figures 7-15 through 7-20 represent the dependence of the different output parameters on the hot water inlet temperature. The comparison of the results obtained by changing the hot water flow rate and inlet temperature confirms the close qualitative similarity between the two cases; temperatures, humidities, concentrations and COP have the same trend of variation. One difference was however observed in the absorber outlet air enthalpy, which remained almost constant in one case and sharply declined in the other. That difference can be explained by the fact that the enthalpy of moist air is a function of both temperature and humidity; in both cases the resulting air is warmer and dryer, and therefore it's enthalpy may either increase or decrease depending on the relative magnitude of the counteracting effects of temperature and humidity.

The above experimental investigation shows the complex interaction between the dehumidification and regeneration processes through the continuous circulation of the liquid desiccant. The main conclusions drawn from this investigation may be summarized by the following

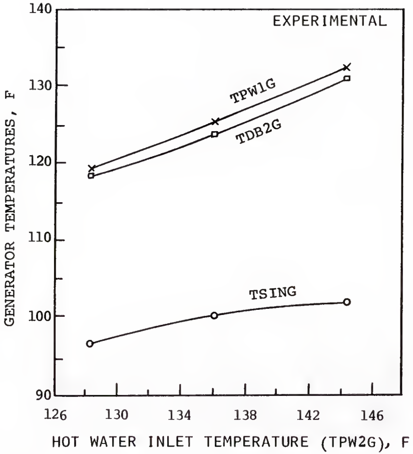

Figure 7-15: Outlet Air and Water, and Inlet Solution Temperatures versus Hot Water Inlet Temperature.

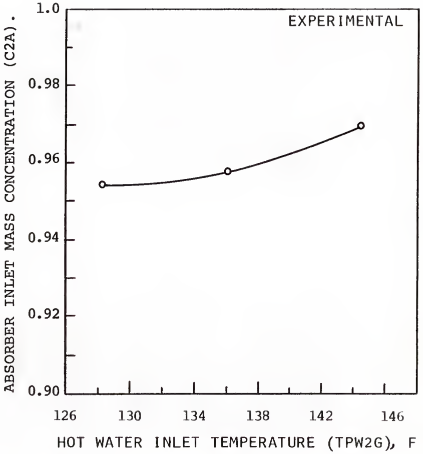

Figure 7-16: Strong Solution Concentration versus Hot Water Inlet Temperature.

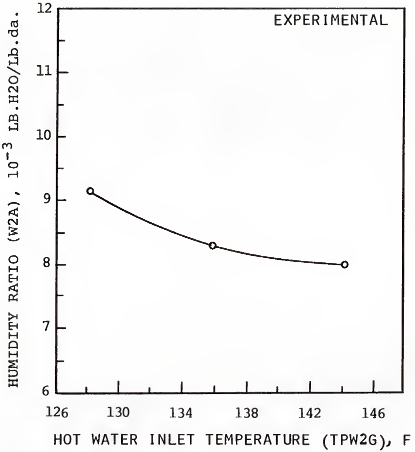

Figure 7-17: Humidity Ratio of Air Leaving Absorber versus Hot Water Inlet Temperature.

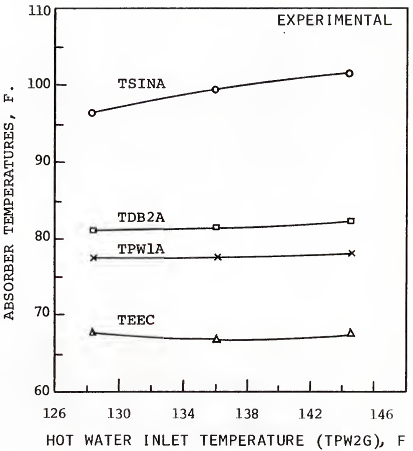

Figure 7-18: Outlet Air and Water, Inlet Solution, and Exit-of Evaporative Cooler Air Temperatures, versus Hot Water Temperature.

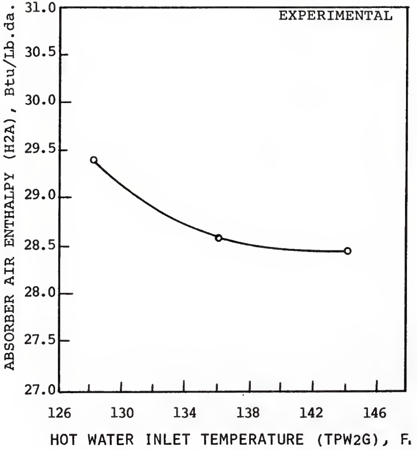

Figure 7-19: Enthalpy of Air Leaving the Absorber versus Hot Water Inlet Temperature.

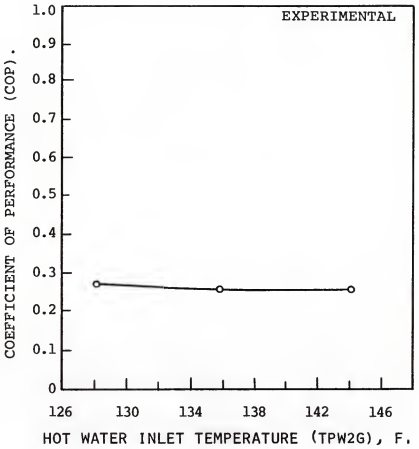

Figure 7-20: System's Coefficient of Performance versus Hot Water Inlet Temperature

The performance of a liquid desiccant air conditioner is best improved by simultaneously maintaining the absorber as cool and the regenerator as hot as possible. Cooler absorbers result in a more efficient moist-air dehumidification. Warmer regenerators, on the other hand, result in higher desiccant concentrations which in turn permit better dehumidification. However, unless appropriate measures are taken, the advantage of the resulting higher concentrations may be offset by the associated higher solution temperatures, entering the absorber, and the larger exhaust losses. This emphasizes the importance of using the solution-to-solution intercooler and air-to-air recovery heat exchanger in addition to the larger water flow rates.

7.4. Comparison of Experimental and Theoretical Results

The theoretical model was discussed in Chapter III and the computer simulation was presented in Chapter IV. However, the use of the computer program DESYST to predict the output of the experimental set-up requires the knowledge of the solution-to-solution intercooler effectiveness ERS, the fin efficiency E and the wetting factor F, in addition to all other inlet parameters. The first was approximated from the measured desiccant solution inlet and outlet temperatures, and an intercooler effectiveness ERS = 0.55 was found to predict closely the temperature of the desiccant entering the absorber. Preliminary calculations showed that, for the finned-tube coils used in the current experimental set-up, the fin efficiency factor is about $E = 0.75$. The wetting factor, which is dependent on several factors such as packing geometry, quality of the spray, viscosity, surface roughness and desiccant and air flow rates, was however impossible to determine experimentally. It was therefore deduced by a trial and error procedure as outlined in the following.

With all other input parameters (dimensions, flow rates, inlet temperatures and humidities) kept constant and equal to those obtained and used in the experiment, the wetting factor was changed in the computer model until best agreement between the calculated and measured output variables (temperatures and humidities) is obtained. The procedure was repeated for all experiments, and a wetting factor $F = 0.15$ was deduced as best fit. Although this value seems to be small, it is judged acceptable for the experimental apparatus used in this work. The lower than expected value of F results from

a) The one nozzle circular spray covers only a part of the rectangular cross section of the packing.

b) Because of the directional spray resulting from a single nozzle, only one side of the fins is wetted.

c) The use of two coils, packed on each other, causes a discontinuity in the flow of the falling film, and therefore a dropwise liquid passage between the coils takes place. This results in a poor liquid distribution on the lower coil.

In the computer program DESYST, written to analyze the operation of the liquid desiccant air conditioner, recovery heat exchangers were included and simulated by the constant effectiveness approach. In the experimental apparatus, however, an electric air duct heater was used to simulate the effect of the air-to-air recovery heat exchanger on the regenerator air inlet temperature. In consequence, to adapt the computer code to the experimental system, the effectiveness of the air-to-air recovery heat exchanger is taken equal to zero, and the regenerator inlet temperature is considered equal to the air temperature after the air duct heater. The evaporative cooling process is assumed adiabatic and its saturation efficiency is kept constant for all the tests. From the measurement of the inlet and outlet temperatures of the evaporative cooler, the saturation efficiency was found to be about 78%.

For each series of tests conducted, where only one parameter of interest is changed, it was attempted to maintain all other independent input parameters constant. In this way, groups of experiments can be compared directly and the effect of one variable may be evaluated. Since it is impossible to exactly reproduce the same conditions, the average values of the supposedly kept constant input data are used in the computer model. The small deviations of the actual data from their average values are considered as sources of error and their effect is discussed in the uncertainty propagation analysis presented in Appendix E.

The theoretical results, corresponding to the three series of tests conducted in this investigation, are presented in Tables D1, 2, and 3 of Appendix D. They are also grouped and plotted in Figures 7-21 through 7-30, together with their experimental counterparts to facilitate the comparison. The estimated measurement errors and a sample of the uncertainties, resulting from the propagation of errors through the theoretical model, are summarized in tables E-1 and E-2 to assist in the evaluation of the results. The details of the uncertainty calculations are discussed in Appendix E.

Upon inspection of the figures mentioned above, it can be concluded that there is a generally good agreement between the experimental and theoretical results, considering the numerous assumptions made as well as numerous potential sources of errors. The figures show that the experimental and theoretical results have the same variation trends in terms of the different controlling parameters.

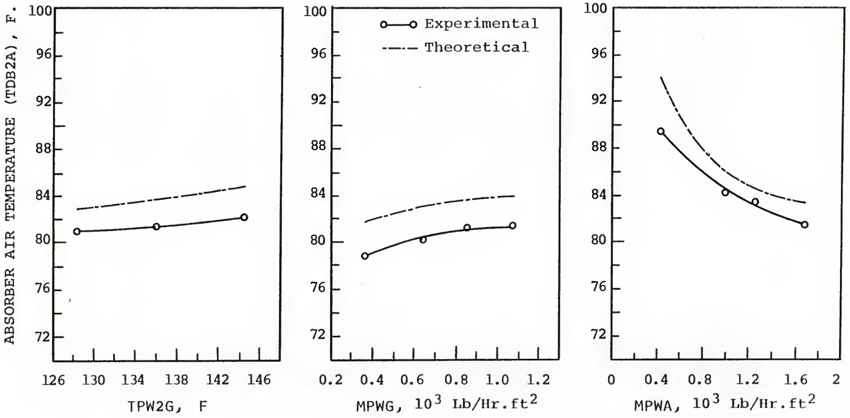

(a) (b) (c)

Figure 7-21: Temperature of Air Leaving the Absorber versus a) Hot Water Inlet Temperature, b) Hot Water Flow Rate, c) Cooling Water Flow Rate.

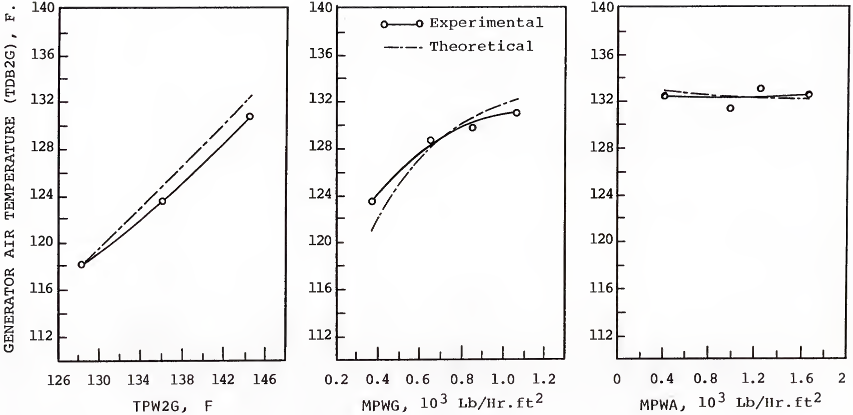

(a) (b) (c)

Figure 7-22: Temperature of Air Leaving the Regenerator versus a) Hot Water Inlet Temperature, b) Hot Water Flow Rate, c) Cooling Water Flow Rate.

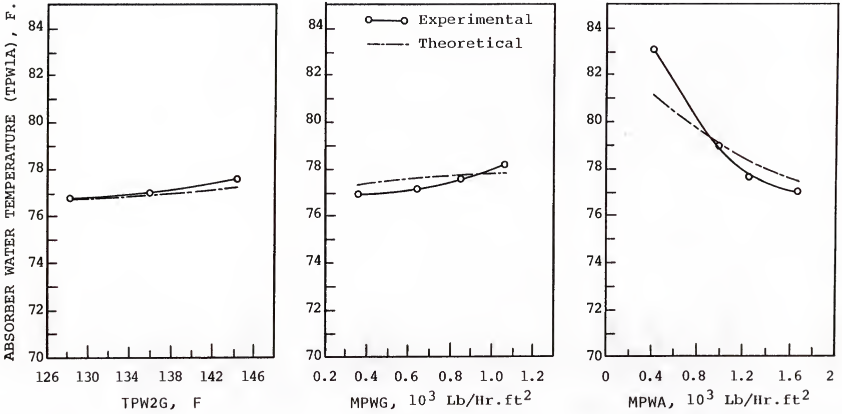

(a) (b) (c)

Figure 7-23: Cooling Water Outlet Temperature versus a) Hot Water Inlet Temperature, b) Hot Water Flow Rate, c) Cooling Water Flow Rate.

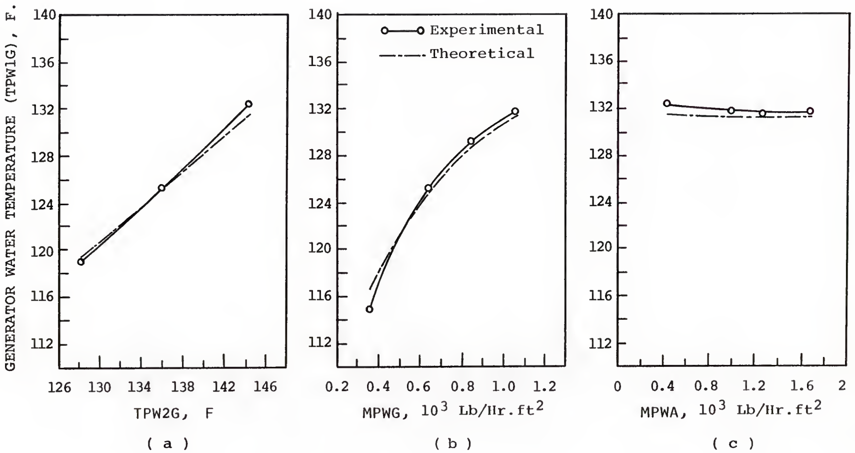

Figure 7-24: Hot Water Outlet Temperature versus a) Hot Water Inlet Temperature, b) Hot Water Flow Rate, c) Cooling Water Flow Rate.

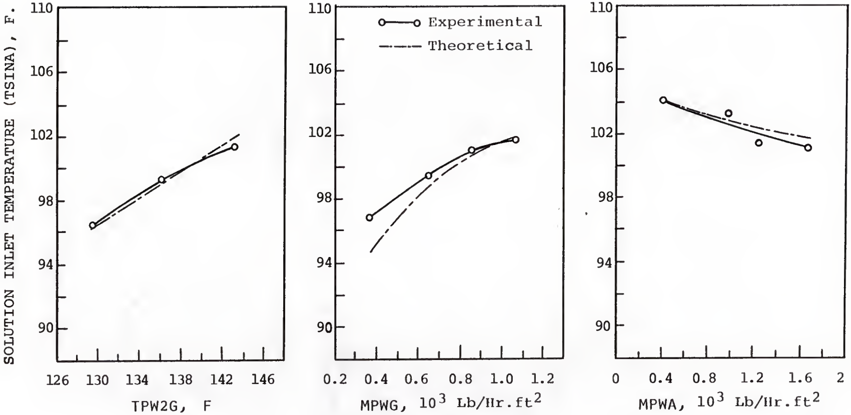

(a) (b) (c)

Figure 7-25: Desiccant Solution Temperature Entering the Absorber versus a) Hot Water Inlet Temperature, b) Hot Water Flow Rate, c) Cooling Water Flow Rate.

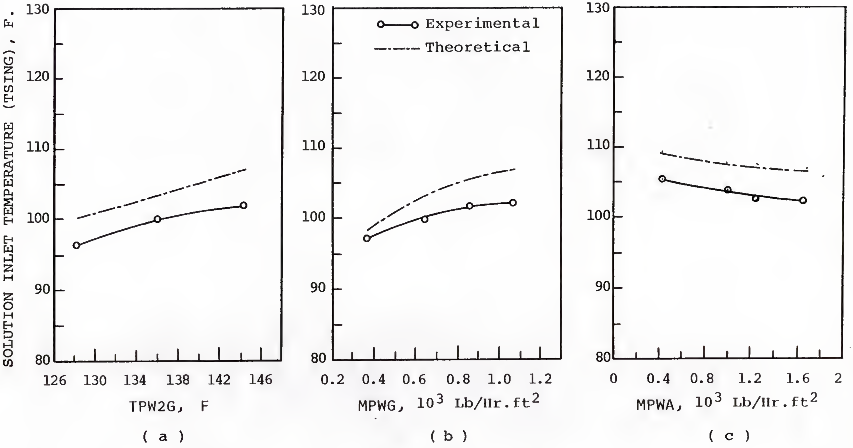

Figure 7-26: Desiccant Solution Temperature Entering the Regenerator versus a) Hot Water Inlet Temperature, b) Hot Water Flow Rate, c) Cooling water Flow Rate.

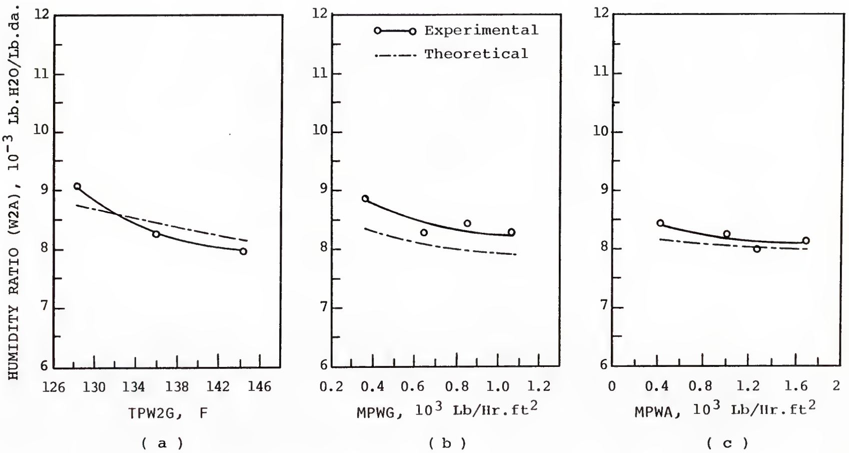

Figure 7-27: Humidity Ratio of Air Leaving the Absorber versus a) Hot Water Inlet Temperature, b) Hot Water Flow Rate, c) Cooling Water Flow Rate.

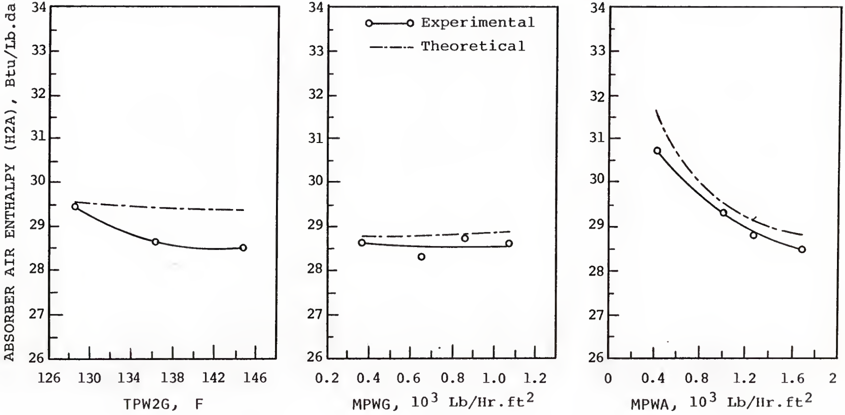

(a) (b) (c)

Figuew 7-28: Enthalpy of Air Leaving the Absorber versus a) Hot Water Inlet Temperature, b) Hot Water Flow Rate, c) Cooling Water Flow Rate.

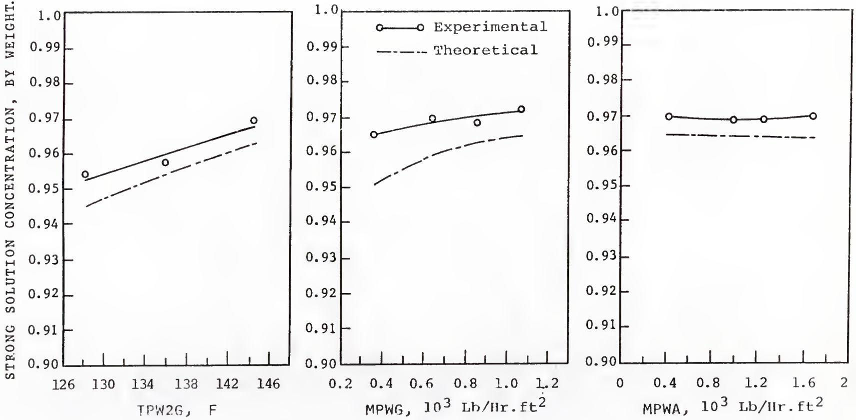

(a)

(b)

(c)

Figure 7-29: Strong Solution Concentration versus a) Hot Water Inlet Temperature b) Hot Water Flow Rate, c) Cooling Water Flow Rate.

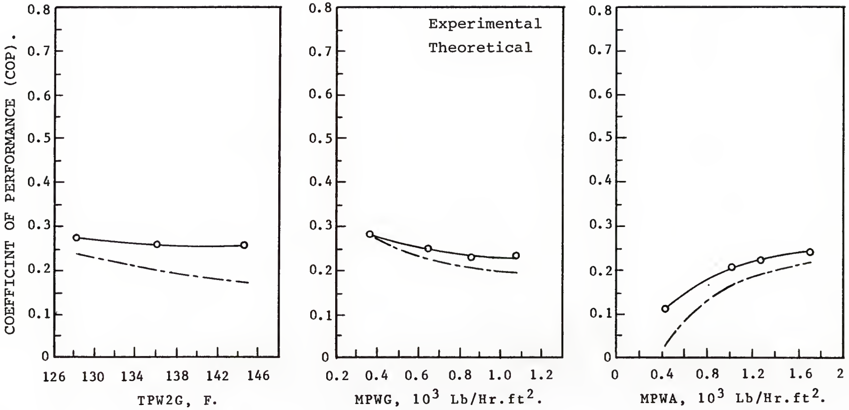

(a)

(b)

(c)

Figure 7-30: System's Coefficient of Performance versus a) Hot Water Inlet Temperature, b) Hot Water Flow Rate, c) Cooling Water Flow Rate.

For the first two series of experiments, where the process water flow rate is changed, one notices that there is a larger deviation between the experimental and theoretical results at low water flow rates. That deviation may be attributed to the fact that, under those conditions, the assumption that the heat capacity of the process water is much larger than that of both desiccant and air is violated, and in consequence the theoretical model results in larger errors.

The inspection of the same figures also reveals that the theoretical model consistently predicts a slightly warmer air, leaving the absorber, than measured. It is suggested that that difference is due to the uncertainty in determining the heat and mass transfer coefficients as well as the finned-tube surface effectiveness and wetting factor. One other noticeable difference between the experimental and theoretical results is observed in the temperature of the solution entering the regenerator. That difference can be explained by the fact that there are heat losses between the intercooler and the environment, and that those heat losses are not taken into account in the theoretical model, where the intercooler effectiveness was estimated based on the temperature of the solution entering the absorber.

Considering the complexity of the phenomena of simultaneous heat and mass transfer between the three countercurrent fluids, the complexity of the continuous interaction between the dehumidification and regeneration processes, and the numerous potential sources of errors due especially to the non measureable properties such as wetting factor, mass and heat transfer coefficients, surface effectiveness and heat interactions with surroundings, it can be concluded that the theoretical model presents a simple and accurate simulation of the process if basic assumptions are met.

CHAPTER VIII
CONCLUSIONS AND RECOMMENDATIONS

8.1. Conclusions

An experimental and theoretical investigation of a liquid desiccant air-conditioner has been conducted. Based on the findings of this work, the following conclusions may be drawn:

1. Liquid-desiccant air-conditioning in hot and humid climates is feasible and economically competitive with commercial vapor-compression units. It can be operated at low regenerating temperatures (140°F), that can be supplied by use of available flat-plate solar collectors.
2. Non-adiabatic dehumidification permits maintaining the desiccant solution cooler throughout the process for a more efficient mass transfer operation, and results in lower concentration requirements. Obvious consequences are the lower regenerating temperatures and the subsequent higher efficiency of the solar collectors.

3. Non-adiabatic regeneration chambers permit keeping the desiccant solution hot throughout the packing, thus causing more water stripping because of the higher partial pressure of water in the hot desiccant solution. The water heated regeneration chamber is a practical choice because of its good performance even in humid climates, its compactness is size, and its suitability for different sources of energy.
4. Because of the open cycle nature of liquid desiccant systems, considerable amounts of energy could be lost to the environment unless appropriate recovery heat exchangers are used to recuperate it from the exhaust hot and humid air.
5. In addition to transferring moisture from the absorber to the regenerator, desiccant solutions introduce non desired heat to the dehumidifier of a continuous process, and should therefore be precooled for better performance.
6. Opposed to their absorption counterparts, liquid desiccant air-conditioners can operate at regenerating temperatures well below the design value. In fact they have a higher C.O.P. at such lower than design temperatures and provide a partial cooling effect, thus adjusting to the

cooling requirements which are in phase with the solar radiation. In a well designed system, no additional back-up source of energy is then required.

7. The blower power requirements of the proposed liquid-desiccant system are well below those of a comparable solid-desiccant unit.
8. The theoretical model, developed in this work, represents a simple and reliable tool to analyze and design liquid desiccant systems, as long as the basic assumptions are satisfied.
9. Special care should be taken in the design of the spray system to insure a uniform wetting of the packing area, and make to most of the available surface useful for mass transfer. Also, reclaimers must be inserted in the system to recuperate the part of the expensive triethylene glycol evaporated in the regenerator, and otherwise exhausted to the environment.

8.2. Recommendations

The following areas are recommended for further research and development:

1. Experimental investigation to accurately determine a) the wetting factor, b) mass transfer properties, c) flooding limitation and d) air side friction losses in terms of the packing geometry and the countercurrent air and desiccant flow rates.
2. Consider the storage of energy in the form of concentrated desiccant - a method that permits storage at ambient temperatures with no thermal losses-.
3. Perform a transient analysis of liquid desiccant air conditioning systems to assist in the development of a control technique.
4. Analyze the seasonal performance of desiccant systems and develop a control technique to monitor both supply air temperature and humidity in terms of instantaneous weather conditions.
5. Investigate the possibility of using liquid desiccant systems as heat pumps, especially in areas with arid winters.

APPENDIX A
SIMPLIFIED MODEL FOR LIQUID DESICCANT AIR-CONDITIONERS

The interface equilibrium mass ratio Y_i' is a function of local temperature, total pressure and solution mass ratio X'

$$Y_i' = Y_i' \, (T_i, X', P_t) \tag{A-1}$$

By differentiation, one obtains

$$d\,Y_i' = \left(\frac{\partial Y_i'}{\partial T_i}\right)_{X',P_t} d\,T_i + \left(\frac{\partial Y_i'}{\partial X'}\right)_{T_i,P_t} dX' + \left(\frac{\partial Y_i'}{\partial P_t}\right)_{X_i,T_i} dP_t. \tag{A-2}$$

Since the system is open to atmospheric pressure and the only pressure changes are those due to small friction losses, the total pressure may be considered constant and equal to one atmosphere. Furthermore, for the small range of working solution temperature and concentration, the partial derivatives may be assumed constant and denoted by

$$\left(\frac{\partial Y_i'}{\partial T_i}\right)_{X',P_t} = a \tag{A-3a}$$

$$\left(\frac{\partial Y_i'}{\partial X'}\right)_{T_i, P_t} = b \tag{A-3b}$$

$$\left(\frac{\partial Y_i'}{\partial P_t}\right)_{T_i, X_i} = 0 \tag{A-3c}$$

Then Equation (A-2) becomes

$$dY_i' = a \cdot dT_i + b\ dX' \tag{A-4}$$

On the other hand, the energy balance on a cross-section differential element of the contractor, with the help of the assumptions made in Chapter III, gives the change of sensible energy $d\dot{Q}_L$ as

$$d\dot{Q}_L = (\dot{L}_s\ C_L' + \dot{M}_w\ C_w)\ dT_i$$

$$= \dot{G}_s\ \{C_G'\ dT_G + d\dot{Y}(\overline{\lambda}_A + \overline{\Delta H}_{m,A}')\} \tag{A-5}$$

Since efficient desiccant systems should operate under nearly isothermal conditions and the enthalpy of mixing is relatively small compared to the latent heat, therefore the energy exchanged with the liquids corresponds mostly to the latent heat and equation (A-5) may be approximated by

$$(\dot{L}_s\ C_L' + \dot{M}_w\ C_w)\ dT_i = \dot{G}_s\ \bar{\lambda}_A\ dY'$$

$$= \dot{L}\ \ \bar{\lambda}_A\ dX' \tag{A-6}$$

or

$$dX' = \frac{\dot{L}_s\ C_L' + \dot{M}_w\ C_w}{\dot{L}_s\ \lambda_A}\ dT_i \tag{A-6a}$$

Substituting for dX' into equation (A-4) and then integrating

$$Y_i' = \left\{a + b\ \frac{\dot{L}_s\ C_L' + \dot{M}_w\ C_w}{\dot{L}_s\ \lambda_A}\right\}\ T_i + B \tag{A-7}$$

or

$$Y_i' = A \cdot T_i + B \tag{A-7a}$$

where A and B are the resulting linearity constants. Notice that if equation (A-6a) is instead used to substitute for dT_i in equation (A-4), then another linearity equation, with constants A' and B', may be deduced

$$Y_i' = A' \cdot X' + B' \tag{A-7b}$$

Now, recall the enthalpy expresion defined by equation (3-70) and evaluate it at the interface conditions

$$H_i^* = C_G'\ T_i + \frac{F}{L_e^{2/3}}\ (\bar{\lambda}_A + \overline{\Delta H}'_{M,A})\ Y_i' \tag{A-8}$$

Replacing Y_i' by its approximate value, given by equation (A-7a), leads to

$$H_i^* = \{C_G' + A \frac{F}{L_e^{2/3}} (\bar{\lambda}_A + \overline{\Delta H}'_{M,A})\} T_i$$

$$+ B \frac{F}{L_e^{2/3}} (\bar{\lambda}_A + \overline{\Delta H}'_{M,A}). \qquad \text{(A-9)}$$

or by lumping together the constants into α and β

$$H_i^* \simeq \alpha T_i + \beta \qquad \text{(A-9a)}$$

These linearity approximations permit considerable simplifications in the analysis and design of liquid desiccant air conditioning systems. A physical interpretation is discussed in chapter III.

Consider equation (A-8), but evaluated at the bulk gas conditions, after differentiation

$$dH_G^* = C_G' \, dT_G + \frac{F}{L_e^{2/3}} (\overline{\lambda_A} + \overline{\Delta H}'_{M,A}) \, dY' \qquad \text{(A-10)}$$

The Lewis number for moist air is about 0.84. In addition, in a well designed system, the desiccant spray should cover most of the packing area, therefore the wetting factor F is close to unity and so is the ratio

$F/Le^{2/3}$. The comparison of equations (A-5) and (A-9) leads to the expression

$$d\dot{Q}_L = (\dot{L}_S\ C_L' + \dot{M}_W\ C_W)\ dT_i = \dot{G}_S\ dH_G^* \qquad \text{(A-11)}$$

Integrating over the contactor height

$$\dot{Q}_L = (L_S\ C_L + M_W\ C_W)\ (T_{i2} - T_{i1}) \qquad \text{(A-12)}$$

$$= \dot{G}_S\ (H_{G2}^* - H_{G1}^*) \qquad \text{(A-12a)}$$

where the subscripts 1 and 2 refer to the end points of the contactor.

Meanwhile, differentiating equation (A-9a) and substituting dT_i by its value from equation (A-5) leads to

$$dH_i^* = \alpha \cdot \frac{d\dot{Q}_L}{(\dot{L}_S\ C_L' + \dot{M}_W\ C_W)} \qquad \text{(A-13)}$$

By combining equations (A-10) and (A-13), it can be deduced that

$$dH_G^* - dH_i^* = d(H_G^* - H_i^*)$$

$$= d\dot{Q}_L\ \left(\frac{1}{\dot{G}_S}\right) - \left(\frac{\alpha}{\dot{M}_W\ C_W + \dot{L}_S\ C_L'}\right) \qquad \text{(A-14)}$$

Recalling Equation (3-71)

$$dQ_L = -\ K_y\ a\ A_c\ E_H\ L_e^{2/3}(H_G^* - H_i^*)\ dZ \qquad \text{(A-15)}$$

then by taking the ratio of equations (A-14) and (A-15) and after rearrangement

$$\frac{d(H^*_G - H^*_i)}{H^*_G - H^*_i} = -K_Y a\ A_c\ E_H\ L_e^{2/3} \left(\frac{1}{\dot{G}_S} + \frac{\alpha}{\dot{L}_S\ C'_L + \dot{M}_W\ C_W}\right) dZ \quad \text{(A-16)}$$

Integration over the contactor's height, with A_o denoting the packing total area, gives

$$\ln \left(\frac{H^*_{G2} - H^*_{i2}}{H^*_{G1} - H^*_{i1}}\right) = -\ K_y\ E\ L_e^{2/3} A_o \left(\frac{1}{\dot{G}_S} + \frac{\alpha}{\dot{M}_W\ C_W + L'_S\ C'_L}\right) \quad \text{(A-17)}$$

Now, replacing $\dot{L}_s\ C_L + \dot{M}_W\ C_w$ and $\dot{G}_S$ by their respective equivalent values deduced from equations (A-12) and (A-12.a)

$$\ln \left(\frac{H^*_{G2} - H^*_{i2}}{H^*_{G1} - H^*_{i1}}\right) = -\ K_y\ E\ L_e^{2/3}\ A_o \left(\frac{H^*_{G2} - H^*_{G1}}{Q_L}\right) - \frac{\alpha(T_{i2} - T_{i1})}{\dot{Q}_L} \quad \text{(A-18)}$$

The temperature difference $(T_{i2} - T_{i1})$ can be expressed in terms of the linearity equation (A-7a) by

$$H^*_{i2} - H^*_{i1} = \alpha\ (T_{i2} - T_{i1}) \quad \text{(A-19)}$$

Finally, equations (A-18) and (A-19), combined and rearranged, give the logarithmic mean enthalpy

$$Q_L = (\dot{L}_S C_L' + \dot{M}_W C_W)(T_{i2} - T_{i1})$$

$$= - K_Y A_o E L_e^{2/3} \Delta H_{1m}^* \qquad \text{(A-20)}$$

where

$$\Delta H_{1m} = \frac{(H_{G2}^* - H_{i2}^*) - (H_{G1}^* - H_{i1}^*)}{\ln \dfrac{H_{G2}^* - H_{i2}^*}{H_{G1}^* - H_{i1}^*}} \qquad \text{(A-20a)}$$

APPENDIX B
THERMODYNAMIC PROPERTIES OF TRIETHYLENE GLYCOL

In order to perform a computer simulation of the liquid-desiccant air conditioner, it is necessary to express the thermodynamic properties in algebraic forms. The only published data on triethylene glycol (TEG), which is used in this investigation, are unfortunately presented in the form of charts. For the purpose of this work, a least square curve fitting of the available data and for the ranges of interest was performed as follows:

Figure 4-6 gives the equilibrium total pressure over aqueous ethylene glycol solutions of different concentrations verus temperatures. Because glycols are much less volatile than water, the given total pressures are expected to be very close to the equilibrium water partial pressures. To confirm that, consider the case of an ideal solution. The equilibrium partial pressures of triethylene glycol $P'_{TEG,l}$ and of water $P'_{H2O,l}$ in the liquid phase and at a specified solution temperature T may then be determined by Raoult's law

$$P'_{TEG} = x_{TEG} \cdot P_{TEG,S}\,(T) \qquad (B\text{-}1)$$

$$P'_{H2O} = x_{H2O} \cdot P_{H2O,S}\,(T) \qquad (B\text{-}2)$$

where x_{H2O} and X_{TEG} denote the molar fractions of water and TEG in the solution, respectively, and $P_{TEG,S}$ and $P_{H2O,S}$ are the saturation pressures of pure substances at the given temperature. The total equilibrium vapor pressure equals the sum of the individual partial pressures

$$P_v = P'_{TEG,1} + P'_{H20,1} \tag{B-3}$$

A sample calculation, performed on a solution with a concentration 85% tryethylene glycol by weight and at a temperature T = 260°F, showed that the TEG partial pressure is 900 times as great as that of water. Furthermore, the comparison of the ideal to the actual total pressures showed that the aqueous solution has a small positive deviation from ideality at the specified temperature and concentration. Note that the sample calculation considered represents a worst case for an operating desiccant system. In view of the above verification, the published equilibrium total pressures will be assumed equal to the water partial pressures.

Reference-substance plots are the most common method used for graphical representation of vapor pressures versus temperatures. They stem from the Clausius-Clapeyron equation which relates the slope of the vapor pressure versus temperature curve of a pure substance to its latent heat of vaporization. The relationship between the vapor pressures of two substances may be given [50] by

$$\log_{10} P = \frac{\lambda}{\lambda r} \log_{10} P_r + \text{Const} \qquad (B-4)$$

where P is the vapor pressure, λ denotes the latent heat, and subscript r refers to the reference substance which is generally chosen as one with well known properties such as water.

Equation (B-4) shows that if log-log coordinates are used, a linear curve will result. Keeping this in mind, the linearity of triethyline glycol data of Figure (4-6) suggests that the reference-substance technique is used. If water is used as reference, then the solution equilibrium water vapor-pressure P_e at a specified temperature T and concentration by weight C would have the form

$$\log_{10}(P_e) = A(C) \log_{10} [P_{H20,s}(T)] + B(C) \qquad (B-5)$$

where A(C) and B(C) are the linearity coefficients and are function of the concentration.

Closer inspection of Figure (4-6) reveals that the curves are parallel up to a concentration of 98% TEG by weight. Therefore, for the purpose of this study where a maximum concentration of 97% may be used, the slope A(C) can be considered constant and be easily deduced from

$$A = \frac{\log_{10} \dfrac{P_{e1}}{P_{e2}}}{\log_{10} \dfrac{P_{H20,s(T_1)}}{P_{H20,s(T_2)}}} \qquad (B-6)$$

where subscripts 1 and 2 refer to any two points of the same constant concentration curve. Once A is known, then B(C) can be determined from

$$B(C) = A \log_{10} [P_{H2Os} (T_1)] - \log_{10} (P_{e1}) \qquad \text{(B-7)}$$

The last step is to make a curve fitting for B(C). A polynomial fitting would result in a large error on P_e due to the fact that a small error on B(C) is greatly amplified by the exponentiation. Therefore a better accuracy of P_e would result if a least square curve fitting is performed on $10^{B(C)}$ instead of B(C). Graphical inspection of $10^{B(C)}$ versus C suggests that a second degree polynomial should be used

$$10^{B(C)} = a_2 C^2 + a_1 C + a_o \qquad \text{(B-8)}$$

The temperatures, concentrations, and equilibrium vapor pressures were read with best possible accuracy from Figure (4-6). Then the application of the above curve fitting procedure leads to the correlation

$$P_e = (-3.07443 + 11.44548C - 8.37558C^2)[P_{H20,s}(T)]^{0.972} \qquad \text{(B-9)}$$

where both pressures P_e and P_{w1s} are expressed in millimeters of mercury. Analytical expressions to compute $P_{H20,s}$ are published in reference [68].

APPENDIX C
ECONOMIC ANALYSIS

This appendix gives the details of the economic analysis. The values attributed to the different variables are those used in this investigation.

Present Worth Technique

Instead of focusing just on the initial cost, the present worth value takes into account the additional costs of energy, operation and maintenance, and system replacements. It permits the discount of all future expenses to a present value. If there is no equipment replacement over the project life, then

$$PW = (EC)\ (PWF) + IC \qquad (C\text{-}1)$$

where

$$PWF = \frac{a\ (a^n - 1)}{(a - 1)} \qquad (C\text{-}1a)$$

$$a = \left(\frac{1 + e}{1 + i}\right) \qquad (C\text{-}1b)$$

PW = Present worth value

EC = Annual energy costs

IC = Initial cost

PWF = Present worth factor

e = Escalation rate of electricity = 8%

i = Cost of money = 10%

η = Project life = 20 years

Annual Energy Use

Heating: Using the degree-day concept, the seasonal energy requirement for heating purposes may be estimated by

$$Q_{HS} = \frac{24\ Q_{HD}\ DD}{(T_i - T_o)\ \eta_H} \tag{C-2}$$

where

Q_{HS} = Seasonal energy use for heating, Btu/year

H_{HD} = Design heating load = 3600 Btuh

T_i = Indoor design temperature = 72°F

T_o = Outdoor design temperature = 31°F

DD = Degree days = 1485 degree days/year

η_H = Efficiency of the heating system = 90%

Domestic hot water: For a four persons, single family residence, the hot water use is about 70 gallons/day. The annual energy requirement for domestic hot water is then

$$Q_{DHW} = \frac{213087\ (T_{HW} - T_{CW})}{\eta_{HW}} \tag{C-3}$$

where

Q_{DHW} = Annual energy use for domestic hot water, Btu/year

T_{HW} = Hot water temperature = 120°F

T_{CW} = Local ground water temperature = 70°F

η_{HW} = Efficiency of hot water system = 90%

Cooling: The seasonal energy requirement for cooling is best estimated by

$$Q_{CS} = \frac{Q_T \text{ SFLEOH}}{\text{COP}} \qquad \text{(C-4)}$$

where

Q_{CS} = Seasonal energy use for cooling, Btu/year

Q_T = Design cooling load, Btuh

COP = Coefficient of performance of the cooling system used

SFLEOH = Seasonal full load equivalent operating hours = 1500 hours/year

Since the solar collections can be used year around to supply energy for heating, domestic hot water, and cooling, then only a fraction of their cost should be charged to the cooling system. That fraction is given by

$$\% = \frac{Q_{CS}}{Q_{CS} + Q_{HS} + Q_{DHW}} \times 100 \qquad \text{(C-5)}$$

Initial Cost Estimation

The following relations are deduced from the most recent cost publications. They give a rough cost estimate of the different components in terms of their size.

Solar collectors and storage system

All costs include installation and are related to the collection area (A_C), expressed in square foot.

- Collectors....................$18/$ft^2$
- Storage......................$ 6/ft^2
- Controls.......................$300
- Pumps, valves, fittings, tubing, insulation, antifreeze.........$($600 + 2A_C$)

- Total.........................$($900 + 26A_C$)

Desiccant system

Finned tube coils.................$$A_{CS}$ (80 + 20NR)

Pumps............................$($80 + 650H_P$)

Blowers..........................$(30 + 0.076 CFM)

Air to air heat exchanger.........$21/1000 Btuh

Liquid to liquid heat exchanger...$7/1000 Btuh

where

A_{CS} = Coil cross section [ft^2]
NR = Coil number of rows
H_p = Bracke horsepower
CFM = Air flow rate [ft^3/min]

The cost of duct work, fittings, valves, tubing, insulation, desiccant and labor are estimated as 60% of the total material cost.

Operating Costs

The total electrical energy use of the desiccant air-conditioner is estimated using the seasonal full load equivalent operating hours concept. The pressure drops through the electrically powered components are estimated as follows:

Desiccant pumps	10 psig
Evaporative cooler pump	20 psig
Absorber blower	$(0.69 + DP_{a,A})$ inch H_2O
Regenerator blower	$(0.59 + DP_{a,G})$ inch H_2O
Hot water pump	$DP_{W,G}$
Cold water pump	$DP_{W,A} + h$
Collector to storage pump	neglegible

where

$DP_{a,A}$, $DP_{W,A}$ = air and water side pressure drops through the absorber packing, respectively, inch H_2O

$DP_{W,A}$, D_{WG} = air and water side pressure drops through the regenerator packing, respectively, inch H_2O

h = cooling water elevation and head loss in the plumbing connecting the source of water and absorber

APPENDIX D
EXPERIMENTAL AND THEORETICAL DATA AND RESULTS

Table D-1: Effect of Cooling Water Flow Rate.

	ABSORBER WATER FLOW RATE , (Lb/hr)			
	426	1016	1282	1706
INPUT PARAMETERS				
MAA, Lb/hr	967	967	967	967
MAG, Lb/hr	870	870	870	870
MD, Lb/hr	203	203	203	203
MPWG, Lb/hr	1077	1077	1077	1077
TPW2A, F	74.2	73.9	74	74
TDB1A, F	78	77.6	77.4	77.6
TWB1A, F	67.9	67.7	67.3	67.3
W1A, Lb/Lb.da	0.01229	0.01229	0.0121	0.0121
TPW2G, F	144.4	143.9	143.9	144.1
TDB1G, F	103	102	104	102
OUTPUT PARAMETERS				
TPW1G, F	132.4	131.9	131.6	131.8
TPW1G*, F	131.55	131.43	131.38	131.33
TSING, F	105	104	102.8	102
TSING*, F	108.9	107.8	107.4	106.94
TSINA, F	104	103.2	101.3	101
TSINA*, F	104.06	102.74	102.26	101.7
TPW1A, F	81.3	79	77.65	77
TPW1A*, F	81.17	79.06	78.32	77.47
TDB2A, F	89.4	84.2	83.4	81.4
TDB2A*, F	94.01	86.03	84.65	83.33
TWB2A, F	66.3	64.3	63.3	63.1
TEEC, F	71.6	68.7	68.2	66.9
W2A, Lb/Lb.da	0.00843	0.00829	0.008	0.00814
W2A*, Lb/Lb.da	0.00816	0.00809	0.00806	0.00803
H2A, Btu/Lb.da	30.7337	29.3092	28.8002	28.47
H2A*, Btu/Lb.da	31.5595	29.5328	29.1679	28.8139
COP	0.1083	0.2075	0.2212	0.2409
COP*	0.0284	0.1723	0.1972	0.2214
C2A	0.9696	0.9686	0.9685	0.9694
C2A*	0.9643	0.964	0.9639	0.9637

---

* Theoretical results based on average input conditions and with EA=EG=0.75, FA=FG=0.15, and ERS=0.55.

Table D-2: Effect of Hot Water Flow Rate.

	REGENERATOR WATER FLOW RATE , (Lb/hr)			
	1077	861.5	646.2	359
INPUT PARAMETERS				
MAA, Lb/hr	967	967	967	967
MAG, Lb/hr	870	870	870	870
MD, Lb/hr	203	203	203	203
MPWA, Lb/hr	1553	1496	1451	1484
TPW2A, F	74.2	74	74.1	74.2
TDBlA, F	77.2	77.1	77.4	77.3
TWBlA, F	67.4	67.3	66.9	67.2
WlA, Lb/Lb.da	0.012143	0.01207	0.01179	0.012
TPW2G, F	144.2	144	144.1	144
TDBlG, F	104	103.5	103	103
OUTPUT PARAMETERS				
TPWlG, F	131.7	129.2	125.2	114.9
TPWlG*, F	131.49	128.94	125.2	116.62
TSING, F	102.2	101.8	99.8	97.1
TSING*, F	107.2	105.7	103.5	98.4
TSINA, F	101.7	101	99.4	96.8
TSINA*, F	101.99	100.74	98.71	94.71
TPWlA, F	78.2	77.6	77.2	77
TPWlA*, F	77.83	77.76	77.65	77.37
TDB2A, F	81.4	81.2	80.2	78.8
TDB2A*, F	84.1	83.72	83.15	81.84
TWB2A, F	63.3	63.3	63	64.2
TEEC	67.3	67.2	66.6	67.6
W2A, Lb/Lb.da	0.008286	0.008429	0.008286	0.008871
W2A*, Lb/Lb.da	0.007927	0.007989	0.008084	0.008347
H2A, Btu/Lb.da	28.6269	28.7351	28.3345	28.6345
H2A*, Btu/Lb.da	28.8898	28.8652	28.8321	28.8016
COP	0.2299	0.2266	0.2499	0.2834
COP*	0.1994	0.2093	0.2263	0.2831
C2A	0.972	0.9682	0.9694	0.9651
C2A*	0.9645	0.9625	0.9594	0.9509

* Theoretical results based on average input conditions and with EA=EG=0.75, FA=FG=0.15, and ERS=0.55

Table D-3: Effect of Hot Water Inlet Temperature.

	GNERATOR INLET WATER TEMPERATURE, F		
	128.2	136.1	144.6
INPUT PARAMETERS			
MAA, Lb/hr	967	967	967
MAG, Lb/hr	870	870	870
MD, Lb/hr	203	203	203
MPWG, Lb/hr	1077	1077	1077
TPW2A, F	73.85	73.9	74
TDB1A, F	76.2	76.2	77.2
TWB1A, F	67.8	67.3	67.5
W1A, Lb/Lb.da	0.012714	0.012286	0.012286
MPWA, Lb/hr	1366	1396	1370
TDB1G, F	102	104	103
UOTPUT PARAMETERS			
TPW1G, F	119.1	125.3	132.5
TPW1G*, F	119.33	125.26	131.64
TSING, F	96.3	100.1	102
TSING*, F	100.35	103.7	107.26
TSINA, F	96.4	99.2	101.3
TSINA*, F	96.27	99.5	102.03
TPW1A, F	77.2	77.5	78.1
TPW1A*, F	77.24	77.51	77.77
TDB2A, F	81	81.4	82.2
TDB2A*, F	82.82	83.84	84.89
TWB2A, F	64	62.9	63.1
TEEC, F	67.6	66.8	67.6
W2A, Lb/Lb.da	0.009143	0.0083	0.008
W2A*, Lb/Lb.da	0.008816	0.008492	0.008192
H2A, Btu/Lb.da	29.4695	28.6423	28.50797
H2A*, Btu/Lb.da	29.556	29.448	29.3746
COP	0.2702	0.2575	0.258
COP*	0.2375	0.2032	0.1751
C2A	0.9542	0.9575	0.9695
C2A*	0.9451	0.9548	0.9633

---

* Theoretical results based on average input conditions and with EA=EG=0.75, FA=FG=0.15, and ERS=0.55.

APPENDIX E
UNCERTAINTY ANALYSIS

Every experimental work is associated with errors that can be classified as systematic or random. The uncertainty of a given variable is the net effect of its contributing sources of error; in particular, the uncertainty of a computed variable is the result of the propagation of errors in the primary measurements. If a result variable R is a given function of the independent variables X_1, X_2, ..., X_n

$$R = R(X_1, X_2, \ldots, X_n) \tag{E-1}$$

then the uncertainty in the result ΔR is expressed in terms of the individual uncertainties in the independent variables ΔX_1, ΔX_2, ..., ΔX_n by

$$\Delta R = \left[\frac{\partial R}{\partial X_1} \Delta {X_1}^2 + \frac{\partial R}{\partial X_2} \Delta {X_2}^2 + \ldots + \frac{\partial R}{\partial N_n} \Delta {X_n}^2 \right]^{1/2} \tag{E-2}$$

Because of the complexity and non linearity of the system of equations encountered in the analysis of the liquid-desiccant air-conditioners, it is impossible to explicitly express each result variable as a function of the independent ones and then calculate the propagation of errors as presented above; therefore, the following approach is adopted

If the output variables $Y_j (j = 1,\dots,m)$ are related to the independent input variables X_i $(i = 1, \dots, n)$ by the system of m non linear equations

$$f_j(Y_1,Y_2,\dots,Y_m,X_1,X_2,\dots,X_n) = 0 \tag{E-3}$$

then, by successive substitutions, the solution can theoretically be written as

$$Y_j = F_j\ (X_1,\ X_2,\ \dots,\ X_n) \tag{E-4}$$

where F_j are still unknown expressions. The uncertainity propagation may thereafter be represented by

$$\Delta Y_j = [\ \frac{\partial F_j}{\partial X_1} \Delta X_1{}^2 + \dots + \frac{\partial F_j}{\partial X_n} \Delta X_n{}^2\ ]^{1/2} \tag{E-5}$$

The partial derivatives $\frac{\partial F_j}{\partial X_i}$ can not be determined analytically since the expressions F_j are unknown, but can be numerically approximated by

$$\frac{\partial F_j}{\partial X_i} = \frac{F_j(X_1,\dots,X_j+\varepsilon_j,\dots,X_n) - F_j(X_1,\dots,X_j,\dots,X_n)}{\varepsilon_j} \tag{E-6}$$

where ε_j is an arbitrary chosen small increment, and

$$F_j(X_1,\ldots,X_n) = Y_j(X_1,\ldots,X_n) \qquad \text{(E-6a)}$$

are deduced from the numerical solution of the system of non linear equations. The knowledge of the partial derivatives and of the uncertainty in the independent variables permit the computation of the desired error propagations using equation (E-5).

The uncertainties of the measured variables are estimated from the least count of the instrumentation, double checking to other equipment or calibration, disturbances, reproducibility and stability. In the analysis of the effect of different parameters on the system performance, the experimental average values of the supposedly kept constant variables input data are used in the simulation model for comparison. To take that into account, the deviations of the actual input data from their average values are also considered as errors. Finally, the errors introduced by the empirical correlations are included by inserting multipliers which are then treated as independent variables.

After preliminary calculations, the uncertainty propagation due to certain variables was found negligible and was then omitted. Table E-1 gives the estimated errors of the measured input parameters and input coefficients. Table E-2 gives a sample of the uncertainty in the computed output variables, resulting from the propagation of errors in the primary input parameters.

Table E-1. Estimated Errors of Different Variables

Variable	Uncertainty	Variable	Uncertainty
MAA	± 10%	MAG	± 10%
MPWA	± 10%	MPWG	± 5%
MDA	± 10%	MDG	± 10%
TSINA	± 1°F	TSING	± 2°F
TPW2A	± 0.5°F	TPW2G	± 0.5°F
TPW1A	± 0.5°F	TPW1G	± 0.5°F
TDB1A	± 0.5°F	TDB1G	± 2°F
TDB2A	± 0.5°F	TDB2G	± 2°F
TWB1A	± 1°F	E	± 15%
TWB2A	± 1°F	F	± 20%
HCA	± 10%	ERS	± 20%

Table E-2. Uncertainty pf Computer Output Variables, Resluting from Error Propagation*

Variable	Uncertainty	Variable	Uncertainty
TDB2A	1.8°F	H2A	0.898 Btu/Lb. da
TDB2G	3.6°F	W2A	0.79 10^{-3}LB.H_2O/Lb.da
TPW1A	0.7°F	C2A	0.46 % by weight
TPW1G	1.3°F	C2G	0.68 % by weight
TSINA	2.7°F	COP	0.1
TSING	2.8°F		

---

* Uncertainties based on the experimental data of Table D-1 with an absorber water flow rate of 1016 Lb/hr.

APPENDIX F
COMPUTER LISTING OF DESYST AND SUBROUTINE DESCON

```
C          ***************************************
C
C                SOLAR POWERED LIQUID DESICCANT
C
C                   AIR CONDITIONING SYSTEM
C
C          ***************************************
C
C          THIS PROGRAM SERVES TO COMPUTE ALL THE OUTPUT
C         PARAMETERS OF THE LIQUID DESICCANT AIR
C         CONDITIONER, USING TRIETHYLENE GLYCOL.
C          THE INPUT PARAMETERS ARE READ FROM A DATA FILE,
C         THAT SHOULD BE FORMATTED ACCORDING TO THE READ
C         STATEMENTS, OR BY INTERACTIVE MEANS.
C          THE INPUT AND OUTPUT VARIABLE NOTATIONS ARE
C         CONSISTENT WITH WHAT WAS USED IN THE TEXT OF
C         THIS DISSERTATION.
C
C          **********   MAIN PROGRAM     **********
C
      IMPLICIT REAL (A-Z)
      INTEGER I,K,L,M,N,NC,TEST
      COMMON W2C,TDB2C,C1C,LAMDA,PT,K
      LOGICAL*1 NAME(20)
      DATA NAME/20*´ ´/
      TYPE*,´ENTER THE TEST DATAFILE NAME´
      READ (7,1)L,(NAME(I),I=1,L)
1     FORMAT(Q,20A1)
      CALL ASSIGN (2,NAME,0,´RDO´)
C  ABSORBER COIL DATA :
      READ(2,8) LA,WA,HA,IDA,ODA,XAA,XBA,YFA
      READ(2,4) NRA,NTPRA,NTFA,NFA
C  GENERATER COIL DATA :
      READ(2,8) LG,WG,HG,IDG,ODG,XAG,XBG,YFG
      READ(2,4) NRG,NTPRG,NTFG,NFG
C  AIR CONDITIONS AND FLOW RATES :
      READ(2,4) TO,WO,TR,WR
      READ(2,4) MAA,MAG,YA,YG
      READ(2,4) MUAA,MUAG,KAA,KAG
C  PROCESS WATER CONDITIONS AND FLOW RATES :
      READ(2,6) MPWA,TPW2A,CPWA,MUWA,KWA,ROUWA
      READ(2,6) MPWG,TPW2G,CPWG,MUWG,KWG,ROUWG
C  DESICCANT SOLUTION DATA :
      READ(2,5) MDA,MDG,CPDA,CPDG,QM
C  EFFECTIVENESS,WETTING SACTOR  TOTAL PRESSURE :
      READ(2,7) ERA,ERG,FA,FG,EA,EG,PT
C  INITIAL GUESSES :
      READ(2,4) C2AIG,W2AIG,T2AIG,T2GIG
C  CONVERGENCE CRITERIA :
      READ(2,4) DW2,DT2,EPSA,EPSC
4     FORMAT(4F10.5)
5     FORMAT(5F10.5)
6     FORMAT(6F10.5)
7     FORMAT(7F10.5)
8     FORMAT(8F8.4)
      LA = 12.0
      LG = 12.0
      WA = 12.0
      WG = 12.0
      TYPE*,'ENTER : TO, WO, TR, WR'
      ACCEPT*,TO,WO,TR,WR
      TYPE*,'ENTER: MAA,MAG,YA'
      ACCEPT*,MAA,MAG,YA
      TYPE*,'ENTER: MPWA,MPWG,TPW2A,TPW2G,MDA,MDG'
      ACCEPT*,MPWA,MPWG,TPW2A,TPW2G,MDA,MDG
      TYPE*,'ENTER: ERA,ERG,ERS'
      ACCEPT*,ERA,ERG,ERS
      TYPE*,'ENTER: FA,FG,EA,EG'
      ACCEPT*,FA,FG,EA,EG
      TYPE*,'ENTER NRA,NRG,NTFA,NTFG,NFA,NFG :'
      ACCEPT*,NRA,NRG,NTFA,NTFG,NFA,NFG
      TYPE*,'ENTER C2AIG :'
      ACCEPT*,C2AIG
C  CONVERGENCE CRITERIA :
      DW2 = 0.000001
      DT2 = 0.01
      EPSC = 0.0001
C  DERIVATION OF CONTACTER  INPUT CONDITIONS IN
C   TERMS OF THE VENTILATION RATE Y :
      YG = (1-YA)*MAA/MAG
      WOG = YG*WR + (1-YG)*WO
      W1G = WOG
      WOA = YA*WR + (1-YA)*WO
      W1A = WOA
      HOG = YG*HMSTA(TR,WR) + (1-YG)*HMSTA(TO,WO)
      HOA = YA*HMSTA(TR,WR) + (1-YA)*HMSTA(TO,WO)
      TDBOG = (HOG-1061.0*WOG)/(0.240+0.444*WOG)
      TDBOA = (HOA-1061.0*WOA)/(0.240+0.444*WOA)
```

```
C  COMPUTATION OF HEAT AND MASS TRANSFER COEFFICIENTS :
      CALL HTX(LA,WA,ZA,XBA,IDA,ODA,NFA,YFA,NTFA,NTPRA,
     $NRA,ROUWA,CPWA,MUWA,KWA,MPWA,MUAA,KAA,MAA,
     $W0A,HCAA,HCWA,HMA,LEA,A0A,ATIA,TPW2A)
      CALL HTX(LG,WG,ZG,XBG,IDG,ODG,NFG,YFG,NTFG,NTPRG,
     $NRG,ROUWG,CPWG,MUWG,KWG,MPWG,MUAG,KAG,MAG,
     $W0G,HCAG,HCWG,HMG,LEG,A0G,ATIG,TPW2G)
C  INITIALISATION :
      LAMDA0 = 1.0
      M = 0
      NC = 0
      K = 0
12    C2AIG = C2AIG - 0.01
      TYPE*,´C2AIG=´,C2AIG,´LAMDAA´,LAMDAA,´LAMDAG´,LAMDAG
      LAMDAA = LAMDA0
      LAMDAG = LAMDA0
      W2G = W0G
      C2A = C2AIG
      TDB2G = TDB0G
C  ABSORBER CALCULATION :
13    LAMDAA = LAMDAA - 0.1
      IF(LAMDAA.LT.0.1) GO TO 12
      TSINA = TPW2G + ERS*(TPW2A-TPW2G)
      TDB2A = TDB0A
      W2A = W0A
100   K = K+1
      CALL CONT(C2A,W2A,TDB2A,W0A,TDB0A,TSINA,TPW1A,MAA,
     $MDA,MPWA,CPDA,CPWA,LEA,HCAA,HCWA,ATIA,A0A,ERA,EA,FA,
     $PT,QM,DW2,DT2,TPW2A,TS1A,TS2A,C1A,QPWA,QLA,TDB1A,
     $AHMA,AMA,H1A,H2A,WE1A,WE2A,N,TEST,LAMDAA)
      M = M + N
      IF(TEST.EQ.1) GO TO 13
      W2A = W2C
      TDB2A = TDB2C
      C1A = C1C
C  GENERATER CALCULATION :
      C2G = C1A
      TSING = TS1A-TSINA+(ERS*TS1A-TSINA)/(ERS-1.)
      GO TO 110
14    LAMDAG = LAMDAG - 0.1
      IF(LAMDAG.LT.0.1) GO TO 12
      W2G = W0G
      TDB2G = TDB0G
110   K = K + 1
      CALL CONT(C2G,W2G,TDB2G,W0G,TDB0G,TSING,TPW1G,MAG,
     $MDG,MPWG,CPDG,CPWG,LEG,HCAG,HCWG,ATIG,A0G,ERG,EG,FG,
     $PT,QM,DW2,DT2,TPW2G,TS1G,TS2G,C1G,QPWG,QLG,TDB1G,
     $AHMG,AMG,H1G,H2G,WE1G,WE2G,N,TEST,LAMDAG)
      M = M + N
      IF(TEST.EQ.1) GO TO 14
      TDB2G = TDB2C
      W2G = W2C
      C1G = C1C
      TSINA = TS1G - ERS*(TS1G-TS1A)
C  CONCENTRATION CONVERGENCE CHECK :
      IF(ABS(C1G-C2A).LT.EPSC) GO TO 200
      C2A = ( C2A + C1G )/2.
      NC = NC + 1
      TYPE*,´LAMDAA=´,LAMDAA,´LAMDAG=´,LAMDAG
      GO TO 100
200   QCOOL = MAA*(H2A-HMSTA(TR,WR))
      QABS = MAA*(H2A-H1A)
      QGEN = MAG*(H2G-H1G)
      QLATA = MAA*(W2A-W1A)*HFGW((TS1A+TS2A)/2.0)
      QLATG = MAG*(W2G-W1G)*HFGW((TS1G+TS2G)/2.0)
      MSA = MDA/C2A
      MSG = MDG/C2G
      QDESA = ((1.-(C1A+C2A)/2.)*CPWA+CPDA)*(TS1A-TSINA)*MSA
      QDESG = ((1.-(C1G+C2G)/2.)*CPWG+CPDG)*(TS1G-TSING)*MSG
      COP = -QCOOL / QPWG
      COPWPH = -QCOOL/(QPWG+MAG*(H1G-H0G))
      TYPE*,´ ´
      TYPE*,´# OF TIMES CONT WAS CALLED:´,K
      TYPE*,´TOTAL # OF IITERATIONS =´,M
      TYPE*,´# OF TIMES C2A HAS CHANGED´,NC
C  PRINT OUT REQUIERED DATA  RESULTS :
      WRITE(7,11) TR,TO,WR,WO
11    FORMAT(//30X,´ROOM CONDITIONS =´,5X,´OUT CONDITIONS =´
     $//10X,´DRY BULB TEMP    =´,F14.7,15X,F10.7/
     $10X,´HUMIDITY RATIO  =´,F14.7,15X,F10.7)
      WRITE(7,33) MAA,MAG,MPWA,MPWG,MDA,MDG,YA,YG,
     $ERA,ERG,EA,EG,FA,FG,TDB0A,TDB0G,W0A,W0G
      WRITE(7,44) TDB1A,TDB1G,H1A,H1G,W0A,W0G,WE1A,WE1G,
     $TDB2A,TDB2G,H2A,H2G,W2A,W2G,W2A,WE2G,C1A,C1G,
     $TS1A,TS1G,C2A,C2G,TS2A,TS2G,TSINA,TSING
      WRITE(7,55) TPW1A,TPW1G,TPW2A,TPW2G,QPWA,QPWG,QLA,QLG,
     $QDESA,QDESG,HCAA,HCAG,HCWA,HCWG,HMA,HMG,A0A,A0G,ATIA,
     $ATIG,ZA,ZG,NRA,NRG,AHMA,AHMG,AMA,AMG,QABS,QGEN,QLATA,
     $QLATG,QCOOL,COP,COPWPH
33    FORMAT(/20X,´ABSORBER :´,12X,´GENERATER :´//
     $10X,´MA     =´,F16.7,6X,F16.7/
     $10X,´MPW    =´,F16.7,6X,F16.7/
     $10X,´MD     =´,F16.7,6X,F16.7/
     $10X,´Y      =´,F16.7,6X,F16.7/
     $10X,´ER     =´,F16.7,6X,F16.7/
     $10X,´E      =´,F16.7,6X,F16.7/
     $10X,´F      =´,F16.7,6X,F16.7//
     $10X,´TDB0   =´,F16.7,6X,F16.7/
     $10X,´W0     =´,F16.7,6X,F16.7/)
44    FORMAT(10X,´TDB1  =´,F16.7,6X,F16.7/
     $10X,´H1     =´,F16.7,6X,F16.7/
     $10X,´W1     =´,F16.7,6X,F16.7/
     $10X,´WE1    =´,F16.7,6X,F16.7//
     $10X,´TDB2   =´,F16.7,6X,F16.7/
     $10X,´H2    =´,F16.7,6X,F16.7/
     $10X,´W2    =´,F16.7,6X,F16.7/
     $10X,´WE2   =´,F16.7,6X,F16.7//
     $10X,´C1    =´,F16.7,6X,F16.7/
     $10X,´TS1   =´,F16.7,6X,F16.7//
     $10X,´C2    =´,F16.7,6X,F16.7/
     $10X,´TS2   =´,F16.7,6X,F16.7/
     $10X,´TSIN  =´,F16.7,6X,F16.7/)
55    FORMAT(10X,´TPW1  =´,F16.7,6X,F16.7/
     $10X,´TPW2  =´,F16.7,6X,F16.7/
     $10X,´QPW   =´,F16.7,6X,F16.7/
     $10X,´QL    =´,F16.7,6X,F16.7/
     $10X,´QDES  =´,F16.7,6X,F16.7//
     $10X,´HCA   =´,F16.7,6X,F16.7/
     $10X,´HCW   =´,F16.7,6X,F16.7/
     $10X,´HM    =´,F16.7,6X,F16.7//
     $10X,´A0    =´,F16.7,6X,F16.7/
     $10X,´ATI   =´,F16.7,6X,F16.7/
     $10X,´Z     =´,F16.7,6X,F16.7/
     $10X,´NR    =´,F16.7,6X,F16.7//
     $10X,´AHM   =´,F16.7,6X,F16.7/
     $10X,´AM    =´,F16.7,6X,F16.7//
     $10X,´QCONT =´,F16.7,6X,F16.7/
     $10X,´QLAT  =´,F16.7,6X,F16.7//
     $10X,´QCOOL =´,F16.7/
     $10X,´COP   =´,F16.7/
     $10X,´COPWPH=´,F16.7)
      STOP
      END

C         **********  SUBROUTINE CONTACTER  *********

C         GIVEN THE PROCESS WATER,DESICCANT SOLUTION
C         AND THE AIR STREAM INLET CONDITIONS; THIS
C         SUBROUTINE COMPUTES THE OUTLET CONDITIONS.

      SUBROUTINE CONT(C2,W2,TDB2,W0,TDB0,TSIN,TPW1,MA,MD,
     $MPW,CPD,CPW,LE,HCA,HCW,ATI,A0,ER,E,F,PT,QM,DW,DT,TPW2,
     $TS1,TS2,C1,QPW,QL,TDB1,AHM,AM,H1,H2,WE1,WE2,N,
     $TEST,LAMDA)
      IMPLICIT REAL(A-Z)
      INTEGER TEST,N,K
      COMMON W2C,TDB2C,C1C
      TEST = 0
      W1 = W0
      N = 0
10    N = N + 1
D     TYPE*,´TDB2´,TDB2
      W2P = W2
      TDB2P = TDB2
      TDB2 = TDB2 + DT
      DMW = MA*(W2-W1)
```

```
 MS2 = MD / C2
 C1 = MD / (MS2 - DMW)
 X2 = (MS2 - MD)/MD
 X1 = (MS2 - MD - DMW)/MD
 TDB1 = (TDB2-TDB0)*ER + TDB0
 H1 = HMSTA(TDB1,W1)
 H2 = HMSTA(TDB2,W2)
 CPL = CPD+CPW*(X1+X2)/2.
 DTLW = -(MD*CPL*(TPW2-TSIN)+MA*(H2-H1)+MA*(W2-W1)*QM)
$/((MPW*CPW+MD*CPL)*(HCW*ATI/(MPW*CPW))+MD*CPL)
 TPW1 = TPW2+(HCW*ATI/(MPW*CPW))*DTLW
 QL = (MD*CPL+MPW*CPW)*(TPW2-TPW1)
 TS1 = TPW1+DTLW
 TS2 = TPW2+DTLW
 WE1 = WESOL(C1,TS1,PT)
 WE2 = WESOL(C2,TS2,PT)
 KYP = HCA / 0.24
 YP1 = W1
 YP2 = W2
 YPE1 = WE1
 YPE2 = WE2
 DYR = (YP1 - YPE1)/(YP2 - YPE2)
 IF(DYR.LE.0.0) GO TO 99
 DYLM = ((YP1-YPE1)-(YP2-YPE2))/ALOG(DYR)
 FF1T = A0*DYLM*KYP*F - MA*(YP1-YP2)
 CPG = 0.240+0.444*(W1+W2)/2.
 TBAR = (TDB1+TDB2)/2.
 HS1 = HSTAR(TDB1,W1,QM,F,CPG,LE,TBAR)
 HS2 = HSTAR(TDB2,W2,QM,F,CPG,LE,TBAR)
 HSI1 = HSTAR(TS1,WE1,QM,F,CPG,LE,TBAR)
 HSI2 = HSTAR(TS2,WE2,QM,F,CPG,LE,TBAR)
 DHSR = (HS2 - HSI2)/(HS1 - HSI1)
 IF(DHSR.LE.0.0) GO TO 99
 DHSLM = ((HS2-HSI2)-(HS1-HSI1)) / ALOG((HS2
$-HSI2) / (HS1-HSI1))
 GG1T = QL + HCA*E*A0*DHSLM / CPG
 TDB2 = TDB2P
 W2 = W2 + DW
 DMW = MA*(W2-W1)
 MS2 = MD / C2
 C1 = MD / (MS2 - DMW)
 X2 = (MS2 - MD)/MD
 X1 = (MS2 - MD - DMW)/MD
 TDB1 = (TDB2-TDB0)*ER + TDB0
 H1 = HMSTA(TDB1,W1)
 H2 = HMSTA(TDB2,W2)
 CPL = CPD+CPW*(X1+X2)/2.
 DTLW = -(MD*CPL*(TPW2-TSIN)+MA*(H2-H1)+MA*(W2-W1)*QM)
$/((MPW*CPW+MD*CPL)*(HCW*ATI/(MPW*CPW))+MD*CPL)
 TPW1 = TPW2+(HCW*ATI/(MPW*CPW))*DTLW
 QL = (MD*CPL+MPW*CPW)*(TPW2-TPW1)
 TS1 = TPW1+DTLW
```

```
      TS2 = TPW2+DTLW
      WE1 = WESOL(C1,TS1,PT)
      WE2 = WESOL(C2,TS2,PT)
      KYP = HCA / 0.24
      YP1 = W1
      YP2 = W2
      YPE1 = WE1
      YPE2 = WE2
      DYR = (YP1 - YPE1)/(YP2 - YPE2)
      IF(DYR.LE.0.0) GO TO 99
      DYLM = ((YP1-YPE1)-(YP2-YPE2))/ALOG(DYR)
      FF1W = A0*DYLM*KYP*F - MA*(YP1-YP2)
      CPG = 0.240+0.444*(W1+W2)/2.
      TBAR = (TDB1+TDB2)/2.
      HS1 = HSTAR(TDB1,W1,QM,F,CPG,LE,TBAR)
      HS2 = HSTAR(TDB2,W2,QM,F,CPG,LE,TBAR)
      HSI1 = HSTAR(TS1,WE1,QM,F,CPG,LE,TBAR)
      HSI2 = HSTAR(TS2,WE2,QM,F,CPG,LE,TBAR)
      DHSR = (HS2 - HSI2)/(HS1 - HSI1)
      IF(DHSR.LE.0.0) GO TO 99
      DHSLM = ((HS2-HSI2)-(HS1-HSI1)) / ALOG((HS2
     $-HSI2) / (HS1-HSI1))
      GG1W = QL + HCA*E*A0*DHSLM / CPG
      W2 = W2P
      DMW = MA*(W2-W1)
      MS2 = MD / C2
      C1 = MD / (MS2 - DMW)
      X2 = (MS2 - MD)/MD
      X1 = (MS2 - MD - DMW)/MD
      TDB1 = (TDB2-TDB0)*ER + TDB0
      H1 = HMSTA(TDB1,W1)
      H2 = HMSTA(TDB2,W2)
      CPL = CPD+CPW*(X1+X2)/2.
      DTLW = -(MD*CPL*(TPW2-TSIN)+MA*(H2-H1)+MA*(W2-W1)*QM)
     $/((MPW*CPW+MD*CPL)*(HCW*ATI/(MPW*CPW))+MD*CPL)
      TPW1 = TPW2+(HCW*ATI/(MPW*CPW))*DTLW
      QL = (MD*CPL+MPW*CPW)*(TPW2-TPW1)
      TS1 = TPW1+DTLW
      TS2 = TPW2+DTLW
      WE1 = WESOL(C1,TS1,PT)
      WE2 = WESOL(C2,TS2,PT)
      KYP = HCA / 0.24
      YP1 = W1
      YP2 = W2
      YPE1 = WE1
      YPE2 = WE2
      DYR = (YP1 - YPE1)/(YP2 - YPE2)
      IF(DYR.LE.0.0) GO TO 99
      DYLM = ((YP1-YPE1)-(YP2-YPE2))/ALOG(DYR)
      FF = A0*DYLM*KYP*F - MA*(YP1-YP2)
      CPG = 0.240+0.444*(W1+W2)/2.
      TBAR = (TDB1+TDB2)/2.
      HS1 = HSTAR(TDB1,W1,QM,F,CPG,LE,TBAR)
      HS2 = HSTAR(TDB2,W2,QM,F,CPG,LE,TBAR)
      HSI1 = HSTAR(TS1,WE1,QM,F,CPG,LE,TBAR)
      HSI2 = HSTAR(TS2,WE2,QM,F,CPG,LE,TBAR)
      DHSR = (HS2 - HSI2)/(HS1 - HSI1)
      IF(DHSR.LE.0.0) GO TO 99
      DHSLM = ((HS2-HSI2)-(HS1-HSI1)) / ALOG((HS2
     $-HSI2) / (HS1-HSI1))
      GG = QL + HCA*E*A0*DHSLM / CPG
      FFT = (FF1T - FF)/DT
      FFW = (FF1W - FF)/DW
      GGT = (GG1T - GG)/DT
      GGW = (GG1W - GG)/DW
      IF(FFT.EQ.0.0.OR.GGT.EQ.0.0) GO TO 11
      GO TO 12
11    DT = 10.0*DT
      GO TO 10
12    DEN = FFT*GGW - FFW*GGT
      TDB2 = TDB2P + LAMDA*(FFW*GG-FF*GGW)/DEN
      W2 = W2P + LAMDA*(FF*GGT-FFT*GG)/DEN
C  CONVERGENCE CHECK :
      IF(ABS(W2P-W2).GT.DW) GO TO 10
      IF(ABS(TDB2P-TDB2).GT.DT) GO TO 10
      W2C = W2
      TDB2C = TDB2
      C1C = C1
      QS = MA*CPG*(TDB2-TDB1)
      AM = MA*(YP1-YP2)/(DYLM*KYP*F)
      QL = (MPW*CPW+MD*CPL)*(TPW2-TPW1)
      AHM = -QL*CPG / (HCA*E*DHSLM)
      QPW = MPW*CPW*(TPW2-TPW1)
      GO TO 100
99    TEST = 1
100   RETURN
      END
C
C         **********  SUBROUTINE HTX  **********
C
C         IT COMPUTES THE HEAT  MASS TRANFER
C         FOR A SPECIFIC FINNED TUBE COIL
C         GEOMETRY  FLUID FLOW CONFIGURATION
C
      SUBROUTINE HTX(L,W,Z,XB,ID,OD,NF,Y,NTF,NTPR,NR,
     $ROUW,CPW,MUW,KW,MPW,MUA,KA,MA,W0,HCA,HCW,HM,LE,A0,
     $ATI,TPW)
      IMPLICIT REAL(A-Z)
C  WATER SIDE HEAT TRANSFER COEFFICIENT (HCW)
      Z = NR * XB
      A = 3.14159*ID**2 /( 4.0*144.0)
      V = MPW / (ROUW*A*NTF)
      REID = ROUW * V * (ID/12.) / MUW
      PRW = MUW * CPW / KW
      IF(TPW.GT.100.0) GO TO 10
      N = 0.4
      GO TO 20
10    N = 0.3
20    HCW = 0.023 * KW * REID**0.8 * PRW**N / (ID/12.)
C  AIR SIDE HEAT TRANSFER COEFFICIENT :
      AFR = L * W / 144.0
      AC = AFR-(NTPR*L*OD+NF*L*Y*(W-NTPR*OD))/144.
      ATI = NTPR * NR * 3.14159 * ID * L / 144.0
      ATO  = NTPR * NR * 3.14159 * OD * L / 144.0
      AO = (2.*NF*L*(W*Z - NTPR*NR*3.14159*OD**2/4.)
     $ + NTPR*NR*3.14159*OD*L*(1. - NF*Y)) / 144.0
      GC = MA / AC
      REOD = GC * (OD/12.) / MUA
      JP = REOD**(-0.4)*(AO/ATO)**(-0.15)
      S = 1. / NF
      RES = REOD * S / OD
      JS = 0.84 + 4.*10.**(-5)*RES**1.25
      JIS = (0.95 + 4.*10.**(-5)*RES**1.25)*(S/(S-Y))**2
      JPS = JP * JS
      JPIS = JP * JIS
      J4 = (2.6144*JPS*10.**2 + 1.3858)*10.**(-3)
      REXB = GC * (XB/12.) / MUA
      NRR = NR
      IF(NRR.LE.10) GO TO 30
      NRR = 10
30    R = (1.-1280.*NRR*REXB**(-1.2))
     $/(1.-5120.*REXB**(-1.2))
      JNR = J4 * R
      CPA = 0.240 + 0.444*WO
      PRA = MUA * CPA / KA
      HCA =  JNR * GC * CPA * PRA**(-2./3.)
      LE = 0.84
C  MASS TRANSFER COEFFICIENT :
      SC = PRA
      JI4 = (2.6144*JPIS*10.**2 + 1.3858)*10.**(-3)
      JINR = JI4 * R
      HM = JINR * GC * SC**(-2./3.)
      RETURN
      END

C          **********  FUNCTION HMSTA(T,W)  **********

C          IT COMPUTES THE ENTHALPY OF MOIST AIR
C          KNOWING THE DRY BULB TEPERATURE IN ´F
C           THE HUMIDITY RATIO W IN LB.H2O/LB.D.A

      FUNCTION HMSTA(T,W)
      HMSTA = 0.240*T + W*(1061.0 + 0.444*T)
      RETURN
      END
```

```
C         **********  FUNCTION HFGW(T)  ***********

C         IT COMPUTES THE WATER LATENT HEAT AT A
C         GIVEN SATURATION TEMPERATURE READ IN ´F

      FUNCTION HFGW(T)
      HFGW = 1053.0 - (52./90.)*(T - 70.0)
      RETURN
      END

C         ************  FUNCTION HSTAR  ************

C         IT COMPUTES THE ENTHALPY HSTAR AT A
C         GIVEN TEMPRATURE (´F), HUMIDITY RATIO
C         (LB.H2O/LB.D.A), HEAT OF MIXING (BTU/LB.H2O)
C         AND WETTING FACTOR.

      FUNCTION HSTAR(T,W,QM,F,CPG,LE,TBAR)
      REAL LE
      HSTAR = CPG*T+F*W*(HFGW(TBAR)+QM)/(LE**(2./3.))
      RETURN
      END

C         ******  FUNCTION WESOL(C,T,P)  **********

C         IT COMPUTES THE EQUILIBRIUM HUMIDITY
C         RATIO OF WATER IN THE DESICCANT SOLUTION

      FUNCTION WESOL(C,T,P)
      IMPLICIT REAL (A-Z)
      TK = (T+459.67)/1.8
      K1 = -5800.2206
      K2 = +1.3914993
      K3 = -0.048640239
      K4 = +0.41764768E-4
      K5 = -0.1445209E-7
      K6 = +6.5459673
      LNPWS = (K1/TK)+K2+K3*TK+K4*TK**2+K5*TK**3+K6*ALOG(TK)
      PWSMMM = 760.*(EXP(LNPWS))/(1.01325E5)
      PWEMMM = (-3.07443142+11.44547558*C-8.37558365*C**2)
     $ *PWSMMM**0.972
      WESOL = 0.62198*PWEMMM/(P-PWEMMM)
      RETURN
      END
```

REFERENCES

1. Dunkle, R.V., "A Method of Solar Air Conditioning," Mech. and Chem. Engr. Trans. Inst. Engrs. Australia., MC1, 73, (May 1985).

2. Dunkle, R.V., "Regenerative Evaporative Cooling Systems," Australian Refrigeration,Air Conditioning and Heating, pp. 13-23, (Jan. 1906).

3. Dunkle, R.V., and Maclaine-Cross, I.L., "Theory and Design of Rotary Regenerators for Air Conditioning," Mech. and Chem. Engr. Transactions, MC6, No. 1, (May 1970).

4. Johnson, R.C.R., "Regenerative Evaporative Air Conditioning with Dehumidification," Australian Refrigeration, Air Conditioning and Heating, 29 (Feb. 1967).

5. Lunde, Peter, "Solar Desiccant System Analysis and Materials," Use of Solar Energy for the Cooling of Buildings, de Winter, F., and de Winter J.W., eds. NTIS # SAN/1122.

6. Lunde, Peter, "Solar Desiccant Air Conditioning with Silica Gel," The Use of Solar Energy for Cooling of Buildings, NTIS # SAN/1122-76/2, 280, (Feb. 1976).

7. Lunde, Peter, Solar Powered Desiccant Air Conditioning System, CEM 4171-526, Center for the Environment and Man, Hartford, CT., (1975).

8. Lunde, Peter, Preliminary Design of a Solar Powered Desiccant Air Conditioning System USing Silica Gel, CEM 4186-55, Center for the Environment and Man, Harford CT., (1976).

9. Nelson, J.S., An Investigation of Solar Powered Open Cycle Air conditioners, M.S. thesis, University of Wisconson, Madison, 1976.

10. Nelson, J.S., Beckman, W.A., Mitchell, J.W., Close, D.J., "Simulations of The Performance of Open Cycle Desiccant Systems Using Solar Energy," Solar Energy, 21, 273, (1978).

11. Banks, P.J., "Coupled Equilibrium Heat and Single Absorbate Transfer in Fluid Flow Through a Porus Medium - I," Chem. Engr. Sci., 27, 1143 (1972).

12. Close, D.J. and Banks, P.J., "Coupled Equilibrium Heat and Single Absorbate Transfer in Fluid Flow Through a Porus Medium II," Chem. Engr. Sci., 27, 1157 (1972).

13. Maclaine-Cross, I.L., and Banks, P.J., "Coupled Heat and Mass Transfer in Regenerators--Prediction Using an Analogy with Heat Transfer," Int. Jour. of Heat and Mass Transfer, 15, 1225, (1972).

14. Pla-Barby, F.E., Solar Desiccant Air Conditioning with Silica Gel Using Solar Energy, Ph.D. Dissertation, University of Texas, Austin, (May 1978).

15. Robison, H.I. et al., "Open Cycle Solar Air Conditioner," Proceedings of the 1978 Annual Meeting of AS/ISES, 667, (1978).

16. Barlow, K. and Collier, K., "Optimizing The Performance of Desiccant Beds for Solar Regenerated Cooling," Proceedings of the 1981 Annual Meeting of AS/ISES, 496, (1981).

17. Schultz, K.J., Mitchell, J.W. and Beckman, W.A., "The Performance of Desiccant Dehumidifier Air-Conditioning Systems Using Cooled Dehumidiers," American Society of Mechanical Engineers, Publication #83-WA/Sol-15.

18. Jurinak, J.J. and Beckman, W.A., "A Comparison of the Performance of Open Cycle Air Conditioners Utilizing Rotary Desiccant Dehumidifiers," Proceedings of the 1980 Annual Meeting of AS/ISES, 3, 215, (June 1980).

19. Lavan, Z., Gidaspow, D., Onischak, M., Perkari, S., "Development of a Solar Desiccant Dehumidifier," Proceedings of the 13th Intersociety Energy Conversion Engineering Conference, 1623, (Sept. 1978).

20. Roy, D. and Gidaspow, D., "Nonlinear Coupled Heat and Mass Exchange in a Cross-Flow Regenerator," Chem, Engr. Sci., 29, 2101, (1974).

21. Worek, W.M. and Lavan, Z., "Cross-Cooled Desiccant Dehumidifier for Solar Powered Cooliilng Systems," Proceedings of the 1980 Annual Meeting of the AS/ISES, 3.1, 224, 1980.

22. Monnier, J.B., Worek, W.M. and Lavan, Z., "Testing of a Solar Powered Cooling System Using Cross-Cooled Desiccant Dehumidifiers," Proceedings of the 1981 Annual Meeting of the AS/ISES, 4.1, 505, (May 1981).

23. Niagara Blower Company, Niagara Hygrol Liquid Desiccant System, Bulleting No. 162.

24. Midland-Ross Corporation, Kathabar Spray-Cel System, Bulletin KSC-175.

25. Midland-Ross Corporation, Kathabar Twin-Cel System, Bulletin TC-810.

26. Lof, G.O.G., "Cooling with Solar Energy," Proceedings of the 1955 Congress on Solar Energy, 171, (Nov. 1955).

27. Lodwig, E., Wilke, D. and Bressman, J., "A Solar Powered Desiccant Air Conditioning System," Proceedings of the 1977 Annual Meeting of the AS/ISES, 1, 1977.

28. Robison, H.I., "Liquid Sorbent Solar Air Conditioner," Alternative Energy Sources, Veziroglu, T.N., ed. Hemisphere Publishers, Washington, D.C., 1978.

29. Robison, H.I., "Liquid Desiccant Solar Heat Pumps for Developing Nations," Solar Energy International Progress, ed., Veziroglu, T.N., Pergamon Press, New York, N.Y., 1978.

30. Mullick, S.C. and Gupta, M.C., "Solar Air Conditioning Using Absorbents," Second Workshop on the Use of Solar Energy for the Cooling of Buildings, de Winter, eds., NTIS # SAN/1122-76/2 (1976).

31. Johannsen, A., "The Application of Liquid Absorbent Open Cycle Systems for Year Round Solar Air Conditioning," Proceedings of the Solar Energy Conference, Cape Town, South Africa, (Sept. 1978).

32. Johannsen, A., "Design and Operation of a Liquid Desiccant Type Solar Air Conditioning System," Sun II: Proceedings of the ISES, Silver Jubilee Congress, 1, 681 (May 1979).

33. Grossman, G. and Shwarts, I., "An Open Absorption System Utilizing Solar Energy for Air Conditioning," Proceeding of the Heat Transfer Conference, Dubrovnik, Yougoslavia, (Sept. 1977).

34. Olsen, T.G., "Desiccant Systems Potential for Cooling in Humid Climates," Solar Cooling and Heating: A National Forum, University of Miami, Conference Series, Dec. 1976.

35. Kapur, J.C., "A Report on the Utilization of Solar Energy for Refrigeration and Air Conditioning Applications," Solar Energy, 4.1, 39, (Jan. 1960).

36. Leboeuf, C.M., Lof, G.O.G., "Open-Cycle Absorption Cooling Using Packed-Bed Absorbent Réconcentration," Proceedings of the 1980 Annual Meeting of the American Section of the ISES, 205 (June 1980).

37. Factor, H.M. and Grossman, G., "A Packed Bed Dehmidifier/Regenerator for Solar Air Conditioning with Liquid Desiccants," Solar Energy, 24, 541 (1980).

38. Peng, C.S.P. and Howell, J.R., "Analysis and Design of Efficient Absorbers for Low Temperature Desiccant Air Conditioners," Journal of Solar Energy Engg., 103, 76 (Feb. 1981).

39. Turner, N.C., Cooling System and Method United State Patent No. 4, 171, 620, (Oct. 1979).

40. Hollands, K.G.T., "The Regeneration of Lithium Chloride brine in a Solar Still for use in Solar Air Conditioning," Solar Energy, 7.2, 39 (1963).

41. Dunkle, R.V., "Solar Water Distillation: The Roof Type Still and a Multiple Effect Diffusion Still," International Developments in Heat Transfer, ASME 5, 895, ASME, (1961).

42. Lof, G.O.G., Eibling, J.A. and Bloemer, J.W., "Energy Balances in Solar Distillers," A. J. CR. E. Journal, 7, 4 (Dec. 1961).

43. Kababaev, A. and Khandurdyer, A., "Absorption Solar Refrigeration Unit with Open Regeneration of Solution," Geliotekhnika, 5.4, 28, (1969).

44. Kababaev, A., et al., "Regeneration Capacity of an Absorption Solar Refrigeration Plant With Flat Glazed Solution Regenerator," Geliotekhnika, 8.2, 60, (1972).

45. Gandhidasan, P., Sriramulu, V., and Cupta, M.C., "Analysis of a Solar Regenerator," Proceedings of the ISES Congress, New Delhi, India, 1567, (Jan. 1978).

46. Gandhidasan, P., Sriramulu, V., and Gupta, M.C., "Theoretical and Experimental Investigations of a Countercurrent Solar Regenerator," Sun II: Proceeding of the ISES, Silver Jubilee Congress, 686, (May 1979).

47. Ganhidasan, P., Sriramulu, V., and Cupta, M.C., "Bouyancy Effects in a Solar Regenerator," Solar Energy, 22.1-B 9, (1979).

48. Mullick, S.C. and Gupta, M.C., "Solar Desorption of Absorbent Solutions," Solar Energy, 16, 19, (1974).

49. Peng, C.S.P., and Howell, J.R., The Performance of Various Types of Regenerators of Liquid Desiccants, A.S.M.E., Pulication 81-WA/Sol-31, (1981)

50. Treybal, Mass Transfer Operations Third Edition, McGraw Hill Company, New York, (1980).

51. Kays, W.M. and Crawford, M.E., Convective Heat and Mass Transfer, Second Edition, McGraw Hill Company New York, (1980).

52. Skelland, A.H.P., Diffusional Mass Transfer, John Wiley and Sons, New York 1976.

53. Chilton, T.H., and Colburn, A.P., "Mass Transfer (Absorption) Coefficients - Prediction from Data on Heat Transfer and Fluid Friction," Industrial and Engineering Chemistry, (Nov. 1934).

54. Threlkeld, J.L., Thermal Environmental Engineering, Second Edition, Prentice Hall Inc. Englewood, N.J., (1970).

55. Schlichting, H., Boundary-Layer Theory, Sixth Edition, McGraw Hill Company, New York, (1968).

56. Peng Chung Shiang Patrick., The Analysis and Design of Liquid Absorbent/Desiccant Cooling/Dehumidifiction Systems for Flor Grade Thermal Energy Applications, Ph.D. Dissertation, Department of Mechanical Engineering, University of Texas, (Dec. 1980).

57. Queiroz, A.G., Orlando, A.F., and Saboya, F.E.M., Performance of an Air Dryer of a Liquid Dehumidifier Solar Air Conditioning System, ASME, Publication 84-WA/Sol-6, (1984).

58. McQuiston, F.C., "Heat, Mass and Momentum Transfer in a Parallel Plate Dehmidifying Exchanger," ASHRAE Trans., 2, 82, (1976).

59. McQuiston, F.C., "Heat, Mass, and Momentum Transfer Data for Five Plate-Fin-Tube Heat Transfer Surfaces," ASHRAE Trans., 1, 84, (1978).

60. McQuiston, F.C., "Correlation of Heat, Mass, and Momentum Transport Coefficients for Plate-Fin-Tube Heat Transfer Surfaces," *ASHRAE Trans.*, *1*, 84, (1978).

61. Rich, D.G., "The Effects of Fin Spacing on the Heat Transfer and Friction Performance of Multirow Smooth Plate Fin-and-Tube Heat Exchangers," *ASHRAE Trans.*, 79, (June 1973).

62. Kays, W.M. and London, A.L., *Compact Heat Exchangers*, McGraw Hill, San Francisco, California, (1964).

63. McQuiston, F.C., "Heat Transfer and Flow Friction Data for Two Fin-Tube Surfaces," *ASME Journal of Heat Transfer*, 93, (May 1971).

64. Parker, J.D., Boggs, J.H., and Blick, E.F., *Introduction to Fluid Mechanics and Heat Transfer*, Addison-Wesley, Reading, Massachusetts, (1969).

65. McQuiston, F.C. and Parker, J.D., *Heating, Ventilating and Air Conditioning--Analysis and Design*, Second Edition, John Wiley & Sons, New York, (1982).

66. ASHRAE, *Ashrae Handbook of Equipment*," ASHARE, Inc. New York, (1983).

67. Gifford, E.W., "Dehmidification by Liquid Sorbents," *Heating, Piping and Air Conditioning*, 156, (Apr. 1957).

68. Dow Chemical Company, *A Guide to Clycols*, Form No. 116-1035-82.

69. ASHRAE, *ASHRAE Handbook of Fundamentals*, ASHRAE Inc., New York, (1985).

70. James, M.L., Smith, G.M., and Wolford, J.C., *Applied Numerical Methods for Digital Computation with FORTRAN and CSMP*, Second Edition, Harper & Row Publishers, Inc., New York, (1977).

71. Roose, R.W., *Handbook of Energy Conservation for Mechanical Systems in Buildings*, Van Nostrand Reinhold Company, New York, (1983).

BIOGRAPHICAL SKETCH

Ammar Chebbah was born in 1954, in Pont du Fahs, Tunisia. He graduated in 1971 from Béja High School (Lycée Technique de Béja), Tunisia. He attended the National School of Engineering of Tunis (E.N.I.T.), Tunisia, where he was awarded the degree of "Ingenieur Diplomé" in mechanical engineering, in 1979.

As a recipient of a national scholarship for graduate studies in the U.S.A., he joined the Graduate School of the University of Florida, Gainesville, Florida, in 1980.

I certify that I have read this study and that in my opinion it conforms to acceptable standards of scholarly presentation and is fully adequate, in scope and quality, as a dissertation for the degree of Doctor of Philosophy.

E. A. Farber, Chairman
Distinguished Service Professsor
of Mechanical Engineering

I certify that I have read this study and that in my opinion it conforms to acceptable standards of scholarly presentation and is fully adequate, in scope and quality, as a dissertation for the degree of Doctor of Philosophy.

H. A. Ingley
Associate Professor of Mechanical
Engineering

I certify that I have read this study and that in my opinion it conforms to acceptable standards of scholarly presentation and is fully adequate, in scope and quality, as a dissertation for the degree of Doctor of Philosophy.

RA Gater

R. A. Gater
Associate Professor of Mechanical
Engineering

I certify that I have read this study and that in my opinion it conforms to acceptable standards of scholarly presentation and is fully adequate, in scope and quality, as a dissertation for the degree of Doctor of Philosophy.

C. K. Hsieh
Professor of Mechanical Engineering

I certify that I have read this study and that in my opinion it conforms to acceptable standards of scholarly presentation and is fully adequate, in scope and quality, as a dissertation for the degree of Doctor of Philosophy.

U. H. Kurzweg

U. H. Kurzweg
Professor of Engineering Sciences

I certify that I have read this study and that in my opinion it conforms to acceptable standards of scholarly presentation and is fully adequate, in scope and quality, as a dissertation for the degree of Doctor of Philosophy.

R Pagano

R. Pagano
Associate in Engineering Sciences

This dissertation was submitted to the Graduate Faculty of the College of Engineering and to the Graduate School, and was accepted as partial fulfillment of the requirements for the degree of Doctor of Philosophy.

May 1987

Dean, College of Engineering

Dean, Graduate School